VTT SCIENCE 183

Chemical behaviour of bentonite in the near field of the...

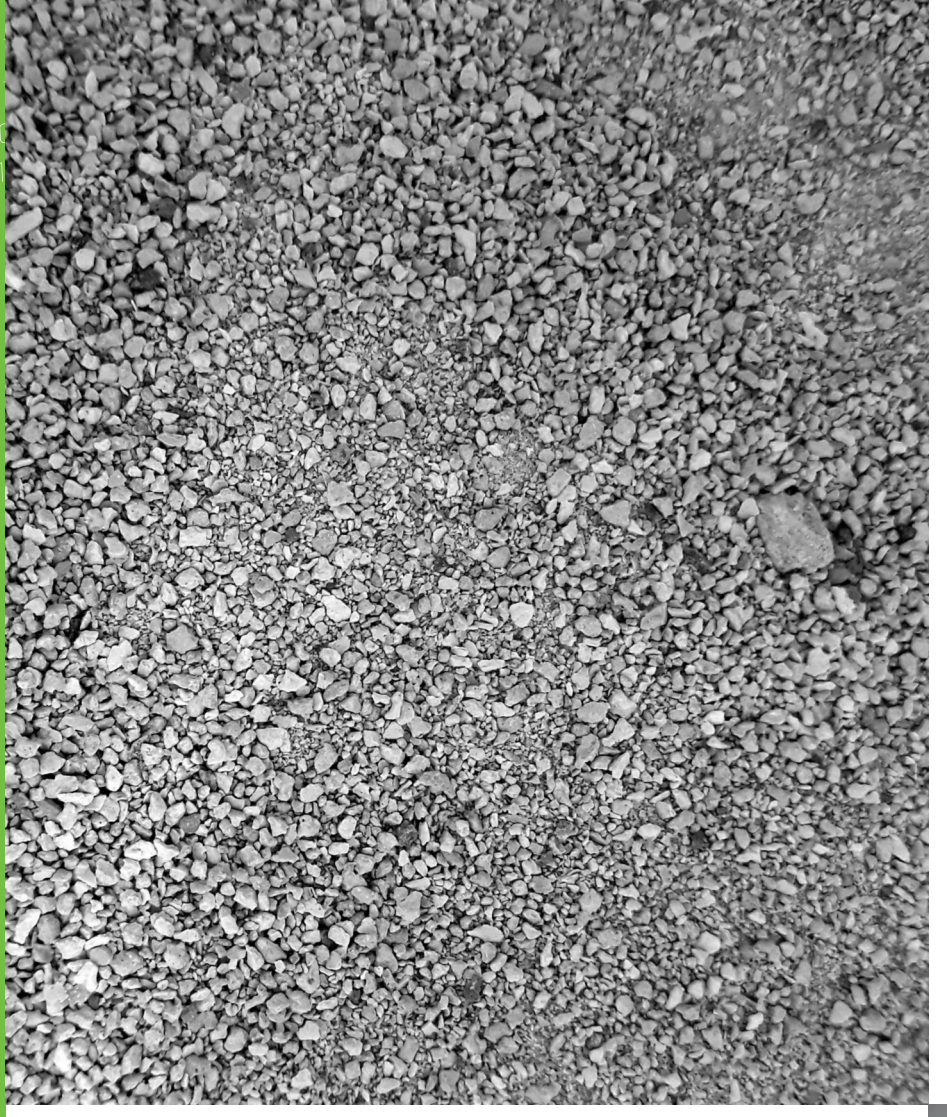

SCIENCE • TECHNOLOGY • RESEARCH HIGHLIGHTS • VISIONS •

Dissertation
183

Chemical behaviour of bentonite in the near field of the KBS-3V concept

Aku Itälä

VTT SCIENCE 183

Chemical behaviour of bentonite in the near field of the KBS-3V concept

Aku Itälä

ACADEMIC DISSERTATION

Thesis for the degree of Doctor of Philosophy to be presented with the permission of the Faculty of Science of the University of Helsinki for public examination in lecture hall D123 (Exactum) of the University of Helsinki, on November 20th, 2018, at 12 o'clock noon.

ISBN 978-951-38-8670-7 (Soft back ed.)
ISBN 978-951-38-8669-1 (URL: http://www.vttresearch.com/impact/publications)

VTT Science 183

ISSN-L 2242-119X
ISSN 2242-119X (Print)
ISSN 2242-1203 (Online)
http://urn.fi/URN:ISBN:978-951-38-8669-1

JULKAISIJA – UTGIVARE – PUBLISHER

Teknologian tutkimuskeskus VTT Oy
PL 1000 (Tekniikantie 4 A, Espoo)
02044 VTT
Puh. 020 722 111, faksi 020 722 7001

Teknologiska forskningscentralen VTT Ab
PB 1000 (Teknikvägen 4 A, Esbo)
FI-02044 VTT
Tfn +358 20 722 111, telefax +358 20 722 7001

VTT Technical Research Centre of Finland Ltd
P.O. Box 1000 (Tekniikantie 4 A, Espoo)
FI-02044 VTT, Finland
Tel. +358 20 722 111, fax +358 20 722 7001

Juvenes Print, Tampere 2018

Abstract

In Finland the spent nuclear fuel final repository of Posiva Oy is based on the Swedish KBS-3V multi-barrier concept. In this concept, the spent fuel rods are placed inside cast iron inserts surrounded by a gastight copper canister. The canister is placed in a vertical borehole and surrounded by bentonite clay rings at a depth of at least 400m in an underground bedrock facility at Olkiluoto. In the KBS-3 concept, the role of bentonite clay is considered to be important. The bentonite acts as a buffer material which gives mechanical and chemical protection, dissipates heat and retards radionuclide diffusion in the event of canister failure. It is crucial to know if the bentonite will retain its performance for at least 100 000 years.

This thesis is compiled of 6 publications in which experiments related to bentonite buffer are modelled, or some parameters of bentonite are studied in laboratory/final repository conditions. In the two first publications the aim was to model the chemical evolution of a final repository during the thermal phase, when the bentonite is only partially saturated in the beginning. In these publications, a case called Long-term test adverse 2 performed in Äspö Hard Rock Laboratory was adopted as a reference case to make the modelling more concrete and to clarify if the phenomena occurring in the experiment must be taken into account in safety assessment. The main chemical change according to the models and the experiment was anhydrite precipitation near the heater interface. No changes affecting the performance of the bentonite was observed.

In addition, during this thesis a few laboratory experiments were conducted and modelled. The effect of temperature on cation-exchange behaviour of purified sodium montmorillonite was studied in three different temperatures (25 ^{o}C, 50 ^{o}C and 75 ^{o}C) using calcium/sodium perchlorate mixtures. The observed results showed similar selectivity for all temperatures.

In the fourth publication, the carbon dioxide partial pressure effect on the pH of bentonite was modelled using Geochemist's Workbench. The results indicated that only the surface protonation sites buffered the pH changes in the compacted bentonite system since the water amount inside the bentonite was small compared to the amount of surface complexation sites. The buffering capacity was approximated to be 0.3pH units/10g of bentonite.

In the fifth publication, a structural model for bentonite was additionally made, which takes into account different kinds of waters inside the bentonite, and the

model was compared to state-of-the-art commercial software and was noted to work well. In the last publication a simplified model was made to model the pore water of the squeezing experiments from compacted bentonite in anoxic laboratory conditions. The model worked well on major ions, but some differences were also observed.

The conclusion from all these studies is that bentonite is a complex material, and the microstructural behaviour is still under dispute. The most common consensus is that there are three different waters (free pore water, diffuse double-layer water and interlamellar water). It is important to understand the microstructure of bentonite so that accurate models can be created which correctly predict the phenomena occurring inside bentonite. Modelling is needed to approximate the final repository behaviour over hundreds of thousands of years, but there are still some uncertainties remaining such as chemical and mechanical parameters, parameters relates to saturation and high temperature behaviour, lack of kinetic data for some minerals as well as reactive surface areas and grain radii.

Acknowledgements

The research for this thesis was conducted in the Nuclear Waste Management team at the VTT Technical Research Centre of Finland during the period of May 2008 to May 2015. The writing of the thesis has been a challenging journey and progressed slowly. I started writing this thesis in April 2016 but had almost a year break and it was not until the end of 2017 I incited myself to finish it. I am grateful for the opportunity to do this thesis at VTT and for our team which made it possible and advised me during my work.

The starting point of this work came from our research professor and my supervisor at VTT Dr. Markus Olin who was encouraging me to start doing this thesis from my current publications, and also the conversations with him and our former team leader Dr. Kari Rasilainen. I'm very grateful for all of their comments on the work as well.

This work would not have been possible without the contribution of my co-authors. I am indebted to M.Sc. Joonas Järvinen, Dr. Arto Muurinen, M.Sc. Veli-Matti Pulkkanen, M.Sc. Michal Matusewicz and M.Sc. Merja Tanhua-Tyrkkö at VTT, and Dr. Mika Laitinen from Numerola Oy and to M.Sc. Jarmo Lehikoinen from STUK who were a great help at the beginning of my career and during it with their comments and work they have also given me.

The research conducted in the thesis was funded by EU projects, KYT (Finnish Research Programme on Nuclear Waste Management) projects, Posiva Oy and VTT which are all acknowledged for their financial support. I would like to thank SKB (Svensk Kärnbränslehantering AB) for providing me the results from LOT experiments performed at the Äspö Hard Rock Laboratory in Sweden.

I am also grateful to Professor Markku Kulmala who made this thesis possible for being my Supervisor at Helsinki University. I am also grateful to my reviewers Daniele Pedretti and Mika Niskanen for their comments and to my opponent Jyrki Mäkelä.

In addition, a lot of support has been given to me financially and mentally by my family; father Seppo Itälä, mother Anne Itälä and my two big brothers Olli and Petri. Biggest thanks from the latest years goes to my girlfriend Jenna Leppänen who has been my support and there for me. I hope after this thesis is finished I am more open about what to do during weekends.

Espoo, 5th of October 2018, Aku Itälä

Academic dissertation

Supervisors	Academian Markku Kulmala, Ph.D. University of Helsinki
	Professor Markus Olin, Ph.D. VTT Technical Research Centre of Finland Ltd
Reviewers	Professor Daniele Pedretti, Ph.D. Geological Survey of Finland
	Doctor Mika Niskanen, Ph.D. Posiva Oy
Opponent	Professor Jyrki Mäkelä, Ph.D. Tampere University of Technology

List of publications

This thesis is based on the following original publications, which are referred to in the text as I–VI. The publications are reproduced with kind permission from the publishers.

I Itälä Aku, Olin Markus. **2011**. Chemical evolution of bentonite buffer in a final repository of spent nuclear fuel during 5 phase. Nuclear Technology, Vol. 174, No. 3, pp. 342-352. doi: 10.13182/NT11-A11744

II Itälä Aku, Olin Markus, Lehikoinen Jarmo. **2011**. Lot A2 test, THC modelling of the bentonite buffer: Elsevier. Physics and Chemistry of the Earth, Parts A/B/C, Vol. 36, No. 17-18, pp. 1830-1837. doi:10.1016/j.pce.2011.10.020

III Itälä Aku, Muurinen Arto. **2012**. Na/Ca selectivity coefficients of montmorillonite in perchlorate solution at different temperatures. MRS Spring Meeting, 9 - 13 April 2012, Buenos Aires, Argentina: Materials Research Society. Materials Research Society Symposium Proceedings, Vol. 1475, pp. 335-340. Doi:10.1557/opl.2012.596

IV Itälä Aku, Järvinen Joonas, Muurinen Arto. **2013**. CO2 effect on the pH of compacted bentonite buffer on the laboratory scale: Mineralogical Society. Clay Minerals, Vol. 48, No. 2, pp. 277 -283. doi:10.1180/claymin.2013.048.2.09

V Itälä, A., Laitinen, M., Tanhua-Tyrkkö, M., Olin, M. **2014**. Modeling Transport of Water, Ions, and Chemical Reactions in Compacted Bentonite: Comparison Among Toughreact, Numerrin, and Comsol Multiphysics. Nuclear Technology, Vol. 18, No. 2, pp. 169-174. doi: 10.13182/NT13-79

VI Järvinen Joonas, Matusewicz Michał, Itälä Aku. **2016**. Methodology for studying the composition of non-interlamellar pore water in compacted bentonite. Clay Minerals, May 2016; Vol. 51, i. 2, pp. 173-187. doi:10.1180/claymin.2016.051.2.01

Author's contributions

Most of the work in these papers was done by the author himself with the help of the co-workers [I-V]. Publication [I] is based on author's Master of Science thesis. In both publications [I-II] an experiment called Long Term test of buffer material (LOT-A2), done in Äspö hard rock laboratory (HRL), was used as an experimental case. The aim was to study the evolution of a final repository's near field during the thermal phase. The model was created with TOUGHREACT in 1-dimensional geometry. The author wrote this paper alone under guidance of the co-author, Dr. Markus Olin.

Publication [I] was a continuation of publication [I], and the model was further developed into semi-3D geometry in axisymmetric 2D cylindrical coordinates. The author was responsible for the modelling work and writing with the help of the co-authors, Dr. Markus Olin and M.Sc. Jarmo Lehikoinen.

In publication [III], cation-exchange selectivities for sodium and calcium in purified sodium montmorillonite were studied at three different temperatures. The experimental work and modelling were conducted by the author with fruitful tips and discussions about the experiments and results with Dr. Arto Muurinen.

The effect of carbon dioxide partial pressure on compacted MX-80 bentonite was studied in publication [IV]. The author performed the modelling work in this paper as well as writing the paper together with Dr. Arto Muurinen and M.Sc. Joonas Järvinen who did the experimental work. The author also contributed in evaluating the experimental results.

In publication [V], three different codes TOUGHREACT, COMSOL Multiphysics and Numerrin were compared by calculating a test case, which included a simple NaCl system with some decaying components. The author did the TOUGHREACT modelling part and helped to develop the numerical model for the COMSOL and Numerrin codes. The co-author Dr. Mika Laitinen did the modelling with Numerrin and Dr. Markus Olin with COMSOL. The co-author M.Sc. Merja Tanhua-Tyrkkö helped in developing the model.

In paper [VI] the author did the modelling part of the paper and also contributed to the experimental parts by analysing the experimental results with other authors and through the modelling results. The paper was written on the ABM experiment in Äspö Hard Rock Laboratory and the MX-80 part of the experiment was analysed at VTT.

Contents

List of abbreviations

α	capacity factor
β	equivalent mole fraction
c	molar concentration (mol/L)
D_e	effective diffusion coefficient (m^2/s)
D_p	pore diffusion coefficient (m^2/s)
D_s	surface diffusion coefficient m^2/s)
ϕ	porosity
K	selectivity coefficient/equilibrium constant
λ_i	linear reaction rate (radioactive decay) for species (1/s)
M	mass (kg)
ρ	density (kg/dm^3)
r	reaction rate
χ	ratio of volume fractions of free and total water volume
X	cation exchange site
z_i	charge of cation i

Abbreviations

BWR	Boiling Water Reactor
CEC	Cation Exchange Capacity
DDL	Diffuse Double Layer
EDL	Electrical Double Layer
EDZ	Excavation Damaged Zone
EOS	Equation of State
GWB	Geochemist's Workbench
IrOx	Iridium Oxide
KBS-3V	Kärnbränslesäkerhet (Nuclear safety) – 3 Vertical
LOT	Long Term Test
MOX	Mixed Uranium-Plutonium Oxide
NMR	Nuclear Magnetic Resonance
PA	Performance Assessment
PWR	Pressurized Water Reactor
RH	Relative Humidity
SAXS	Small-Angle X-ray Scattering
THC	Thermo-Hydro-Chemical
THM	Thermo-Hydro-Mechanical
TOT	Tetrahedral-Octahedral-Tetrahedral
VVER	Vodo-Vodjanoi Energetitšeski Reaktor (Water-Water Energetic Reactor)

1. Introduction

All countries that utilize nuclear power for energy production have to solve the problem of how to safely dispose of spent nuclear fuel rods, which after use are highly radioactive spent nuclear waste.

According to the Nuclear Energy Act, nuclear waste generated in Finland must be stored and disposed of in Finland. As a result, the Finnish nuclear power companies (Fortum and TVO) and their affiliated company Posiva Oy have made a plan to dispose of the spent fuel in a geological repository at 450m depth in the bedrock. The repository was granted a construction license at the end of year 2015. [1,2]

The safe disposal is based on the Swedish KBS-3 method [3], which is elaborated in Chapter 2, including the characteristics of the Olkiluoto site in Eurajoki. In this method the long-term isolation and containment of radionuclides needs to be secured. In the event of canister failure and the release of radionuclides, the engineered barrier system and the rock matrix should also retard the release of these nuclides.

The performance of this system is based on a few safety functions. The first component of the system is the ceramic state of the fuel and thus the slowly dissolving solid uranium pellets inside gastight metal rods, which also slow down the release of radioactive nuclides.

The second component of the system is the copper canister that functions to provide the stable and safe containment of the radionuclides. This function is maintained by the mechanical strength of the canister's cast iron insert and the corrosion resistant copper around it.

Thirdly, there is the bentonite clay buffer, which should protect the canister from external chemical and mechanical processes by limiting and retarding the release of radionuclides from the canisters in the case of canister failure.

The fourth barrier is the host rock/bedrock, which isolates the repository from the surface and which offers predictable and favourable conditions for the other barriers whilst also retarding the release of nuclides from the repository.

Lastly, there are the other system components such as backfilling materials, e.g. pellets and backfill blocks, which are used between the barriers and to fill the deposition tunnels. The purpose of the backfill materials is to prevent creation of flow paths, to keep the buffer around the canister in place, to support the

surrounding rock and to prevent chemical disturbances to the canister, buffer and bedrock [4].

The final disposal system used in Finland was initially developed in Sweden, and has already been studied and reported for almost 40 years. However, in Finland it was started a little later than in Sweden [3,5–14]. In the Swedish KBS-3 concept, the nuclear waste is placed inside copper covered steel canisters into the bedrock at a depth of about 450 m. Each canister contains between 1.4-2.2 tons of uranium [15]. The total weight of the canisters is between 18-30 tons [14]. This design has changed very little over the years [15,16].

The work represented in this thesis provides insight in how to handle the Thermo-Hydro-Chemical (THC) modelling of the near field of the nuclear waste repository and also represents a few experiments related to chemical behaviour of bentonite. The behaviour of the final repository must be predicted by modelling since the repository needs to prevent the release of radionuclides for thousands of years and experimental time is short in comparison. The work is concentrated around the bentonite barrier and its properties in repository conditions during the first 10 000 years when the nuclear fuel is still generating heat. This phase is called the thermal phase and the work is carried out through both modelling and experiments.

1.1 Research problem and objectives (the purpose of this study)

This study was started as an analysis of the chemical evolution of the bentonite buffer in the final repository of spent nuclear fuel during the thermal phase which ends approximately after 10 000 years. In this thermal phase, the incoming water from the bedrock saturates the bentonite under the effects of thermal gradient. During this thermal phase, the bentonite may undergo different chemical alterations. The effect of these phenomena on bentonite evolution is crucial in order to know which kind of bentonite can be used in the final repository. The research question was whether the bentonite would last hundreds of thousands of years in the final repository, maintain its useful features, and are the changes possibly reversible. The research objectives were:

1. To further develop the expertise from mineralogy, hydraulics and physical sciences, so that readiness to perform scientifically challenging safety-specific studies about the behaviour of the near field of the spent nuclear fuel repository, can be achieved.
2. The initial purpose of the study was to design a model that would reliably predict how the bentonite has chemically evolved after the thermal period. However, the target soon appeared too ambitious compared to resources, and the scope of the study was changed so that only a case in which the bentonite was exposed to adverse temperature conditions (120-150 ^{o}C) and high temperature gradients was modelled. These elevated temperatures were set to describe the thermal load of the full 10 000-year period during an approximately 6-year experiment. Thus, the 10 000-year heating period was not modelled as originally planned. Only simplified

modelling, using the LOT A2 test as a source of data and for verification of the model, was undertaken.

3. To further develop the modelling know-how and understanding of behaviour of bentonite material itself by modelling of the laboratory experiments.
4. To verify selected data used in the modelling through experiments.
5. To gain better understanding of bentonite microstructure via modelling and experimental expertise.

2. Geological disposal concept

The final disposal concept of spent nuclear fuel is typically based on the use of multiple barriers. These barriers are planned to ensure that no or a very little amount of radionuclides is released in the biosphere or comes into contact with people in harmful amounts. If one of the barriers fails, it does not endanger the performance of the whole containment system according to the KBS-3 concept. The barriers included in the disposal concept are the physical and chemical state of the fuel, the canister, bentonite barrier, filling materials of the tunnels and the bedrock. The system studied in this thesis is based on the KBS-3 method.

2.1 KBS-3 method

The Finnish Parliament endorsed a Decision-in-Principle (DIP) in 2001 which states that the disposal of spent nuclear fuel shall take place in a geological repository [1,17]. In the KBS-3 method, the spent nuclear fuel rods are sealed inside watertight and gastight copper canisters, which are closed by welding. Inside the copper canister is a cast iron insert surrounding the fuel and giving mechanical protection against e.g. hydrostatic pressure and rock movements. The canister system is then installed in a borehole at a depth of at least 400 m.

In KBS-3 there are two different types of designs where one is vertical (V) and other is horizontal (H). The format chosen to be used in the Finnish final repository by Posiva is currently the KBS-3V design [17].

The adopted KBS-3V system design is based on a multi-barrier system (Fig. 2.1) in which the copper-iron covered fuel canisters are placed in vertically drilled boreholes surrounded by bentonite rings at the bottom of the deposition tunnels. The deposition tunnels and central tunnels are going to be backfilled with materials of low permeability containing bentonite and rock-bentonite mixtures while the final natural barrier is the rock itself.

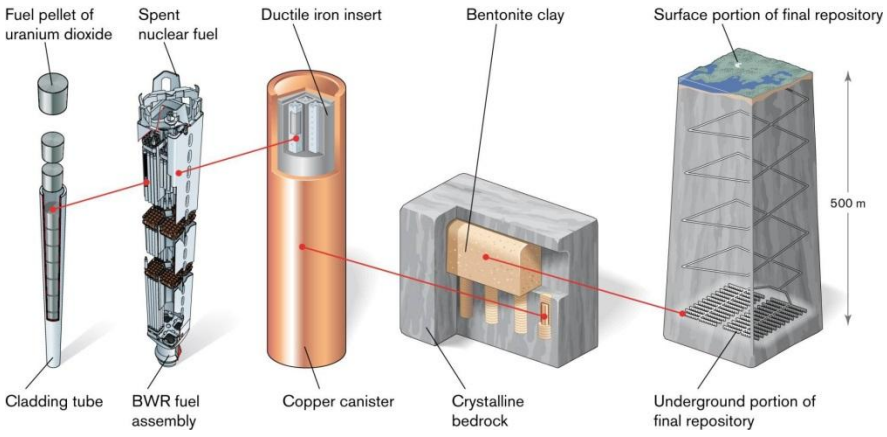

Figure 2.1. KBS-3V concept (Figure is courtesy of SKB) [18].

2.2 Safety functions and requirements

Each barrier mentioned earlier has certain safety requirements to fulfil which are engineered by specialists and regulated by the radiation and nuclear safety authorities (STUK in Finland).

Posiva is responsible for spent fuel final disposal of TVO's and Fortum's waste. Posiva and Fennovoima have to ensure that the residual heat generated by the spent nuclear fuel is removed safely after deposition to bedrock. They must also ensure that any release of radioactive waste is kept to a minimum and that effective protection of individuals, society and environment is taken care of. Posiva must consider the chemical, biological and other hazards caused by spent nuclear fuel and also try to keep the risks below the aforementioned safety requirements [19,20].

The engineered barriers are designed to support long-term containment of radioactive nuclear waste. Besides providing protection for the canisters, the design must ensure that any radionuclides released from defective or broken canisters will be retarded and diluted by barriers as much as possible before reaching the surface so that the hazardous radiation value is not surpassed. More importantly, the barriers are needed to slow down the release, advective transport and diffusion of radionuclides. The transport barriers seen in Figure 2.1 and their related safety functions are [21]:

- Canister [15]: The copper canister with iron insert must be tight and maintain its integrity for at least 100 000 years according to criteria defined by Posiva. For this reason, the canister must have good corrosion resistance and during expected evolution should remain intact [22,23]. Some results have shown faster corrosion [24] but this is not in line with most studies [23,25] or natural analogues. The canister must also protect the environment by only allowing heat and low-level gamma and neutron radiation through canister. It must also be able to withstand mechanical stress from bentonite swelling, rock movements, glacial age and hydrostatic pressure.
- Buffer: The purpose of the bentonite buffer is to protect the canister from bedrock displacements as well as the effects of groundwater flow by directly halting it near the canister vicinity (only diffusion as transport mechanism following from low enough permeability of bentonite) [21,26–29]. The buffer must have high thermal conductivity to dissipate the heat from the canister to the rock and provide chemical and mechanical protection to canister and other barriers.
- Tunnel backfill and sealing materials must be chemically and mechanically stable, and prevent the groundwater flow in tunnels and excavation disturbed zones (EDZ).
- The bedrock must provide a long-term stable and favourable environment for the repository. It is assumed to have four safety functions which are chemically, hydrologically, mechanically and thermally favourable conditions.

2.3 Spent nuclear fuel

There are two different kinds of reactors in use in Finland called Boiling Water Reactors (BWR) in Olkiluoto and Pressurised Water Reactors (PWR also named Veda-Vodanoi Energetitsheski Reaktor (VVER)) in Loviisa, which differ slightly through the water-boiling mechanisms. Olkiluoto 3 will also be one type of PWR reactor called European Pressurized Water Reactor (EPR).

The enriched fuel is composed of uranium dioxide which contains 3-5% fissile Uranium-235 and mostly non-fissile Uranium-238. The fission produces a lot of unstable fission products, which in turn generate heat through decay and radioactivity. The fission products dominate the radioactivity during the first century, but after that heavier elements with a long half-life play a more dominant role in the residual radiotoxicity [35].

Spent nuclear fuel is one of the most hazardous man-made materials. The spent fuel when removed from the nuclear reactor after use can cause death or cancer in a few minutes under radiation exposure [36]. The fuel after removal is thus positioned for cooling in water pools for years (as water works as a coolant and already a few meters retards the radiation totally). The risks are that these water pools might be susceptible, for example, to terrorist attacks or natural disasters and need to be guarded carefully. The radioactive half-life of some materials can be days, whereas thousands of years for other materials.

The spent fuel needs to remain in water pools for at least 20 years also due to the thermal dimensioning criteria in the final repository. This criterion is that the maximum temperature at the canister/buffer interface is set to be +100 ^{o}C but for practical reason it is set for 95 ^{o}C to leave 5 degree margin for changes in host rock properties. This criterion is the same for BWR, VVER as well as for EPR fuel canisters in Finland [37]. After this criterion is fulfilled, the canisters containing spent fuel can be moved to the final repository. In Finland, the construction licence was granted for Posiva Oy in 2015 and the operation licence application is aimed to be submitted in early 2020 and the final disposal is scheduled to be started in first half of 2020s [38].

3. Characterization, chemistry and behaviour of bentonite buffer

Bentonite is chosen to be used as a barrier material to support the canister in many planned final repositories around the world. In Finland in the KBS-3 method MX-80 Wyoming bentonite is chosen to be the buffer material used to isolate the copper canister and bedrock from each other. The copper canisters are placed on deposition holes (Fig. 3.1.) which are filled with c.a. 17-21 tonnes of bentonite. The volume filled with bentonite is approximately 8-10 m^3 of the total volume of depositions hole. The empty area around the bentonite rings is around 2-3 m^3 before the water saturates and swells the bentonite. The dimensions vary depending on the fuel type used in the nuclear power plants. The radius of the deposition hole is always the same but the length varies. [39]

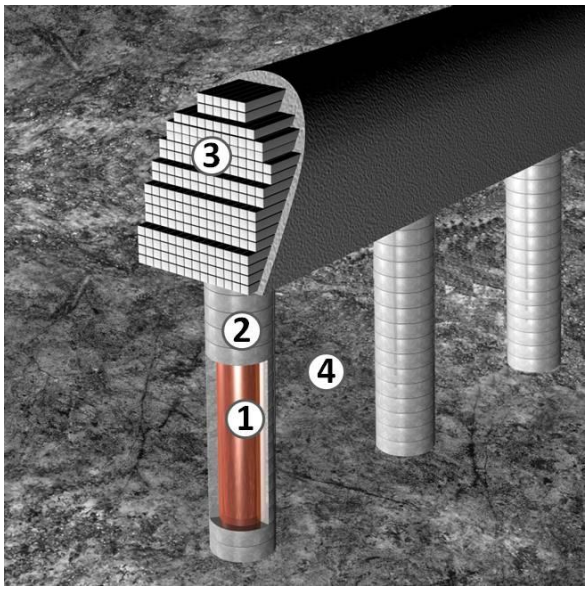

Figure 3.1. Release barriers in the KBS 3-V system: 1. Copper canister, 2. Bentonite, 3. Tunnel backfill, 4. Bedrock. [40]

3.1 Technical safety criteria and performance targets of the buffer

The function of the bentonite buffer in the final repository is to protect the copper canister in which the spent fuel is placed. The canister may face mechanical stress

during, for example, earthquakes or bedrock movements, and bentonite is planned to be able to buffer these effects. [41]

The safety functions of the buffer barrier are as follows: It should provide favourable and predictable mechanical, geochemical and hydrological conditions for the canister. It should protect the canister from external processes, whilst limiting and retarding the radionuclide release in the case of a defective canister and prevent high microbiological activity. [41,42]

The performance targets set for the buffer to fulfil the aforementioned safety criteria for over hundreds of thousands of years in the expected repository conditions are as follows [41]:

- The buffer transfers heat from the canister efficiently to keep the buffer temperature <100 ^{o}C.
- The buffer allows gases to pass through without damaging the barrier system.
- The buffer limits the microbial activity and provides chemical protection.
- The buffer mitigates the impact of rock movements on the canister.
- The buffer possesses low permeability, to limit mass transfer of corroding substances and limit radionuclide transport from the canister to bedrock.
- The buffer provides mechanical support to the deposition hole walls and to the canister to prevent canister movement.
- The swelling pressure should be high and generate fast enough to make the deposition hole tight and stable, and minimize any microbial activity.

3.2 Characterization and structure of bentonite

Bentonite was named after the deposits in the Benton Shale near Rock River in Wyoming by Wilbur C. Knight in 1898. After that, the deposits in which the minerals are called bentonite included more formations around Wyoming and in other places around the world. However, around 70% of the world's bentonite production comes from Wyoming, U.S.A. The bentonite forming in Wyoming is the result of chemical changes occurring in ancient volcanic ash. [43]

Bentonite is commonly described as a material predominantly composed of clay minerals which again belong to the smectite group [44]. The specific bentonite material studied in this thesis is Wyoming MX-80 bentonite, which consists of hydrous alumina silicate more commonly known as montmorillonite. Bentonite has many applications as it can be used, for example, in kitty litter (as it can swell up to 16 times its original volume), drilling mud, binder in moulds and even cosmetics besides the barrier material in a final repository [45–47]. MX-80 is a commercial name used to describe Wyoming bentonite in sodium form. The excavated water content of the bentonite is about 30%. During excavation, the material is crushed and dried after which it is processed into products. For example by sieving and grinding, the grain size of the bentonite can be adjusted as wanted for commercial use.

Bentonites differ by mineralogical composition, with the main mineral, however, being montmorillonite. The special properties of this mineral include the exchange

of Na/Ca cations inside the structure and the ability of the mineral lattice to bound water and swell accordingly. Secondary minerals can be, for example, silicates like quartz, tridymite, cristobalite, feldspars, muscovite/illite, sulphides, pyrite, hematite, gypsum and some trace minerals.

3.2.1 Montmorillonite

Montmorillonite is a swelling clay and belongs to smectite mineral group which includes minerals like beidellite, saponite, sauconite, and hectorite, etc. besides montmorillonite [48]. Montmorillonite is the main mineral on the bentonite structure comprising 65-90% of the bentonite mass and is composed of 1nm thin plates, which can be 200-400nm in diameter. The swelling properties of bentonite are determined mainly by this mineral.

The chemical formula of montmorillonite can be written commonly as:

$$M_x(Al_{2-x}Mg_x)Si_4O_{10}(OH)_2 \cdot nH_2O \quad (1)$$

where *M* is mostly Na^+ and $0.5Ca^{2+}$ and small amounts of K^+ and Mg^{2+} depending on the surrounding conditions. The *x* in the equation is the equivalent amount of exchangeable cations which is usually approximately about 0.3 order of magnitude for montmorillonite and between 0.2-0.6 for other smectites [49]. The fundamental structure of montmorillonite consists of edge sharing 2:1 tetrahedral-octahedral-tetrahedral (TOT) sheets. Between the TOT layers are the exchangeable cations balancing the permanent negative charge. The permanent negative charge of the TOT layers is caused by the isomorphic substitutions of lattice cations Si^{4+} with Al^{3+} on tetrahedral sheet and Al^{3+} with Mg^{2+} or Fe^{2+} (Fe^{3+}) on the octahedral sheet (see Fig. 3.2). This permanent negative charge represents the cation-exchange capacity (*CEC*), which is a measure of how many cations can be bound to material surface, and the *x* in equation 1. [47,50,51]. The negative charge is primarily balanced by cations located in the interlayer space or on the external basal surface. This region, where cation adsorption and anion exclusion occur, is called the electrical double layer (EDL). Anion exclusion in this case means exclusion of anions from a liquid zone adjacent to negatively charged surfaces though some anions may penetrate this area.

Figure 3.2 illustrates how two TOT layers combine to form platelets and how layers are formed by silica and aluminium. The platelets are a few montmorillonite layers thick and bigger clay particles are composed of platelet stacks (3-5 in Na-montmorillonite and 10-20 in Ca-montmorillonite) [52]. The cations in the interlayer space compensate the negative charge and can undergo a stoichiometric exchange with the cations in the external solutions (see e.g. [47,53]). The cation-exchange capacity of montmorillonite varies from 70 to 120 meq/100g depending on the method used for measurement [54].

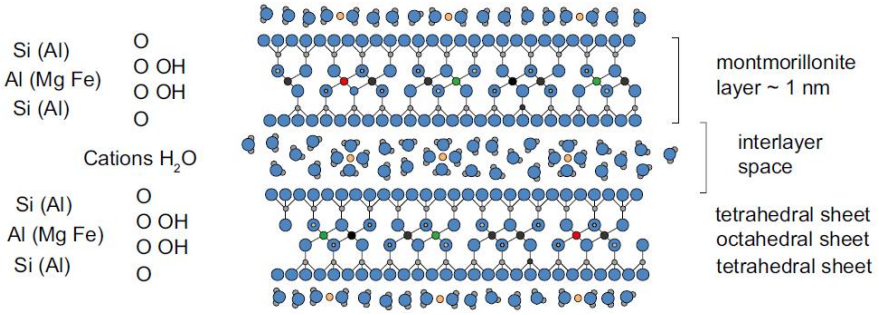

Figure 3.2. A schematic view of two montmorillonite TOT layers with interlayer cations and water molecules. [55]

The montmorillonite mineral structure contains three types of oxygen atoms: basal O_b atoms that connect neighbouring tetrahedra, e.g. SiO_4 and form a plane of O atoms, apical O_a atoms between the tetrahedra and octahedra, e.g. AlO_6 and octahedral O_o atoms that connect the octahedra and carry a proton (OH). Montmorillonite mineral has two basal siloxane surfaces (O_b planes). In the TOT layer there are always two O_o atoms and four O_a atoms in each octahedral site but the configuration may differ. [50]

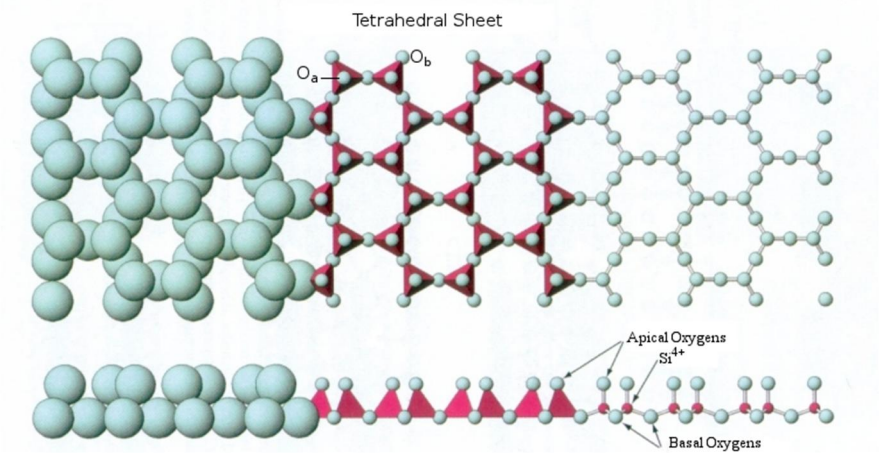

Figure 3.3. A schematic view explaining the 3D structure of tetrahedral sheet and positions of apical and basal oxygen atoms. [56]

The amount of pore water in montmorillonite is small compared to the number of bound cations. Thus, the montmorillonite as a cation exchanger acts as a powerful buffer for the cation composition of the pore water, and it determines the pore water components (see e.g. [57]) together with the interacting external solution (for example groundwater in a repository). This occurs in basal surfaces.

Montmorillonite mineral edges carry a pH-dependent proton surface charge, which arises from the deprotonation/protonation of edge surface hydroxyl groups

(OH^-). The edge surface capacity is approximately one tenth of the CEC [57] and can be studied by acid-base titrations. These surface sites behave as a pH buffer in bentonite and can also bind cations, anions and molecules through short-range interactions [58] depending on the pH. Non-specific interactions compensating the charge of the edge surface explain the pH dependence of CEC in clays [59].

3.2.2 Wetting and water on bentonite

The air-dry bentonite is not completely dry but contains approximately 10-15% of water of the total mass. The amount of water in saturated bentonite depends on the compaction level and the available space, since in the presence of water bentonite swells to fill in any void space.

The hydration of bentonite is a multiscale process, and in the beginning when mesoscopic void space between mineral and sodium bentonite particles is partly filled with water, the mesoscopic swelling is starting when the interlayer space is only filled with one layer of water molecules (see Figure 3.4). According to Salles et al. 2009 [60], at low relative humidity (RH<10%) the hydration of Na-Bentonite starts on the bentonite particle surfaces (external surfaces, diffuse double layer water (DDL) in Figure 3.4) with one layer of water molecules. The second phase for RH higher than 10% the water enters into the interlayer space surrounding the cations and partially hydrating the internal surfaces. At the same time, water also fills fully the mesoscopic porosity between the clay and mineral particles. At 54% RH the mesopores are all filled (free/pore water in Figure 3.4). After this, the interlayer space starts to fill, further increasing the distance between the TOT layers, the particles start to break into smaller parts, and the volume of porosity increases. This process is called swelling [61–63] and is typical for bentonite during saturation with water. For calcium bentonites the swelling phenomenon is slightly different and is more limited than for sodium bentonites (MX-80), which can swell indefinitely and disperse even to single colloidal clay platelets if there nothing to restrict the swelling. Besides the cation form of the bentonite, also the environmental factors such as temperature, pressure and surrounding solutions are known to affect the swelling properties of bentonite [64–66].

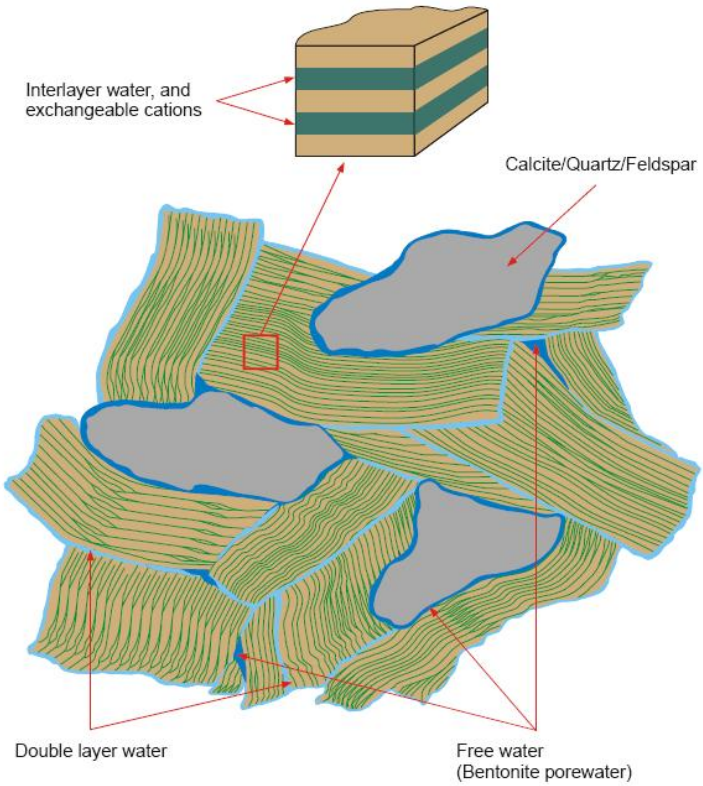

Figure 3.4. A schematic view of the waters and microstructure of bentonite [57].

As can be seen in Fig. 3.4, there are waters in three different positions inside the bentonite (see e.g. [57,67–71]). The first water type is the interlamellar (interlayer) water between the clay platelets where the polar water molecules surround the cations compensating the negative charge of the clay platelets. The interlamellar space has a high concentration of cations and tries to bind as many polar water molecules as possible. The external water can be categorized as diffuse double layer water at the external surfaces of the clay stacks and as free water, also called as pore water, which can be around the other mineral particles or between the clay stacks and secondary minerals.

3.2.3 Chemical phenomena in bentonite

Bentonite has a complicated structure, and while in final repository conditions it will interact with its surroundings with different phenomena. There is a high negative charge at the edges of the clay sheets. The cations compensating this charge between the clay sheets are loosely attached and can undergo a stoichiometric

exchange with the cations in the surrounding pore/groundwater while the same space between the sheets is partially prohibited from anions (anion exclusion).

In final repository conditions, the bentonite interacts with pore water and flowing groundwater, which is coming through fractures. The edge charge in montmorillonite changes with pH such that when the pH is low the charge is positive, and when the pH is high the charge is negative. These sites are called surface complexation sites. The secondary minerals inside the bentonite and bedrock can interact through precipitation/dissolution. The chemical interactions are described in Figure 3.5.

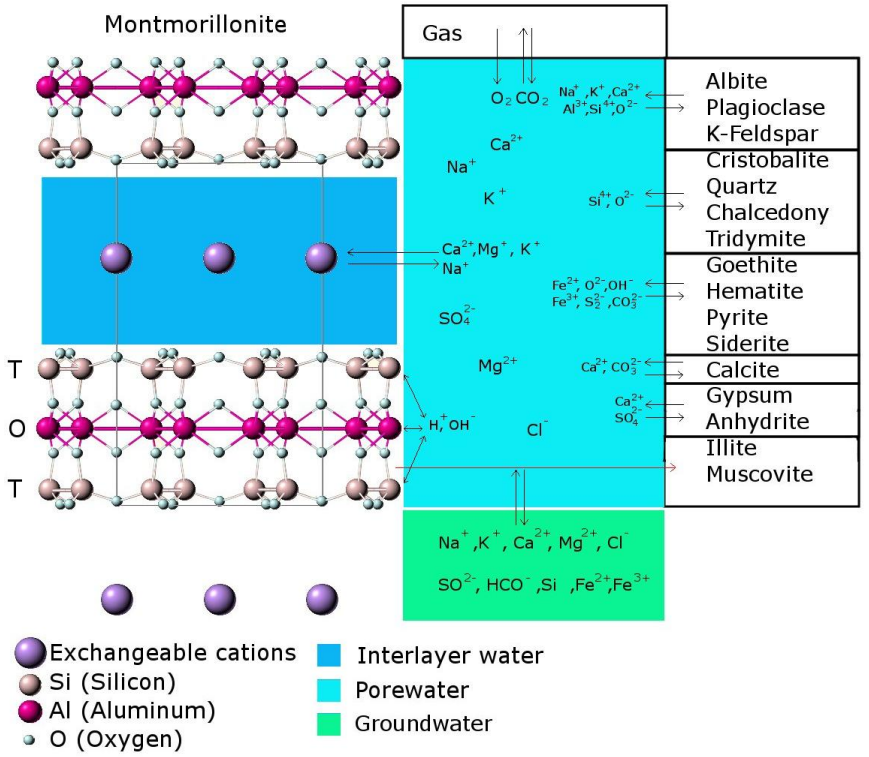

Figure 3.5. Geochemical processes in bentonite-water system in final repository conditions[69].

4. Experimental studies on bentonite

The bentonite structure varies depending on the degree of saturation, density and on the batch used. The bentonites from various areas can include, for example, different accessory minerals and different amounts of montmorillonite in varying cation form (Ca, Na, Mg, K). The chemical conditions in pore water specify the speciation, solubility and diffusion/sorption behaviour of radionuclides in the bentonite. However, laboratory experiments are often performed with loose bentonite, which might even have hundreds of litres of water per bentonite kilogram, while in the repository conditions the amount of water interacting is small. The dry density is aimed at approximately 1,600 kg/m^3 (grain density 2,750 kg/m^3) and porosity being around 43%, and thus these loose bentonite laboratory experiments do not necessarily represent the repository conditions well enough, and compacted bentonite experiments are therefore needed. These laboratory tests to study bentonite behaviour normally span from days to a few years, depending what parameters are studied and the scale of the experiments. For example, diffusion distance is dependent on square root of time.

In this chapter, the emphasis is on THC experiments, and mechanical aspects are not discussed. Phenomena like erosion, swelling behaviour, freezing etc. are not discussed.

4.1 pH buffering behaviour of MX-80 bentonite

The buffering capacity of bentonite related to pH has been studied mainly on loose material (see e.g. [72,73]), and there are only a few studies on the same subject on compacted bentonite. The information about the pH behaviour is crucial for performance assessment (PA) since pH affects the mobility of radionuclides (see e.g. [74]. Mainly high pH experiments to mimic a high pH plume resulting from the alteration of cements in the underground final repository have been conducted, since the groundwater is almost in a neutral region, and no acidic conditions will occur in final repository conditions. Cement is used in deposition tunnel plugs separating the deposition tunnel backfill bentonite from bentonite-rock mixture used in filling of central tunnels. It cannot be ruled out that part of pH plume may enter fractures in host rock and increase the pH in buffer bentonite.

4.1.1 Loose bentonite samples

In loose bentonite samples the solid/liquid ratio is normally really low and even the high solid/liquid mass-ratios used might be only 2% solid/w suspension. The pH of these suspensions is influenced by carbonates (e.g. calcite) even in minor amounts because the number of protons in the liquid is much higher than in the bentonite for it to buffer the changes, whereas calcite can react with water and form CO_2(aq), which again forms weak acid.

Kaufhold et al. 2008 [72] studied cation exchange between Na^+ and Ca^{2+} and its effect on the pH on loose bentonites. They observed that the exchange to calcium form increased pH, which is not the case in highly compacted bentonites [72,75]. However, this has been only noticed in suspensions where the excess salts were removed, and the phenomenon was not explicitly explained because it was proposed that this kind of behaviour might have to do with the delamination and hydrolysis, which depend on the ionic strength of the solution. [72]

Heikola et al. 2013 [73] studied Ca and Na bentonites in four different alkaline waters in the pH range from 8.3 to 12 in batch reactions for 554 days. Also Vuorinen et al. 2006 [76] studied the effects of salinity and high pH on bentonite and crushed rock on batch and flow through experiments (from 6 to 540 days). In these studies, it was found that buffering of pH occurred in the beginning of the experiments. Also, a decrease in Ca and increase in Na were observed in water due to ion exchange from Na to Ca and a small amount of released silica and Al. Only minor changes in mineralogy were observed on highest pH samples at 11.3 and at 12 pH, but some precipitation of calcium minerals (e.g. calcite) was suggested as well as dissolution of gypsum. However, in hyperalkaline solution (pH 13.5), the solid bentonite was completely destroyed, and zeolite and silicate phases formed. In the highest pH experiment, an increase in the carbonate content and decrease in montmorillonite content as well as some calcium silicate hydrate phases which influenced on higher tetrahedral charge (higher CEC) were observed. It was also confirmed that the higher the pH, the more unstable the swelling clay component, as it might change to beidellite. [73,76]

Bradbury and Baeyens 2003 [57] hypothesized that the pH and buffering capacity in highly compacted bentonite systems can be predicted from the initial state of the bentonite powder and the surface hydroxyl groups [57]. In 2009 [77] they proved their hypothesis by conducting some batch experiments from 1.5 to 12 pH to confirm the expected results and modelled them with PHREEQC. In the batch experiments by Pulkkanen et al. 2012 [78], an acetate buffer of 0.3M NaCl and 0.0125M acetic acid adjusted to pH 5 with NaOH was used together with 1g of purified sodium bentonite (pH 7). The experiment was performed such that during certain time intervals (1-2 days) some new solution was added after some of the old solution had been removed from the batch after equilibrium was reached in the old solution. After every step, the pH of the removed solution was measured; the experiment lasted 22 days. The results can be seen in Figure 4.1 and the time steps and more detailed explanation can be found in [78]. Cation exchange had no effect on the results since the solution was NaCl and the montmorillonite was in sodium form. From the results, it was clearly seen that remnants of calcite are still left in the purified sodium bentonite. Since without calcite the modelling results are not even close to the experimental results, it can be concluded that the buffering capacity of bentonite is quite large and almost 1:90 solid/liquid ratio is needed to reach the original pH of the solution used.

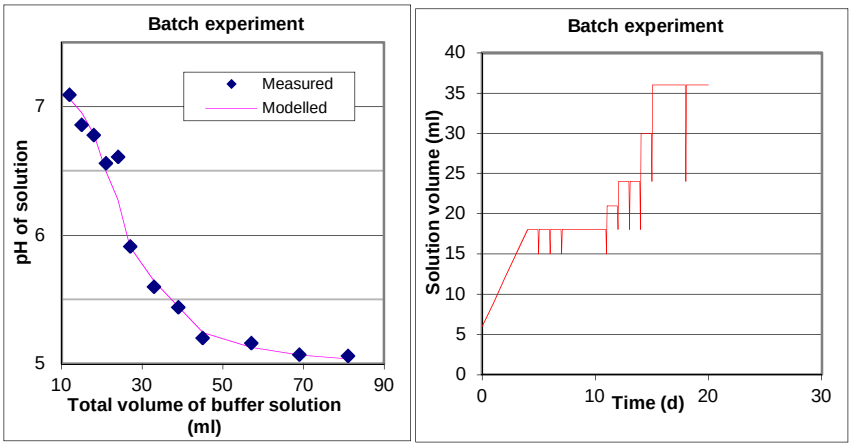

Figure 4.1. pH measured from the removed solutions as a function of total removed solution (left) and solution volume as a function of time (right) [78]. The modelling software used was PHREEQC.

4.1.2 Compacted bentonite

The loose bentonite pH experiments might not correlate with the real repository conditions where the bentonite is compacted tightly and the water amount in the pores is maximum of 43% of the volume. In compacted cases, the reactions can only occur via diffusion if the saturation phase is not included. Thus, compacted bentonite experiments are needed, but there are only a few compacted bentonite experiments related to pH since the experiments are slow and analysing the samples is hard. Almost always, the compositions of pore waters given for highly compacted bentonites are calculated values and simplifications since reliable water samples from compacted material are very hard to obtain even from squeezing at high pressures (the high pressure affects the water chemistry).

The pH behaviour subject for compacted bentonites has been earlier studied only on a few occasions [67,78]. Wersin in 2003 [67] modelled the experimental results of Muurinen & Lehikoinen, 1999 [79], who studied the pore water changes in different ionic strengths and solid/liquid ratios in compacted bentonite. Wersin found that the reactions controlling the pore water chemistry were mainly calcite/gypsum equilibrium, surface complexation reactions and Na/Ca ion exchange. Wersin also suggested that diffusion experiments for compacted bentonite are needed to study the pH dependent surface reactions concentrating on surface exchange and sorption reactions [67].

In the paper by Pulkkanen et al. 2012 [78], the pH was directly measured from compacted samples inside bentonite using Iridium-Oxide (IrOx) pH electrodes in argon atmosphere [68,75]. The experimental device used in the experiment is presented in Fig. 4.2. The bentonite was compacted to a dry density of 1.5 g/cm^3 (mass was approx. 8.7g) and the solution used in the external cells was 30mL of 0.3M NaCl and 0.1M acetic acid adjusted to pH 5 with NaOH. The cells were in

<contact with the bentonite through sinters. The electrodes were in two different positions 5mm and 9.2mm from solution-bentonite interface. The results can be seen in Figure 4.3.

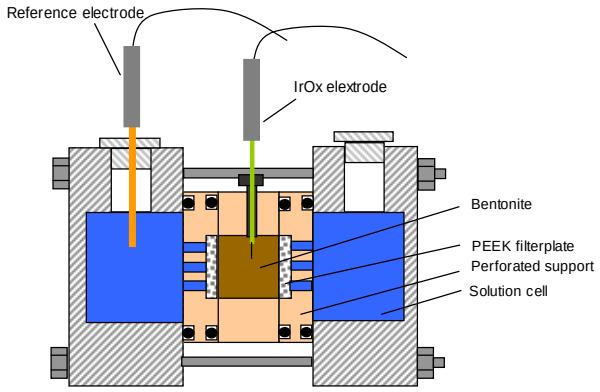

Figure 4.2. Schematic representation of the diffusive cell in the experiment. [78]

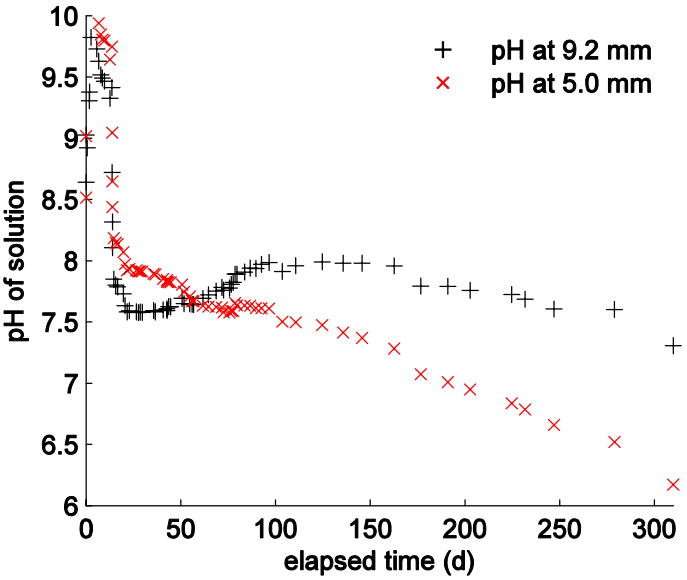

Figure 4.3. The pH values measured from the 2 different positions. The distance is from the solution-bentonite interface. [78]

The peaks at the start (Fig 4.3) are caused by the low concentration of ions in the pore water (deionized water at start), and thus the potential difference is too low to be measured before the system equilibrates with argon atmosphere and the external solution. These results indicate that the pH of the pore water of bentonite

can be directly measured from the inside of the compacted sample. However, the ionic strength must be high enough (for the potential difference) and calibration of the electrodes must be done before and after the experiment, and there is always a risk that the electrodes might break, which was the reason to terminate these experiments and final calibration could not be done. The results again showed the great buffering capacity of bentonite.

In 2013 Itälä et al. [IV] continued the work from Pulkkanen et al. 2012 [78] and studied the bentonite pH behaviour by using CO_2(g) atmosphere in three different partial pressures and in 25^{o}C to see the effects on the pH of compacted bentonite samples. The bentonite used here was Wyoming MX-80 bentonite which includes some small amounts of other minerals [80] (quartz, calcite, feldspar etc.) and mainly montmorillonite mineral. The experimental setup [IV] consisted of a hermetic box, diffusion cell, pH electrodes, cylindrical bentonite sample (dry density 1.57g/cm^3 and mass 9.86g) and external water reservoirs of 50mL each. The cell was similar to the one presented in Figure 4.2. The solution inside the cells was 0.1M NaCl. The samples were saturated with deionized water before the experiment. The experiment duration was 160 days and was modelled using Geochemist's Workbench version 8.

The results of Itälä et al. 2013 [IV] indicate that only the surface protonation sites buffer the pH changes in a compacted bentonite system since the water volume inside the bentonite is minimal compared to the number of surface complexation sites. In addition, the dissolving calcium minerals increase the calcium content in the exchanger, even though the solution is purely NaCl. From the results, it could be seen that, in the conditions where the water/bentonite ratio (liquid/solid) is high 10:1, the bentonite buffering capacity can only last a few tens of days and is insufficient for a longer period. The buffering capacity is approximately 0.3 pH units/10g of bentonite.

The bentonite buffering capacity has been studied widely. However, most studies have been conducted on low solid/liquid (S/L) ratios and in suspensions, and only a few studies have mainly focused on buffering capacity for highly compacted bentonite. More studies are still needed to confirm the amount of buffering capacity bentonite can maintain in under final repository conditions, where the pH is always over neutral conditions and can go higher if, for example, a high pH plume from cement comes into contact with the bentonite.

4.2 Cation exchange

Cation-exchange and surface complexation have been studied widely on clays, especially for MX-80. Cation exchange (Ca^{2+}, Mg^{2+}, Na^{+} and K^{+}) is closely related to diffusion since in compacted bentonite the mass transfers occurs via diffusion after saturation. Most of these studies have been conducted on low solid/liquid mass ratio (e.g. 1/100) water solutions and at room temperature.

The cation exchange in MX-80 is related to montmorillonite mineral (see e.g. [81,82]). The cation exchange with the external water occurs with diffusion through the pores in bentonite.

The most used cation exchange and surface complexation selectivity values in modelling for MX-80 are from Bradbury and Baeyens 2002 [57]. These selectivity coefficients were calculated for compacted MX-80 at room temperature and used the Gaines-Thomas [83] formulation for cation exchange. In this thesis, only the Gaines-Thomas formulation is used. The other common formulations are the Vanselow [84] and Gapon [85] formulations. The Gaines-Thomas formulation is given below [III]:

$$K_{ex}^{i \to j} = \frac{E_{C_j}}{E_{C_i}} \frac{\left\{ C_i^{z_i +} \right\}^{1/z_i}}{\left\{ C_j^{z_j +} \right\}^{1/z_j}} \quad (2)$$

where E_{Ci} denotes the fractional contribution of cation C_i to the total number of moles of charge of exchangeable cations. z_i is the charge of the cation. K is the selectivity coefficient with regard to the cations i and j. The brackets denote the activities of cations C_i and C_j in aqueous solution. These selectivity coefficients are not thermodynamic equilibrium constants and may change depending on the solution concentration/activities and other conditions (e.g. interfering ions/complexes, diameter of ions).

4.2.1 Effect of temperature on cation-exchange selectivity

The effect of temperature on the clay cation-exchange selectivities has been little studied. However, similar studies have been conducted at room temperature for compacted bentonite (see e.g. [57]) and for non-compacted bentonite [86–93]. However, none of these studies took into consideration the effect of changing temperature on the cation-exchange selectivities of bentonite.

In the paper by Itälä and Muurinen 2012 [III] this question was studied, and the Na/Ca cation-exchange selectivities were calculated from experiments at three different temperatures (25°C, 50°C and 75°C). Five different ratios of $NaClO_4/Ca(ClO_4)_2$ with 0.1 cation normality solution (30ml, pH 6.2) were used to react with 1 gram of purified sodium bentonite (MX-80) powder. Perchlorate solution was chosen to be used as a solution to avoid the forming of complexes with cations [82,87]. The clay and solution were separated using a syringe after five days of shaking.

The cations in solution were analysed using ICP-AES. The CEC was determined using the Cu-Trien method [94]. The results can be seen in Figure 4.4 [III] compared to the results of Sposito, 1983 [87] in 25°C and also modelled by PHREEQC. There are only small differences in the cation-exchange selectivities in this temperature range. In 75 °C there is a slightly higher tendency to take calcium inside. The Gaines-Thomas selectivity varied from 4.9 to 6.8, which is in agreement with earlier studies where it has been 2-11 [87,95,96] for Na-montmorillonite.

However, to ascertain the temperature effect on the pH of bentonite repeat experiments would be needed for compacted purified bentonite as well as for non-purified bentonite to see the effect of temperature and to adjust the ionic strength,

which might also affect the exchange selectivities indirectly through the activities of ions. Then again, in non-purified bentonite impurities like gypsum or calcite minerals might affect the cation behaviour by releasing more calcium ions to the solution. Nevertheless, this is only speculation and would need to be studied in higher temperatures as well in laboratory conditions.

Other studies have also shown that the calcium-sodium exchange is a key process affecting bentonite pore water in the KBS-3 concept since less potassium and magnesium are normally present in groundwater and also in exchange sites [79,97,98].

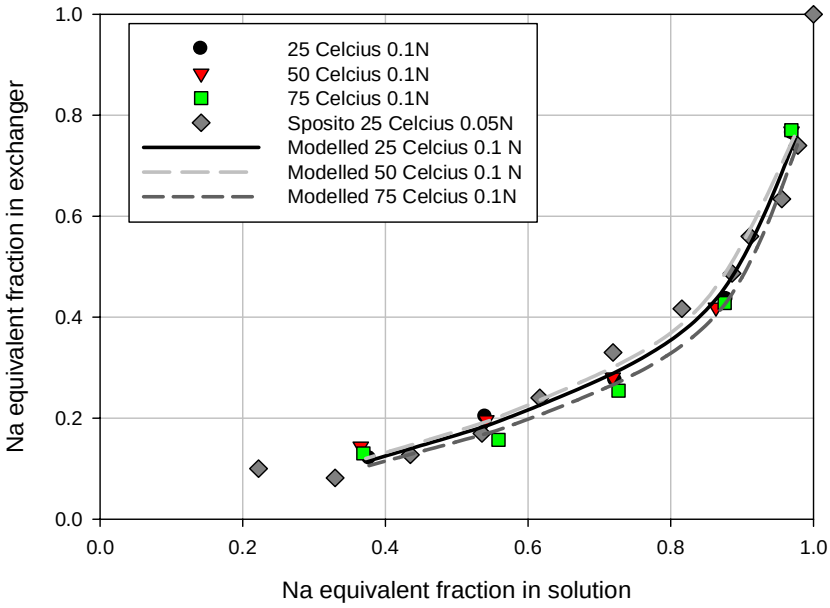

Figure 4.4. Na^+ exchange isotherm on Na-montmorillonite in perchlorate background in Na-Ca solution [III].

5. Thermo-hydro-chemical modelling of bentonite

While the bentonite barrier in the final repository of spent nuclear fuel goes through multiple phenomena during thousands of years, it should protect the copper canister for as long as possible. These phenomena include iron/copper interaction from the corrosion of the canister, interaction with changing groundwater, variating temperature, saturation, swelling, interaction with cement, and dissolution/precipitation of minerals, climate change affecting the ground water etc.

There are tens of parameters affecting bentonite behaviour, which need to be coupled to each other. The complexity of these couplings makes the modelling very challenging. Thus, simplifications are often made in models. These simplifications are most often tested in simplified laboratory experiments where the conditions are manageable, and it is easier to see if the predictions are correct. These data compiled from laboratory tests are then applied to models.

5.1 Modelling software

Three different modelling software were used for modelling in this thesis. All of them are capable of THC calculations. The biggest difference between these programs is the capability to calculate different types of geometries. Water transport in all these programs can occur through diffusion/dispersion/advection. All of these programs below are based on the law of mass action (LMA), whereas there are programs also based on the Gibbs energy minimization method (GEM). One major difference between these programs is that the old version 1.2 of TOUGHREACT used in this thesis did not include surface complexation.

5.1.1 PHREEQC

PHREEQC [99] is a computer program written by C and C++ for geochemical modelling in batch and 1-D geometries. It is capable of speciation and saturation-index calculations, transport calculations with reversible and irreversible reactions. These reactions include mineral dissolution/precipitation, aqueous, gas, solid-solutions, surface complexation, ion exchange through equilibrium and kinetics in different temperatures and pressures. It also includes different activity models for low and high salinity waters. This modelling program was used in the batch experiments of this thesis [III, VI].

5.1.2 Geochemist's Workbench

Geochemist's Workbench [100] is a geochemical modelling program capable of calculating multiple chemical reactions. It includes the same abilities as PHREEQC, and it can solve different kinds of diagrams (piper, ternary, durow, etc.), but can be also used as a numerical simulation solver in batch, 1-D and 2-D geometries to

solve reaction paths, equilibrium and kinetical problems. In addition, it includes microbial growth calculations and flow/well calculations. This modelling program was used to model the pH experiments in paper [IV].

5.1.3 TOUGHREACT

The TOUGH family of codes is being developed in Lawrence Berkeley National Laboratory (LBNL) and includes many modules including TOUGHREACT [101] which is a numerical simulation program for non-isothermal flows of multiphase fluids in 1-D, 2-D and 3-D porous and fractured media. It is developed on TOUGH2 multiphase flow code. It includes changing porosity, permeability, saturation and flow properties, as well as all the same chemical phenomena as PHREEQC. However, the old version TOUGHREACT v 1.2 used in the papers of this thesis did not include surface complexation reactions. The code and the used equation state modules are better described in Itälä, 2009 [69]. This software was used in papers [I-II, V]

5.2 Modelling of laboratory experiments

Most laboratory experiments can be modelled as a batch model or simplified 1-D model. However, the data needed for models can be a lot more extensive than the information studied in the experiment. For example, in simple batch model calculations for bentonite ion exchange, surface complexation, and mineral structure, etc. related data is needed. Luckily, most of the basic THC-data for MX-80 has already been studied over the years, although some of these parameters change with every batch of clay and need to be studied from every batch separately. These parameters are, for example, mineral composition, cation-exchange composition and CEC. In this chapter, modelling of simple batch and 1-D experiments is discussed.

Batch calculations have been made for as long as models have existed, with the first codes made as early as 1965 [102]. One of the first simple batch calculation software programs was EQ3/6, which was developed in the mid-1970s by Thomas Wolery, and was able to calculate simple aqueous solutions and equilibrium [103]. It was later further developed as one of the most thermodynamically accurate programs. This software was the starting point, for example, for the other codes mentioned above and was the first geochemical program the author used.

5.2.1 Modelling of pH behaviour of bentonite

The pH of bentonite is closely related to external water interacting with the bentonite. There are other factors, which also affect this behaviour, like minerals, cation exchange and surface complexation. The buffering capacity of bentonite is partly related to all of these (e.g. calcite dissolution), but mainly it is the effect of the hydroxyl groups at the edge sites of the montmorillonite mineral on bentonite. These

hydroxyl groups can exchange with the pore water and affect the bentonite pH (see e.g. Fig. 3.4 and [73,76]). The parameters to model the surface exchange can be measured and fitted to known experimental results. The parameters used for MX-80 and other bentonites in most studies are taken from Bradbury and Baeyens (2002) [57]. The minerals affecting the pH are mostly carbonates like calcite and rapidly dissolving minerals like gypsum. Thus, the original amounts of these minerals need to be known before modelling. In addition, the surface complexation and cation-exchange parameters need to be known, since the cation exchange and surface complexation behaviour might affect the solubility of these minerals and pH. In the paper by Pulkkanen et al. 2012, the pH behaviour of purified montmorillonite was studied using acetate buffer [78]. The modelling in this paper was performed by the author of this thesis and the results fitted accurately. From the results, it could be seen that even the purified montmorillonite still contains some calcite mineral. The results also showed how well one gram of montmorillonite can buffer against the lower pH 5 solution. A 60 millilitre solution was needed to get the pore water pH near 5 for 1g of montmorillonite. In this modelling exercise, besides the solution composition, a small amount of calcite was included in the model together with the surface complexation sites. In addition, the cation-exchange effects were tested but found negligible. The results are shown in Figure 4.1. [78]

The modelling of the pH behaviour of non-purified bentonite was continued in the article by Itälä et al. 2013 [IV]. In this article the pH experiments in a diffusion cell measured with Iridium-Oxide electrodes was continued from the paper by Pulkkanen et al. 2012 [78]. In these experiments, the CO_2(g) atmosphere was adjusted. The software used in this modelling exercise was Geochemist's Workbench (GWB). The results were not as accurate as those obtained previously in the batch experiments and the model was designed as a 1-D diffusion model. It was noticed that the GWB v. 8 had problems of its own. While modelling the pH, the minerals included in the model were equilibrated with the bentonite. The experiment had water cells on both sides of the bentonite and both boundaries were modelled with Dirichlet's boundary condition. The GWB v.8, however, failed to recognize that the mineral phases were only set to certain cells and equilibrated them to water cells as well at initial conditions, which affected the results. In addition, the surface complexation and ion-exchange sites were set only to bentonite but were also included in the water cells by the software. The results are shown below in Figures 5.1 and 5.2., from the partial pressures of CO_2(g) varying from 0.3 to 1. GWB does not include the option to vary the diffusion coefficient or tortuosities for different ions, and therefore the same diffusion coefficient was used, which also explains some of the model differences.

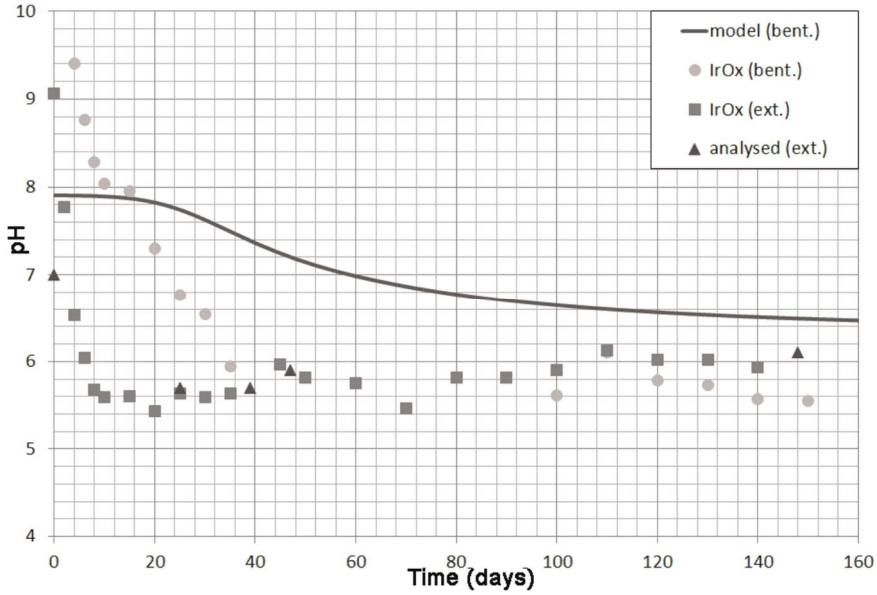

Figure 5.1. Results of test case with a CO_2 partial pressure of 0.3.

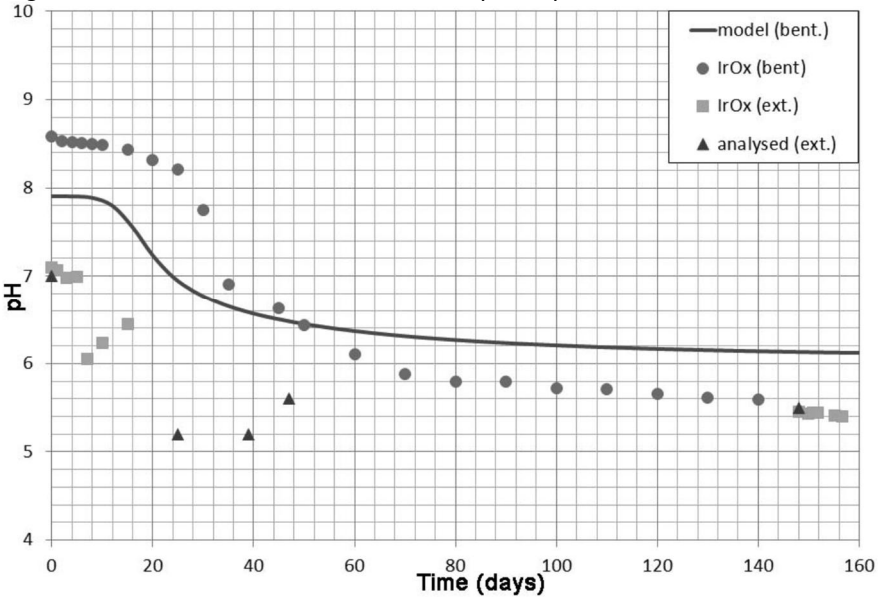

Figure 5.2. Results of test case with a CO_2 partial pressure of 1.

5.3 Structural modelling of bentonite

Most of the transport models and PA models known to the author used to model chemical behaviour of porous materials (bentonite in this case), assume that all of the porosity is available for the so-called pore water (e.g. TOUGHREACT, GWB etc.). However, bentonite has two different kinds of porous spaces (see Section 3.3.2) and could be considered more as a very dense solution of colloidal particles [V]. The two spaces are interlamellar space and free porosity near the mineral surfaces or between the clay stacks. Even then, the spaces between clay stacks can behave differently for anions and cations since the clay stacks are negatively charged. Bentonite differs from typical porous materials as the effective cation diffusivity can be quite high and anion diffusivity quite low. Anions seem to occupy much less porosity than cations, which makes bentonite transport modelling more complicated. In addition, the available free pore water can affect the cation exchange and surface complexation behaviour. The dominant transport mode inside the clays, is diffusion affected by concentration gradients, electrical interactions, accessible porosities, tortuosity and retardations. Data from diffusion experiments can be fitted with transport models. The diffusion follows Fick's law:

$$\frac{\partial}{\partial t}\left(c_i + c_{\mathrm{s},i}\,\frac{\rho_{\mathrm{b}}}{\phi_{\mathrm{a},i}} \right) = D_{\mathrm{e},i}\,\frac{\partial^2 c_i}{\partial x^2} \tag{3}$$

where t is time (s), c_i is the concentration in accessible pore water (mol/L), $c_{s,i}$ is concentration in solid (mol/kg), ρ_b is bulk density of bentonite (kg/L), $\phi_{a,i}$ is accessible porosity, $D_{e,i}$ is effective diffusion coefficient (m^2/s) and i is the i:th component.

5.3.1 Developed model

In the paper by Itälä et al. 2014 [V] a conceptual approach was introduced to handle the porosity issue and the different kinds of waters inside the bentonite. This was continuation to the work by Olin [104,105]. The model was then calculated with two different numerical platforms NUMERRIN [106] and COMSOL and compared to the original TOUGHREACT model.

Compacted bentonite consists of solid (montmorillonite and secondary minerals), water and possibly air in partially saturated cases. The concept of bentonite structure is described in Figure 5.1.

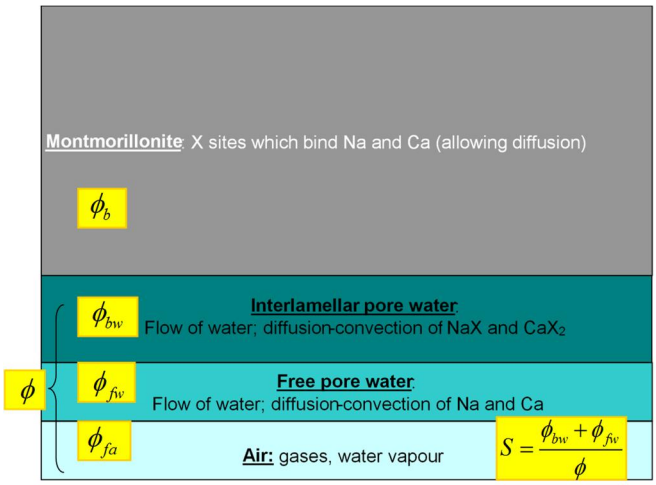

Figure 5.1. Concept of montmorillonite pore structure [V]

The total mass of bentonite in volume *V* can be expressed as (air density is very low compared to water and bentonite density and as such equation (4) can be simplified):

$$\begin{aligned} M &= M_b + M_{bw} + M_{fw} + M_{fa} \\ &\cong \left[\rho_b \phi_b + \rho_w \phi_{bw} + \rho_w \frac{\chi}{1-\chi} \phi_{bw} \right], \end{aligned} \tag{4}$$

and the density of bentonite can be expressed as:

$$\rho \cong \rho_b \phi_b + \frac{\rho_w \phi_{bw}}{1-\chi}, \tag{5}$$

where

M_i = mass of dry bentonite (kg), b; water bound on bentonite, bw; free water, fw; or free air, fa

ρ_b = specific dry density of bentonite (kg/L)

ρ_w = density of water (assumed the same on both bound and free water) (kg/L) ϕ_i = volume fraction of component i

χ = ratio of volume fractions of free and total water volume, where $\chi = \phi_{fw} / (\phi_{bw} + \phi_{fw})$

For example, the sodium ion content in cation exchanger (CEC as mol per kilogram bentonite [mol/kg]) per bound water volume can be expressed as:

$$c_{NaX} = \frac{M_{NaX}}{\phi_{bw} V} = \frac{\phi_b}{\phi_{bw}} CEC \rho_b \beta_{NaX} \tag{6}$$

If we consider a simple model with only two sodium isotopes (^{s}Na and ^{r}Na) and two chloride isotopes (^{s}Cl and ^{r}Cl) with cation-exchange site (X), then sodium can form complexes with X according to the reaction:

$$^{s}\mathrm{NaX} + {}^{r}\mathrm{Na}^{+} \underset{k}{\overset{k}{\rightleftharpoons}} {}^{r}\mathrm{NaX} + {}^{s}\mathrm{Na}^{+} \tag{7}$$

where k is the kinetic constant, upper-case s stands for stable and upper-case r stands for radioactive. At equilibrium we get:

$$\frac{\beta_{\mathrm{rNaX}}}{\beta_{\mathrm{sNaX}}} = \frac{c_{\mathrm{rNa}}}{c_{\mathrm{sNa}}} \tag{8}$$

where c_{iNa} is the concentration (mol/m^3) and β_i the equivalent fraction of cation isotope *i*. For the purpose of implementation of our own code, concentrations are used instead of equivalent fractions of cation-exchange sites. The total mass of each element must be conserved in bound and free water phases and the charge balance must be kept:

$$\begin{aligned} c_{\mathrm{X}} &= c_{\mathrm{sNaX}} + c_{\mathrm{rNaX}} \\ c_{\mathrm{sCl}} + c_{\mathrm{rCl}} &= c_{\mathrm{sNa}} + c_{\mathrm{rNa}} \end{aligned} \tag{9}$$

The total reaction rate can be written:

$$r = r_{\mathrm{f}} - r_{\mathrm{r}} = k_{\mathrm{c}} \left(c_{\mathrm{sNaX}} c_{\mathrm{rNa}} - c_{\mathrm{rNaX}} c_{\mathrm{sNa}} \right) \tag{10}$$

Free and bound water diffusion constants have usually been named pore (D_{p}) and surface diffusion D_{s} respectively[107]. The transport equations for this simple system can be written as:

$$
\begin{aligned}
\partial_t c_{\mathrm{sCl}} &= D_{\mathrm{p}} \nabla^2 c_{\mathrm{sCl}} \\
\partial_t c_{\mathrm{rCl}} &= D_{\mathrm{p}} \nabla^2 c_{\mathrm{rCl}} - \lambda_{\mathrm{Cl}} c_{\mathrm{rCl}} \\
\partial_t c_{\mathrm{sNa}} &= D_{\mathrm{p}} \nabla^2 c_{\mathrm{rNa}} + \phi_{\mathrm{fw}} r \\
\partial_t c_{\mathrm{sNaX}} &= D_{\mathrm{s}} \nabla^2 c_{\mathrm{sNaX}} - \frac{\phi_{\mathrm{fw}}}{\phi_{\mathrm{bw}}} r \\
\partial_t c_{\mathrm{rNa}} &= D_{\mathrm{p}} \nabla^2 c_{\mathrm{rNa}} - r - \lambda_{\mathrm{Na}} c_{\mathrm{rNa}} \\
\partial_t c_{\mathrm{rNaX}} &= D_{\mathrm{s}} \nabla^2 c_{\mathrm{rNaX}} + \frac{\phi_{\mathrm{fw}}}{\phi_{\mathrm{bw}}} \left[r - \lambda_{\mathrm{Na}} c_{\mathrm{rNaX}} \right]
\end{aligned}
\tag{11}
$$

where λ_i (i=Cl,Na) is the linear reaction rate, e.g. radioactive decay.

The difference between TOUGHREACT [101] compared to COMSOL and NUMERRIN is that the latter ones can use surface diffusion and exchange kinetics, whereas TOUGHRECT applies traditional porous media diffusion and assumes exchange equilibrium (uses K_d value which can be defined as concentration in solid/concentration in water).

In equilibrium state the effective diffusivity for traditional and surface diffusion can be written as [105]:

$$
\begin{aligned}
D_{\mathrm{e}}^{\mathrm{t}} &= \phi^{\mathrm{t}} D_{\mathrm{p}}^{\mathrm{t}} \\
D_{\mathrm{e}}^{\mathrm{s}} &= \phi^{s} D_{\mathrm{p}}^{s} + \left(1 - \phi^{s}\right) K_{\mathrm{d}}^{\mathrm{s}} \rho_{\mathrm{d}} D_{\mathrm{s}}
\end{aligned}
\tag{12}
$$

where t stands for traditional and s for surface diffusion, and for apparent diffusion coefficients we can write

$$
\begin{aligned}
D_{\mathrm{a}}^{\mathrm{t}} &= \frac{D_{\mathrm{e}}^{\mathrm{t}}}{\alpha^{\mathrm{t}}} = \frac{\phi^{\mathrm{t}} D_{\mathrm{p}}^{\mathrm{t}}}{\phi^{\mathrm{t}} + \left(1 - \phi^{\mathrm{t}}\right) K_{\mathrm{d}}^{\mathrm{t}} \rho_{\mathrm{d}}} \\
D_{\mathrm{a}}^{\mathrm{s}} &= \frac{D_{\mathrm{e}}^{\mathrm{s}}}{\alpha^{\mathrm{s}}} = \frac{\phi^{s} D_{\mathrm{p}}^{s} + \left(1 - \phi^{s}\right) K_{\mathrm{d}}^{\mathrm{s}} \rho_{\mathrm{d}} D_{\mathrm{s}}}{\phi^{\mathrm{s}} + \left(1 - \phi^{\mathrm{s}}\right) K_{\mathrm{d}}^{\mathrm{s}} \rho_{\mathrm{d}}}
\end{aligned}
\tag{13}
$$

where α is capacity factor and is written as $\alpha = \phi + (1-\phi) K_d \rho$.

While comparing the results of these two different models, effective traditional and surface diffusivity as well as apparent traditional and surface diffusivity should have equal values and the parameter values which can be applied to a traditional model by surface diffusion parameters can be written:

$$D_{\mathrm{p}}^{\mathrm{t}} = \chi D_{\mathrm{p}}^{\mathrm{s}} + \left(\frac{1}{\phi} - \chi\right) K_{\mathrm{d}}^{\mathrm{s}} \rho_{\mathrm{d}} D_{\mathrm{s}}$$
$$K_{\mathrm{d}}^{\mathrm{t}} = \frac{(\chi - 1)\phi + (1 - \chi\phi) K_{\mathrm{d}}^{\mathrm{s}} \rho_{\mathrm{d}}}{(1 - \phi)\rho_{\mathrm{d}}} \tag{14}$$

A very simple column test case was studied in paper [V]. In this test case a column model with open and closed boundary was studied. In TOUGHREACT traditional pore diffusion was used and in COMSOL and NUMERRIN surface diffusion with kinetics. To be able to compare the results, high kinetical rates were used for the latter models and it was seen that the results agree very well and our model works. The test case results can be seen in Figure 5.2.

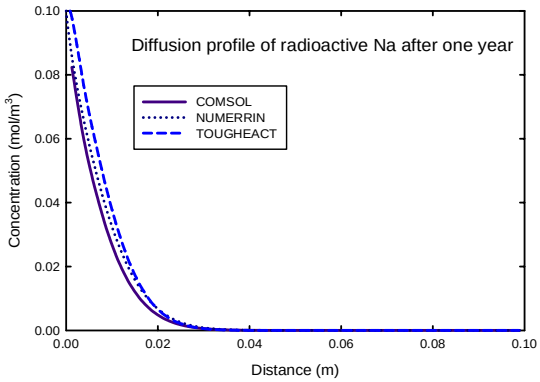

Figure 5.2. Comparison between models [V]

5.4 Squeezing experiments modelled with PHREEQC

In publication [VI] the author used PHREEQC to model experiments in anoxic laboratory conditions. In these squeezing experiments a methodology for studying the composition of non-interlamellar pore water by combining squeezing, chemical analyses, microstructure measurements and modelling was described. The squeezing tests were conducted in four different pressures ranging from 60 MPa to 120 MPa with four parallel samples. The origin of the pore water was measured using SAXS and NMR to determine which part of the water in the compacted sample was interlamellar (IL) and non-interlamellar water. The model was used to determine what happens inside bentonite during squeezing. The pore water yield was between 32-48% from the initial amount of water in the bentonite, depending on the squeezing pressure. About 35% of the water was found to be from interlamellar pores and the ratio seemed to remain constant in different pressures.

The material used was MX-80 from the Alternative Buffer Material (ABM) test. In the experiment, 11 different clays were used which interacted with each other at a heater temperature of 130°C for about 7 years. The MX-80 sample was altered by temperature gradient and Ca-rich solution, which changed the dominant cation in

the sample [VI]. The squeezed sample was cylindrical, 20mm by diameter and the same height, and the squeezing was done under anoxic conditions. More information about the material, sampling and methods can be found in publication [VI] and about the ABM experiment in Svensson et al. (2011) [108].

A simplified conceptual model was created using PHREEQC. The pore water was divided into two types, IL and non-IL waters. The exclusion effect was omitted from the geochemical model. Assumptions were made that cations stay in the interlamellar space during squeezing and the deionized water in the IL space will mix with the non-IL pore water. The model was designed as a batch model using PHREEQC geochemical code [99]. Due to squeezing and the deformation of bentonite the normal 1-D diffusion model with PHREEQC was thought to be irrelevant in this case and the experiment was modelled as a batch model.

In the first phase the minerals, cation exchange and surface complexation sites were equilibrated with assumed pore water of bentonite and later it was mixed with the assumed deionized IL water in the ratio determined by SAXS. In the third phase, the mixed water was equilibrated with bentonite to model the squeezed pore water composition. The model was designed as a target calculation where the composition of the mixed water in the third phase was iterated to respond to the squeezed pore water. More about the used parameters can been found in Järvinen et al. 2016 [VI].

Using the model, the complicated phenomena occurring inside the bentonite was simplified quite successfully. Of course, this model did not take into account that during squeezing it is possible that the size of the free pores becomes smaller, whereas the amount of diffuse double layer water increases compared to free pore water in which chloride ions, for example, reside. This can effectively mean that almost all the chloride is pushed away from the bentonite and the concentration of anions and cations in squeezed water becomes higher. The assumed non-IL water/pore water could not be measured and was iterated backwards so that the squeezed water could be modelled. Approximately 40% of the squeezed water (based on SAXS measurements) came from the interlamellar space and this was also used in the model. The results from some anions, cations and ionic strength (IS) can be seen below in Fig 5.3 and Fig. 5.4.

The original modelling results [VI] matched well, except for carbonate and sulphate which were later corrected for this thesis. While mixing interlamellar water with non-interlamellar water, the original model had an excess of gypsum left in equilibrium with the mixed water, which seemed not to happen in the experiment. During the squeezing, the non-IL pores became smaller and the highly concentrated non-IL water was already saturated by gypsum, and while mixing the anion exclusion and smaller pore space seem to prevent dissolution of gypsum from the bentonite. The non-IL water also might come out from different pores than the IL-water. This was corrected by omitting the gypsum equilibrium at the mixing phase and the results matched very well. No big changes in cation exchanger were observed. The main observation was, according to our modelling, that the initial pore water must be much more concentrated compared to squeezed water when there is very mild water mixing with pore water from the IL space. Also, in the

corrected model the Pitzer database was used instead of the Thermoddem database. Ionic strength was high which makes the Pitzer database more suitable.

The modelling could have been designed as a diffusion 1-D model but then again the mechanical squeezing would have been omitted even though PHREEQC supports multidiffusional models with different diffusion coefficients for species as well as DDL and anion exclusion [109,110]. In this case, this simplified model worked well.

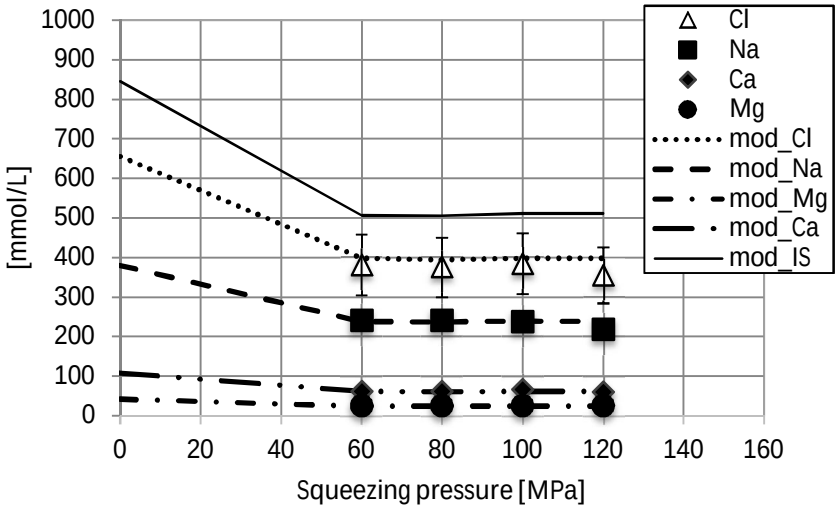

Figure 5.3. Initial non-IL water composition according to modelling (0 MPa), and squeezed pore water (60, 80, 100, 120 MPa) composition according to modelling and experimental results for the main ions. Lines indicate modelling and dots indicate experimental results [VI].

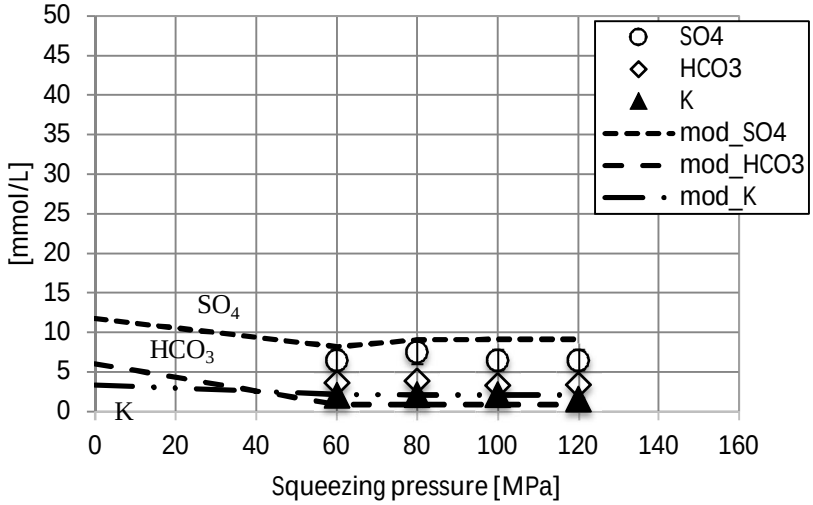

Figure 5.4. Initial non-IL water composition according to modelling (0 MPa), and squeezed (60, 80, 100, 120 MPa) pore water composition according to modelling

and experimental results for the minor ions. Lines indicate modelling and dots indicate experimental results [VI].

5.5 Near field modelling

Determining the long-term stability of bentonite buffer in final repository conditions must be based on numerical modelling, since experimental testing would require millennia to acquire reliable results. These models can then be used in PA studies. Near field modelling of the final repository of spent nuclear fuel has been a research topic for almost two decades (see e.g. [97,111–118] and it has been under continuous development. Combinations of thermo-hydro-mechanical (THM) and thermo-hydro-chemical (THC) models (see e.g. [119]) are common, but combinations of THMC are not or are made only for very narrow applications. In this thesis, the work conducted is only THC modelling excluding mechanical phenomena (e.g. swelling) occurring inside bentonite. Publications [I, II] both model the same LOT-A2 experiment but the latter expands the model to semi 3-D coordinates (cylindrical 2-D).

The THC models concentrate on modelling the temperature effects on the bentonite buffer in a spent nuclear fuel repository during the thermal phase. The model introduced in this thesis is a simplified version of the complex phenomena occurring in the near field of the final repository. In order to make the modelling more realistic, a case called Long-term buffer test adverse 2 (LOT-A2) at the Äspö Hard Rock laboratory (HRL) in Sweden was used as a reference case.

5.5.1 LOT-A2 test

The LOT-A2 test was conducted in adverse temperature conditions (maximum temperature 130 ^{o}C) exposed to field conditions in HRL at a depth of 450m [26]. Adverse in this case means higher than normal temperature and temperature gradient, which accelerate alteration processes, when the normal temperature limit now is set to 100^{o}C in the spent fuel final repository. The test lasted approximately 6 years. The test parcel dimensions were smaller compared to the KBS-3V deposition hole in order to shorten the saturation period, to get higher temperature gradient and ease the lifting of the parcel. More details about the test parcel and the test results can be found in the report by Karnland et al. 2009 [26], Muurinen 2006 [120] and in [I,II].

5.5.2 Modelling concept

The aim of the studies in papers [I] and [II] was to investigate the THC phenomena affecting the bentonite in a deposition hole intersected by a fracture, since the long-term safety of the final repository might partly depend on the composition of the bentonite after the thermal phase. The thermal phase will last a few thousand years, but most of the phenomena is assumed to occur during the first thousand years as the temperature gradient is highest [121].

In the models presented in papers [I] and [II], it is assumed that three phases (solid, liquid and gas) are present in the porous media. Montmorillonite is assumed an insoluble mineral, but it is able to absorb ions and exchange them with solution (Old version of TOUGHREACT did not support surface complexation back then). Precipitated minerals are part of the solid phase. The gas phase is water vapour and air, while the liquid phase consists of dissolved species. Equilibrium is assumed for chemical reactions except kinetics for minerals. The copper canister and rock matrix are inert, except the canister is the heat source (set to produce heat with constant heat flux which keeps the temperature profile the exact same as in the experiment). Mineral precipitation/dissolution can affect the porosity and permeability of the matrix. Host rock and fracture were set to be fully saturated at all times (no capillary pressure), and the bentonite is partially saturated in the beginning. The models were created using TOUGHREACT v.1.0 modelling software Equation of state 3 (EOS) module.

In the first paper [I], the copper canister generating heat was surrounded by bentonite and a water-conducting fracture. The model was made from the fracture position so that the chemical changes were highest. This is the most conservative version and in the real case, the changes would be lower on other positions of the bentonite barrier.

In the second paper [II], the model was axisymmetric with the symmetry axis in the middle of the canister and thus only half the canister was modelled. The grid had 962 cells with a calculation time of 10 hours of the model. The parameters used were taken from known sources [I, II] and not changed to fix the results to get closer to experimental data.

5.5.3 Results

In the models, no big chemical changes occurred inside the bentonite apart from anhydrite precipitation near the heater, which can slightly affect porosity and the amount of calcite and sulphate near the canister surface. Nothing compromising the functionality of the bentonite buffer/montmorillonite was found. The porosity changes were minimal, and the saturation took place in approximately one year as in the experiment. Small amounts of calcite dissolved near the heater as well. The kinetics of quartz and K-feldspar are slow and would need a lot longer time to dissolve/precipitate than the 10 year period simulated, and temperature did not have much effect on them.

The results in the first paper [I] on some parts of the chemical species were slightly higher than in the experiments like sodium and chloride, which was expected since the model described the fracture position. It was also concluded that more of the water during saturation was transported as vapour in the experiment than in the model. The cation-exchange results differ from the experimental results probably due to the different anhydrite profile and because of the fracture position [I]. In the experiment, not many changes were observed in cation exchanger [26].

In paper [II], the results were presented from two positions from the inlet position (fracture) at the bottom of the canister and 1.1 m above it from the middle of the

heater. The inlet position results were in agreement with paper [I]. The saturation took place in 200 days next to fracture and over 93% saturation was reached in 1.5 years at 1.1 m position, which was in agreement with the experimental results. Some difference in mineral behaviour was noticed in different locations of the model. However, anhydrite precipitation near the heater was the main reaction. Calcium and chloride results in 1.1 m position were in better agreement with the experimental result [120] than in paper [I], which is explained with less water entering further away from the fracture.

Overall, no dramatic chemical changes were observed, which could affect the performance of the bentonite barrier. More detailed explanations about the results can be found in publications I and II. Saturation and anhydrite precipitation near the heater can be seen in Figure 5.5.

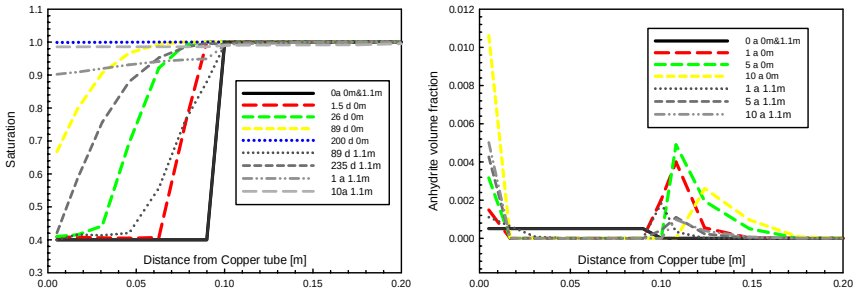

Figure 5.5. Saturation on the left and Anhydrite volume fraction on the right as a function of distance from the heater at various times. Note that anhydrite seems to precipitate also in rock matrix.

5.5.4 Model limitations

The simplified models had a few important limitations. The bentonite was assumed to be fully swollen in the beginning of the model. Montmorillonite was set as insoluble mineral. The models did not include different kinds of water inside the bentonite. Nevertheless, all porosity was assumed to be available for the pore water. In the 1-D version, sharper gradients were observed than in the experiment and the model did not properly take into account the water evaporation/condensation process near the heater, which was assumed to occur in the experiment due to the behaviour of some salts [26]. Surface complexation was excluded from this version of TOUGHREACT. Only one diffusion coefficient was used for all ions. The material parameters were constant and the temperature effects on these were excluded. Van Genuchten parameters for capillary pressure/saturation were not best for this case, which was proven later by Sena et al. 2014 [122,123] who modelled the same case with TOUGHREACT and used Leverett's function for capillary pressure instead. The initial conditions of the bentonite also might differ from the experimental, while in the model quite dilute solution is used to get the exchanger compositions correct in the beginning, which is not exactly the case in the real experiment.

6. Discussions/conclusions

The current situation in understanding of chemical behaviour of bentonite is that it is still under dispute how the microstructure of bentonite actually works. However, the most common consensus is that there are three different kinds of water, which should all be taken into account in modelling. This view has become stronger in recent years. The main transport mechanism of water and other components in compacted bentonite is diffusion after the initial saturation period, while the water through fractures moves by advection. If there is no erosion in the bentonite, diffusion is the mechanism that moves the chemical species.

Chemical reactions coupled with temperature, water flow, precipitation/dissolution of minerals, swelling and surface exchange reaction in bentonite form a complex system, which is not easy to understand or to model. However, while modelling these reactions, the modeller must also have a thorough understanding of these phenomena and often needs to validate the models as well. High heat generated near the spent nuclear fuel canister can induce local equilibria between water vapour and liquid water. This can also affect the precipitation/dissolution of minerals, since chemical species mostly move with liquid water. Taking into account all these phenomena is not easy and usually simplified models are needed, especially if the model grid is complicated, which might unreasonably lengthen the calculation times.

Chemical modelling can be used as a tool to plan the experiments, for example to find out which kind of unwanted phenomena might occur before the experiment is even started. Modelling is a powerful tool when used correctly. It can be also used to explain the phenomena occurring in the experiments, since results analysed after the tests only show the final state, and not what is happening in the experiment during it. New modelling codes are being built all the time and the old ones are also developing, some of them are free and some require a license to be bought.

Now THC modelling seems to be suitable option for many experiments to estimate the behaviour of minerals and bentonite in a short time frame, but to a time scale of thousands of years challenges still exist to obtain accurate enough models. There are always variables that could arise in the years to come which we have not thought of and some parameters should be studied further.

6.1 Uncertainties/challenges in modelling

Most of the models do not take into account the three different kinds of water in bentonite. This is fine in non-compacted batch experiments but not while doing compacted fully saturated experiments with diffusion as the governing transport mechanism. This mechanism should be taken into account, since anion exclusion near clay surfaces and near closed pores in which clay stacks overlap is bound to happen as well as in interlamellar space which only allows the diffusion of cations.

Fully coupled THCM models are very challenging since so many chemical phenomena can affect the mechanical behaviour of the bentonite, for example, cation form, temperature, dissolution/precipitation and pH, and coupling all these to

mechanical parameters is highly challenging. Most of the time, existing fully coupled THCM models work only for a very limited range of parameters.

Some of the chemical and mechanical parameters are still uncertain, like the wetting mechanism of the bentonite and correct parameters to describe it. Uncertainties in high-temperature thermodynamic data may exist and lack of kinetic data for some minerals is an issue since laboratory-based values are not necessarily applicable to the field situation. In addition, reactive surface areas and grain radii of minerals are highly uncertain due to the lack of data. Diffusion coefficients under higher temperatures should also be studied more, since diffusion tends to be faster at higher temperatures [122].

Modelling long-term behaviour to thousands of years is highly uncertain, since it is unknown what natural phenomena might occur so far in to the future, for example, the glacial period could come as soon as in 10 000 years or green-house effect could postpone it to much more distant future ~100 000 years from now.

6.2 Future aspects

While all modelling codes are advancing one step at a time, currently the best free modelling software for chemical species known to the author is PHREEQC, which offers wide variability of model parameters and a 1-D diffusion possibility. Coupled with some other software, which handle transport in more complex geometries, PHREEQC offers the most suitable environment. It includes the possibility to alter diffusion coefficients, tortuosities and geometries for different major species as well as surface diffusion, dead-end pores, Donnan exclusion, exchange reactions as well as the possibility of dual porosity structure and three component division of the pore space in free pore water, DDL water and interlayer water [124]. With all these variables it is possible to accurately model diffusion in compacted clays.

Combining mechanical phenomena with THC models has been a long-term plan for multiple waste management organizations for a long time, but a working THCM model which covers a broad area of applications is not yet available. In this thesis THC coupling has been studied and the know-how in this area can be of help in the future while considering THCM couplings.

7. References

[1] Posiva Oy 2012. Safety Case for the Disposal of Spent Nuclear Fuel at Olkiluoto - Description of the Disposal System 2012, Posiva Report 2012-05, Posiva Oy, Olkiluoto, Finland.

[2] Posiva Oy 2015. Posiva press release. . http://www.posiva.fi/media/tiedotteet/posiva_sai_rakentamisluvan_kaytetyn_polttoaineen_loppusijoituslaitokselle.3224.news

[3] SKBF/KBS 1983. Final Storage of Spent Nuclear Fuel - KBS-3 - Vol I-IV, SKBF/KBS - Swedish Nuclear Fuel Supply Co/Division KBS, Stocholm, Sweden.

[4] Hansen, J., Korkiala-tanttu, L., Keski-Kuha, E. & Keto, P. 2009. Deposition Tunnel Backfill Design for a KBS-3V Repository, Working Report 2009–129, Posiva Oy, Olkiluoto, Eurajoki, Finland.

[5] SKB 1999. Deep repository for spent nuclear fuel. SR-97-Post-closure safety. Volume I and II, Technical Report TR-99-06, SKB - Swedish Nuclear and Waste Management Co, Stockholm, Sweden.

[6] SKB 2011. Long-Term Safety for the Final Repository for Spent Nuclear Fuel at Forsmark - Volumes I-III, Technical Report TR-11-01, SKB AB - Swedish Nuclear Fuel and Waste Management Co, Stocholm, Sweden.

[7] Posiva Oy 1996. Final Disposal of Spent Fuel in the Finnish Bedrock, Detailed Site Investigations 1993-1996 (in Finnish), Posiva Report 96–19, Posiva Oy, Olkiluoto, Finland.

[8] SKB 1986. Handling and Final Disposal of Nuclear Waste Part I-III, SKB AB - Swedish Nuclear Fuel and Waste Management Co, Stocholm Sweden.

[9] SKB 1989. Handling and final disposal of nuclear waste: Programme for research development and other measures Part I-II, SKB AB - Swedish Nuclear Fuel and Waste Management Co, Stockholm, Sweden.

[10] SKBF/KBS 1978. Handling and Final Storage of Unprocced Spent Nuclear Fuel, Volumes I-II. Nuclear Fuel Safety Project (KBS) of the Swedish power utilities, SKBF/KBS - Swedish Nuclear Fuel Supply Co/Division KBS, Stocholm Sweden.

[11] Kärnbränslesäkerhet 1978. Handling of Spent Nuclear Fuel and Final Storage of Vitrified High Level Reprocessing Waste, Kärnbränslesäkerhet (now SKB), Stockholm, Sweden.

[12] Nordman, H. & Vieno, T. 1996. Interim report on safety assessment of spent fuel disposal, Posiva Report 96–17, Posiva Oy, Olkiluoto, Finland.

[13] Posiva Oy 2008. Safety Case Plan 2008, Posiva Report 2008-05, Posiva Oy, Olkiluoto, Finland.

[14] SKB 2006. Long-term safety for KBS-3 repositories at Forsmark and Laxemar – a first evaluation : Main Report of the SR-Can project, Technical Report TR-06-09, SKB AB - Swedish Nuclear Fuel and Waste Management Co, Stocholm, Sweden.

[15] Raiko, H. 2005. Disposal Canister for Spent Nuclear Fuel – Design Report, Posiva Report 2005-02, Posiva Oy, Olkiluoto, Finland.

[16] Raiko, H. 1999. Design report of the disposal canister for twelve fuel assemblies, Posiva Report 99–18, Posiva Oy, Olkiluoto, Finland.

[17] Posiva Oy 2012. Safety Case for the Disposal of Spent Nuclear Fuel at Olkiluoto – Performance Assessment 2012, Posiva Report 2012-04, Posiva Oy, Olkiluoto, Finland.

[18] SKB 2011. Environmental Impact Statement, Interim Storage, encapsulation and final disposal of spent nuclear fuel, Swedish Nuclear Fuel and Waste Management Co, Stocholm Sweden.

[19] STUK 2014. Joint Convention on the Safety of Spent Fuel Management and on the Safety of Radioactive Waste Management, 5th Finnish National Report STUK-B 180, Radiation and Nuclear Safety Authority, STUK, Helsinki, Finland.

[20] Posiva Oy & SKB 2017. Safety functions, performance targets and technical design requirements for a KBS-3V repository, Posiva SKB Report 01, Posiva Oy, SKB AB - Swedish Nuclear and Waste Management Company Co., Olkiluoto, Finland and Stockholm, Sweden.

[21] Vieno, T. & Ikonen, A. 2005. Plan for Safety Case of Spent Fuel Repository at Olkiluoto, Posiva Report 2005-01, Posiva Oy, Olkiluoto, Finland.

[22] King, F., Ahonen, L., Taxén, C., Vuorinen, U. & Werme, L. 2001. Copper Corrosion under Expected Conditions in a Deep Geological Repository, Posiva Report 2002-01, Posiva Oy, Olkiluoto, Finland.

[23] Kwong, G.M. 2011. Status of Corrosion Studies for Copper Used Fuel Containers Under Low Salinity Conditions, NWMO TR-2011-14, Nuclear Waste Management Organization, Toronto, Ontario, Canada.

[24] Szakálos, P., Hultquist, G. & Wikmark, G. 2007. Corrosion of Copper by Water. Electrochem. Solid-State Lett.10(11), C63–C67. doi:10.1149/1.2772085

[25] Swedish Government 2010. Nuclear Waste State of the Art Report 2010 - challenges for the final repository programme, SOU 2010:6, Swedish Government, Stocholm, Sweden.

[26] Karnland, O., Olsson, S., Dueck, A., Birgersson, M., Nilsson, U. & Hernan-Håkansson, T. 2009. Long term test of buffer material at the Äspö Hard Rock Laboratory, LOT project - Final report on the A2 test parcel, Technical Report TR-09-29, Stocholm, Sweden.

[27] Villar, M.V., Sánchez, M. & Gens, A. 2008. Behaviour of a bentonite barrier in the laboratory: Experimental results up to 8years and numerical simulation. Phys. Chem. Earth, Parts A/B/C33S476–S485. doi:10.1016/j.pce.2008.10.055

[28] Pusch, R. 1980. Permeability of highly compacted bentonite, Technical Report 80–16, SKBF/KBS - Swedish Nuclear Fuel Supply Co/Division KBS, Stockholm, Sverige.

[29] Komine, H. 2008. Theoretical Equations on Hydraulic Conductivities of Bentonite-Based Buffer and Backfill for Underground Disposal of Radioactive Wastes. J. Geotech. Geoenvironmental Eng.134(4), 497–508. doi:10.1061/(ASCE)1090-0241(2008)134:4(497)

[30] Keto, P., Hassan, M., Karttunen, P., Kiviranta, L., Kumpulainen, S., Korkiala-tanttu, L., et al. 2013. Backfill Production Line 2012 Design, Production and Initial State of the Deposition Tunnel Backfill and Plug, Posiva Report 2012–18, Posiva Oy, Olkiluoto, Finland.

[31] Arvidsson, A., Josefsson, P., Eriksson, P., Sandén, T. & Ojala, M. 2015. System design of backfill Project results, Techical Report TR-14-20, SKB AB - Swedish Nuclear Fuel and Waste Management Co, Stocholm, Sweden.

[32] Ahonen, L., Hakkarainen, V., Kaija, J., Kuivamäki, A., Lindberg, A., Paananen, M., et al. 2011. Geological safety aspects of nuclear waste disposal in Finland., Geoscience for Society 125th Anniversary Volume Geological Survey of Finland (GTK), Espoo, Finland.

[33] Pitkänen, P., Luukkonen, A. & Partamies, S. 2007. Buffering against intrusion of groundwater of undesirable composition, in: Stab. Buffering Capacit. Geosph. Long-Term Isol. Radioact. Waste Appl. to Cryst. Rock, OECD/NEA Workshop Proceedings, Manchester, United Kingdom

[34] Vidstrand, P., Follin, S., Selroos, J.-O., Näslund, J.-O. & Rhén, I. 2013. Modeling of groundwater flow at depth in crystalline rock beneath a moving ice-sheet margin, exemplified by the Fennoscandian Shield, Sweden. Hydrogeol. J.21(1), 239–255. doi:10.1007/s10040-012-0921-8

[35] Ansolabehere, S., Deutch, J., Driscoll, M., Gray, Paul, E., Holdren, John, P., Joskow, Paul, L., et al. 2003. The Future of Nuclear Power, An Interdisciplinary MIT Study Massachusetts Institute of Technology (MIT), Massachusetts, United States.

[36] GAO 2003. Spent Nuclear Fuel: Options Exist to Further Enhance Security, GAO-03-426, United States General Accounting Office, Washington, United Sates.

[37] Ikonen, K. & Raiko, H. 2012. Thermal dimensioning of spent fuel repository, Working Report 2012–56, Posiva Oy, Olkiluoto, Finland.

[38] General Time Schedule for Final Disposal - Posiva. . http://www.posiva.fi/en/final_disposal/general_time_schedule_for_final_disposal (accessed March 4, 2016)

[39] Saanio, T., Ikonen, A., Keto, P., Kirkkomäki, T., Kukkola, T., Nieminen, J., et al. 2013. Design of the Disposal Facility 2012, Working Report 2013–17, Posiva Oy, Olkiluoto, Finland.

[40] Basics of the final disposal - Posiva. . http://www.posiva.fi/en/final_disposal/basics_of_the_final_disposal (accessed April 6, 2016)

[41] Juvankoski, M. 2012. Buffer Design 2012, Posiva Report 2012–14, Posiva Oy, Olkiluoto, Finland.

[42] Posiva Oy 2012. Safety Case for the Disposal of Spent Nuclear Fuel at Olkiluoto - Design Basis 2012, Posiva Report 2012-03, Posiva Oy, Olkiluoto, Finland.

[43] Sutherland, W.M. 2014. Wyoming Bentonite, Wyoming State Geological Survey, Wyoming, Usa.

[44] Hosterman, J.W. & Patterson, S.H. 1992. Bentonite and fuller's earth resources of the United States, U.S. Geological Survey Professional Paper 1522, . http://pubs.er.usgs.gov/publication/pp1522

[45] Virta, R.L. 2005. Clays, U.S. Geological Survey MIneral Commodity Summaries 2005 U.S. Geological Survey, . https://minerals.usgs.gov/minerals/pubs/commodity/clays/190496.pdf

[46] Murray, H.H. 1999. Applied clay mineralogy today and tomorrow. Clay Miner.3439–49. doi:10.1180/000985599546055

[47] Bergaya, F., Theng, B.K.G. & Lagaly, G. 2006. Development of Clay Science Vol 1. Handbook of Clay Science, 1st ed., Elsevier Ltd., Elsevier, Amsterdam, Netherlands.

[48] Ross, C.S. & Hendricks, S.B. 1945. Minerals of the Montmorillonite Group Their Origin and Relation to Soils and Clays, Geological Survey Washington, United Sates.

[49] Brigatti, M.F., Galan, E. & Theng, B.K.G. 2006. Chapter 2 Structures and Mineralogy of Clay Minerals, in: Dev. Clay Sci., Elsevier, doi:10.1016/S1572-4352(05)01002-0

[50] Tournassat, C., Steefel, C.I., Bourg, I.C. & Bergaya, F. 2015. Developments in Clay Science - Volume 6. Natural and Engineered Clay Barriers, Elsevier Ltd, Amsterdam, Netherlands.

[51] Sposito, G., Skipper, N.T., Sutton, R., Park, S. -h., Soper, A.K. & Greathouse, J.A. 1999. Surface geochemistry of the clay minerals. Proc. Natl. Acad. Sci.96(7), 3358–3364. doi:10.1073/pnas.96.7.3358

[52] Pusch, R., Karnland, O. & Hökmark, H. 1990. GMM — A general microstructural model for qualitative and quantitative studies of smectite clays, SKB Technical Report TR-90-43, SKB AB - Swedish Nuclear Fuel and Waste Management Co., Stockholm, Sweden.

[53] van Olphen, H. 1963. An Introduction to Clay Colloid Chemistry, John Wiley & Sons, New York, USA.

[54] Bergaya, F., Lagaly, G. & Vayer, M. 2006. Chapter 12.10 Cation and Anion Exchange, in: Dev. Clay Sci., Elsevier, doi:10.1016/S1572-4352(05)01036-6

[55] Karnland, O., Olsson, S. & Nilsson, U. 2006. Mineralogy and sealing properties of various bentonites and smectite-rich clay materials, SKB Technical Report TR-06-30, SKB AB - Swedish Nuclear Fuel and Waste Management Co., Stocholm Sweden.

[56] Aubrey, J.D. n.d. Minerals Ionic Solids Types of bonds Covalentbonding e-s shared equally Ionic coulombic attraction between anion and cation e-s localized Ionic / covalent. . http://images.slideplayer.com/26/8808128/slides/slide_19.jpg (accessed May 12, 2016)

[57] Bradbury, M.H. & Baeyens, B. n.d. Porewater Chemistry in Compacted Re-Saturated MX-80 Bentonite : Physico-Chemical Characterisation and Geochemical Modelling, PSI Bericht 02-10, Villigen, Switzerland.

[58] Lagaly, G. & Dékány, I. 2013. Colloid Clay Science, in: Dev. Clay Sci., Elsevier, doi:10.1016/B978-0-08-098258-8.00010-9

[59] Borisover, M. & Davis, J.A. 2015. Adsorption of Inorganic and Organic Solutes by Clay Minerals, in: Dev. Clay Sci., Elsevier, doi:10.1016/B978-0-08-100027-4.00002-4

[60] Salles, F., Douillard, J.-M., Denoyel, R., Bildstein, O., Jullien, M., Beurroies, I., et al. 2009. Hydration sequence of swelling clays: Evolutions of specific surface area and hydration energy. J. Colloid Interface Sci.333(2), 510–522. doi:10.1016/j.jcis.2009.02.018

[61] Teich-McGoldrick, S.L., Greathouse, J.A., Jové-Colón, C.F. & Cygan, R.T. 2015. Swelling Properties of Montmorillonite and Beidellite Clay Minerals from Molecular Simulation: Comparison of Temperature, Interlayer Cation, and Charge Location Effects. J. Phys. Chem. C119(36), 20880–20891. doi:10.1021/acs.jpcc.5b03253

[62] Pusch, R. 2006. Chapter 6 Mechanical Properties of Clays and Clay Minerals, in: Dev. Clay Sci., Elsevier, doi:10.1016/S1572-4352(05)01006-8

[63] Segad, M., Jönsson, B., Åkesson, T. & Cabane, B. 2010. Ca/Na Montmorillonite: Structure, Forces and Swelling Properties. Langmuir26(8), 5782–5790. doi:10.1021/la9036293

[64] Laird, D.A. 2006. Influence of layer charge on swelling of smectites. Appl. Clay Sci.34(1–4), 74–87. doi:10.1016/j.clay.2006.01.009

[65] Zhang, F., Zhang, Z.Z., Low, P.F. & Roth, C.B. 1993. The Effect of Temperature on the Swelling of Montmorillonite. Clay Miner.28(1), 25–31. doi:10.1180/claymin.1993.028.1.03

[66] Villar, M.. & Lloret, A. 2004. Influence of temperature on the hydro-mechanical behaviour of a compacted bentonite. Appl. Clay Sci.26(1–4), 337–350. doi:10.1016/j.clay.2003.12.026

[67] Wersin, P. 2003. Geochemical modelling of bentonite porewater in high-level waste repositories. J. Contam. Hydrol.61(1–4), 405–422. doi:10.1016/S0169-7722(02)00119-5

[68] Muurinen, A. & Carlsson, T. 2007. Development of methods for on-line measurements of chemical conditions in compacted bentonite. Phys. Chem. Earth, Parts A/B/C32(1–7), 241–246. doi:10.1016/j.pce.2006.02.059

[69] Itälä, A. 2009. Chemical Evolution of Bentonite Buffer in a Final Repository of Spent Nuclear Fuel During the Thermal Phase, VTT Publications 721, VTT - Technical Research Centre of Finland, Espoo, Finland.

[70] Muurinen, A., Carlsson, T. & Root, A. 2013. Bentonite pore distribution based on SAXS, chloride exclusion and NMR studies. Clay Miner.48(2), 251–266. doi:10.1180/claymin.2013.048.2.07

[71] Push R. Lehikoinen J., Bors J., Eriksen T., M.A. 1999. Microstructural and chemical parameters of bentonite as determinants of waste isolation efficiency, Nuclear Science and Technology Project Report EUR 18950, European Commission, Luxembourg.

[72] Kaufhold, S., Dohrmann, R., Koch, D. & Houben, G. 2008. The pH of Aqueous Bentonite Suspensions. Clays Clay Miner.56(3), 338–343. doi:10.1346/CCMN.2008.0560304

[73] Heikola, T., Kumpulainen, S., Vuorinen, U., Kiviranta, L. & Korkeakoski, P. 2013. Influence of alkaline (pH 8.3 – 12.0) and saline solutions on chemical, mineralogical and physical properties of two different bentonites. Clay Miner.48(2), 309–329. doi:10.1180/claymin.2013.048.2.12

[74] Kohličková, M. & Jedináková-Křižová, V. 1998. Effect of pH and Eh on the sorption of selected radionuclides. J. Radioanal. Nucl. Chem.229(1–2), 43–48. doi:10.1007/BF02389444

[75] Muurinen, A. & Carlsson, T. 2010. Experiences of pH and Eh measurements in compacted MX-80 bentonite. Appl. Clay Sci.47(1–2), 23–27. doi:10.1016/j.clay.2008.05.007

[76] Vuorinen, U., Lehikoinen, J., Luukkonen, A. & Ervanne, H. 2006. Effects of Salinity and High pH on Crushed Rock and Bentonite – Experimental Work and Modelling E, Posiva Report 2006-01, Posiva Oy, Olkiluoto, Finland.

[77] Bradbury, M.H. & Baeyens, B. 2009. Experimental and modelling studies on the pH buffering of MX-80 bentonite porewater. Appl. Geochemistry24(3), 419–425. doi:10.1016/j.apgeochem.2008.12.023

[78] Pulkkanen, V.-M.S., Itälä, A.-K.P. & Muurinen, A.K. 2012. Buffering of pH conditions in sodium bentonite. MRS Proc.1475 doi:10.1557/opl.2012.593

[79] Muurinen, A. & Lehikoinen, J. 1999. Porewater chemistry in compacted bentonite. Eng. Geol.54(1–2), 207–214. doi:10.1016/S0013-7952(99)00075-7

[80] Kumpulainen & Kiviranta 2010. Mineralogical and Chemical Characterization of Various Bentonite and Smectite-Rich Clay Materials, POSIVA Working report 2010–52, Posiva Oy, Olkiluoto, Finland.

[81] Tournassat, C., Bourg, I.C., Steefel, C.I. & Bergaya, F. 2015. Surface Properties of Clay Minerals, in: Dev. Clay Sci., Elsevier, doi:10.1016/B978-0-08-100027-4.00001-2

[82] Sposito, G. 1981. The Thermodynamics of Soil Solution, Oxford University Press, New York, USA.

[83] Gaines, G.L. & Thomas, H.C. 1953. Adsorption Studies on Clay Minerals. II. A Formulation of the Thermodynamics of Exchange Adsorption. J. Chem. Phys.21(4), 714. doi:10.1063/1.1698996

[84] Vanselow, A.P. 1932. The Utilization of the Base-Exchange Reaction for the Determination of Activity Coefficients in Mixed Electrolytes. J. Am. Chem. Soc.54(4), 1307–1311. doi:10.1021/ja01343a005

[85] Gapon, E.N. 1933. On the Theory of Exchange Adsorption in Soils. Russ. J. Gen. Chem.(3), 144–160.

[86] Sposito, G., Holtzclaw, K.M., Johnston, C.T. & LeVesque-Madore, C.S. 1981. Thermodynamics of Sodium-Copper Exchange on Wyoming Bentonite at 298°K1. Soil Sci. Soc. Am. J.45(6), 1079. doi:10.2136/sssaj1981.03615995004500060014x

[87] Sposito, G., Holtzclaw, K.M., Charlet, L., Jouany, C. & Page, A.L. 1983. Sodium-Calcium and Sodium-Magnesium Exchange on Wyoming Bentonite in Perchlorate and Chloride Background Ionic Media. Soil Sci. Soc. Am. J.47(1), 51. doi:10.2136/sssaj1983.03615995004700010010x

[88] Sposito, G., Holtzclaw, K.M., Jouany, C. & Charlet, L. 1983. Cation Selectivity in Sodium-Calcium, Sodium-Magnesium, and Calcium-Magnesium Exchange on Wyoming Bentonite at 298 K. Soil Sci. Soc. Am. J.47(5), 917. doi:10.2136/sssaj1983.03615995004700050015x

[89] Fletcher, P., Sposito, G. & LeVesque, C.S. 1984. Sodium-calcium-magnesium exchange reactions on a montmorillonitic soil: I. Binary exchange reactions. Soil Sci. Soc. Am. J.481016–1021. doi:10.2136/sssaj1984.03615995004800050013x

[90] Fletcher, P., Holtzclaw, K.M., Jouany, C., Sposito, G. & LeVesque, C.S. 1984. Sodium-Calcium-Magnesium Exchange Reactions on a Montmorillonitic Soil: II. Ternary Exchange Reactions1. Soil Sci. Soc. Am. J.48(5), 1022. doi:10.2136/sssaj1984.03615995004800050014x

[91] Sposito, G. & Fletcher, P. 1985. Sodium-calcium-magnesium exchange reactions on a montmorillonitic soil: III. Calcium-magnesium exchange selectivity. Soil Sci. Soc. Am. J.49(5), 1160–1163. doi:10.2136/sssaj1985.03615995004900050017x

[92] Dolcater, D.L., Lotse, E.G., Syers, J.K. & Jackson, M.L. 1968. Cation Exchange Selectivity of Some Clay-Sized Minerals and Soil Materials1. Soil Sci. Soc. Am. J.32(6), 795. doi:10.2136/sssaj1968.03615995003200060026x

[93] Dohrmann, R. 2006. Cation exchange capacity methodology I: An efficient model for the detection of incorrect cation exchange capacity and exchangeable cation results. Appl. Clay Sci.34(1–4), 31–37. doi:10.1016/j.clay.2005.12.006

[94] Meier, L.P. & Kahr, G. 1999. Determination of the Cation Exchange Capacity (CEC) of Clay Minerals Using the Complexes of Copper(II) Ion with Triethylenetetramine and Tetraethylenepentamine. Clays Clay Miner.47(3), 386–388. doi:10.1346/CCMN.1999.0470315

[95] Appelo, C.A.J. & Postma, D. 2007. Geochemistry, Groundwater and Pollution, 2nd ed., A.A. Balkema Publishers, Leiden, Netherlands.

[96] Bruggenwert, M.G.M. & Kamphorst, A. 1979. Chapter 5: Survey of Experimental Information on Cation Exchange in Soil Systems, in: Dev. Soil Sci., Elsevier, doi:10.1016/S0166-2481(08)70660-3

[97] Wallis, I., Idiart, A., Dohrmann, R. & Post, V. 2016. Reactive transport modelling of groundwater-bentonite interaction: Effects on exchangeable cations in an alternative buffer material in-situ test. Appl. Geochemistry7359–69. doi:10.1016/j.apgeochem.2016.07.005

[98] Arcos, D., Grandia, F., Domènech, C., Fernández, A.M., Villar, M. V., Muurinen, A., et al. 2008. Long-term geochemical evolution of the near field repository: Insights from reactive transport modelling and experimental evidences. J. Contam. Hydrol.102(3–4), 196–209. doi:10.1016/j.jconhyd.2008.09.021

[99] Parkhurst, D.L. & Appelo, C.A.J. 1999. User's Guide To PHREEQC (version 2) — a Computer Program for Speciation, and Inverse Geochemical Calculations, Water-Resources Investigations Report 99–4259, U.S Geological Survey, Denver, Colorado, U.S.A. doi:10.3133/wri994259

[100] Bethke, C.M. 2007. Geochemical and Biogeochemical Reaction Modeling, 2nd ed., Cambridge University Press, Cambridge, United Kingdom. doi:10.1017/CBO9780511619670

[101] Xu, T., Sonnenthal, E., Spycher, N. & Pruess, K. 2006. TOUGHREACT—A simulation program for non-isothermal multiphase reactive geochemical transport in variably saturated geologic media: Applications to geothermal injectivity and CO2 geological sequestration. Comput. Geosci.32(2), 145–165. doi:10.1016/j.cageo.2005.06.014

[102] Kincaid, C.T., Morrey, J.R. & J., R.E. 1984. Geohydrochemical Models for Solute Migration: Volume 1. Process Description and Computer Code Selection, Electric Power Research Institute, Battelle. Pacific Northwest Laboratories, Palo Alto, California, Usa.

[103] Wolery, T. 1979. Calculation of chemical equilibrium between aqueous solution and minerals: the EQ 3/6 software package, UC-11, Lawrence Livermore Laboratory, Livermore, California, USA.

[104] Olin, M., Valkiainen, M. & Aalto, H. 1997. Matrix diffusion in crystalline rocks: coupling of anion exclusion. surface diffusion and surface complexation, Posiva Report 96–25, Posiva Oy, Olkiluoto, Finland.

[105] Olin, M. 1994. Diffusion in crushed rock and in bentonite clay, Dissertation, University of Helsinki.

[106] Itälä, A., Laitinen, M., Tanhua-Tyrkkö, M., Pulkkanen, V.-M. & Olin, M. 2010. COMSOL Multiphysics, TOUGHREACT and Numerrin Comparison in Some Modelling Tasks of Spent Nuclear Fuel Disposal, in: Comsol Conf. 2010, Comsol, Espoo, Finland

[107] Rasmuson, A. & Neretnieks, I. 1983. Surface migration in sorption processes, Technical Report TR 83-87, SKBF/KBS - Swedish Nuclear Fuel Supply Co/Division KBS, Stockholm, Sweden.

[108] Svensson, D., Dueck, A., Nilsson, U., Olsson, S., Sandén, T., Lydmark, S., et al. 2011. Alternative buffer material. Status of the ongoing laboratory investigation of reference materials and test package 1, Technical Report TR-11-06, SKB AB - Swedish Nuclear Fuel and Waste Management Co, Stockholm, Sweden.

[109] Appelo, C.A.J., Van Loon, L.R. & Wersin, P. 2010. Multicomponent diffusion of a suite of tracers (HTO, Cl, Br, I, Na, Sr, Cs) in a single sample of Opalinus Clay. Geochim. Cosmochim. Acta74(4), 1201–1219. doi:10.1016/j.gca.2009.11.013

[110] Appelo, C.A.J. & Wersin, P. 2007. Multicomponent Diffusion Modeling in Clay Systems with Application to the Diffusion of Tritium, Iodide, and Sodium in Opalinus Clay. Environ. Sci. Technol.41(14), 5002–5007. doi:10.1021/es0629256

[111] Luukkonen, A. 2004. Modelling Approach for Geochemical Changes in the Prototype Repository Engineered Barrier System, Posiva Working Report 2004–31, Posiva Oy, Olkiluoto, Finland.

[112] Idiart, a., Maia, F. & David Arcos, D. 2013. Geochemical Evaluation of the Near-Field for Future HLW Repository at Olkiluoto, Posiva Report 2013-05, Posiva Oy, Olkiluoto, Finland.

[113] Gens, A., Guimaräes, L. do N., Olivella, S. & Sánchez, M. 2010. Modelling thermo-hydro-mechano-chemical interactions for nuclear waste disposal. J. Rock Mech. Geotech. Eng.2(2), 97–102. doi:10.3724/SP.J.1235.2010.00097

[114] Arcos, D., Bruno, J. & Karnland, O. 2003. Geochemical model of the granite–bentonite–groundwater interaction at Äspö HRL (LOT experiment). Appl. Clay Sci.23(1–4), 219–228. doi:10.1016/S0169-1317(03)00106-6

[115] Toprak, E., Mokni, N., Olivella, S. & Pintado, X. 2013. Thermo-Hydro-Mechanical Modelling of Buffer Synthesis Report, Posiva Report 2012–47, Posiva Oy, Olkiluoto, Finland.

[116] Clara, S., Salas, J. & Arcos, D. 2010. Aspects of geochemical evolution of the SKB near field in the frame of SR-Site, SKB Technical Report 10–59, SKB AB - Swedish Nuclear Fuel and Waste Management Co, Stocholm, Sweden.

[117] Pitkänen, P., Partamies, S. & Luukkonen, A. 2003. Hydrogeochemical Interpretation of Baseline Groundwater Conditions at the Olkiluoto Site. Posiva Report 2003-07, Posiva Report 2003-07, Posiva Oy, Olkiluoto, Finland.

[118] Pitkänen, P., Luukkonen, A., Ruotsalainen, P., Leino-Forsman, H. & Vuorinen, U. 1998. Geochemical modelling of groundwater evolution and residence time at the Olkiluoto, Posiva Report 98–10, Posiva Oy, Olkiluoto, Finland.

[119] Steefel, C.I., Appelo, C.A.J., Arora, B., Jacques, D., Kalbacher, T., Kolditz, O., et al. 2015. Reactive transport codes for subsurface environmental simulation. Comput. Geosci.19(3), 445–478. doi:10.1007/s10596-014-9443-x

[120] Muurinen, A. 2006. Chemical Conditions in the A2 Parcel of the Long-Term Test of Buffer Material in Äspö (LOT), Working Report 2006–83, Posiva Oy, Olkiluoto, Finland.

[121] Pastina, B. & Hellä, P. 2006. Expected evolution of a spent nuclear fuel repository at Olkiluoto, Posiva Report 2006-05, Posiva Oy, Olkiluoto, Finland.

[122] Salas, J., Sena, C. & Arcos, D. 2014. Hydrogeochemical evolution of the bentonite buffer in a KBS-3 repository for radioactive waste. Reactive transport modelling of the LOT A2 experiment. Appl. Clay Sci.101521–532. doi:10.1016/j.clay.2014.09.016

[123] Sena, C., Salas, J. & Arcos, D. 2010. Thermo-hydro-geochemical modelling of the bentonite buffer - LOT A2 experiment, Technical Report TR-10-65, Stocholm, Sweden.

[124] Appelo, C.A.J., Van Loon, L.R. & Wersin, P. 2010. Multicomponent diffusion of a suite of tracers (HTO, Cl, Br, I, Na, Sr, Cs) in a single sample of Opalinus Clay. Geochim. Cosmochim. Acta74(4), 1201–1219. doi:10.1016/j.gca.2009.11.013

PUBLICATION I

Chemical evolution of bentonite buffer in a final repository of spent nuclear fuel during the thermal phase

In: Nuclear Technology (2011), Vol 174, No.3, pp. 342-452.

CHEMICAL EVOLUTION OF BENTONITE BUFFER IN A FINAL REPOSITORY OF SPENT NUCLEAR FUEL DURING THE THERMAL PHASE

RADIOACTIVE WASTE MANAGEMENT AND DISPOSAL

KEYWORDS: *THC, temperature dependence modeling, cation exchange*

AKU ITÄLÄ* and MARKUS OLIN

VTT Technical Research Centre of Finland, P.O. Box 1000, FI-02044 VTT, Finland

Received February 19, 2010
Accepted for Publication June 28, 2010

Finnish spent nuclear fuel final disposal is planned to be based on the Kärnbränslesäkerhet 3-Vertical concept, which was originally planned for fractured crystalline bedrock. Within this concept, the role of the bentonite buffer is considered central. The aim of the study was to model the evolution of the final repository during the thermal phase (heat-generating period of spent fuel) when the bentonite is initially only partially saturated. There is an essential need to determine how temperature influences saturation and how both of these factors affect the chemistry of bentonite.

In this study the Long-Term Test of Buffer Materials A2 parcel test at the Äspö hard rock laboratory in Sweden was modeled using TOUGHREACT code. The results focused on the following phenomena occurring in the bentonite: cation exchange, changes of bentonite pore water, mineral alterations, saturation, and pressure changes in bentonite buffer.

The results show similarity with experimental data. However, the results are open to questions, and further study is needed to confirm the validity of the results. Differences between modeled and experimental results can be explained, for example, so that the experimental results are not from the fracture position as our one-dimensional model assumes.

I. INTRODUCTION

Finnish spent nuclear fuel final disposal is planned to be based on the Kärnbränslesäkerhet 3-Vertical (KBS-3V) concept (Fig. 1), which was originally planned for crystalline bedrock. Within this concept, bentonite will be used as a buffer material in high-level radioactive waste disposal. Upon saturation with groundwater, bentonite swells and thus seals repository tunnels. However, the thermal, hydrological, mechanical, and chemical phenomena and processes taking place in the bentonite buffer may change the mechanical and chemical properties of the bentonite. Determination of the long-term stability of bentonite under final repository conditions must be based on modeling, since empirical testing would require millennia to implement.

In this work, we concentrate on modeling the temperature effects on bentonite during the thermal phase, when the bentonite is initially only partially saturated. However, the complexity of the in situ conditions and computing power limitations preclude models that include all processes. We are therefore forced to consider only simplified repository site models.

To make the modeling more concrete, an example experimental case was adapted: the Long-Term Test of Buffer Materials (LOT) A-2 parcel test at the Äspö Hard Rock Laboratory (HRL) in Sweden.[2] This experiment was modeled, and the experimental results have been compared with the model.

Differences in the thermodynamic properties of minerals cause a redistribution of minerals within the bentonite. For example, laboratory tests indicate gypsum dissolution and anhydrite precipitation near the heater-bentonite interface. Incoming groundwater will also affect the bentonite pore water. Since these changes may affect the properties of bentonite, it must be determined whether these phenomena are to be taken into account in safety assessment.

*E-mail: aku.itala@vtt.fi

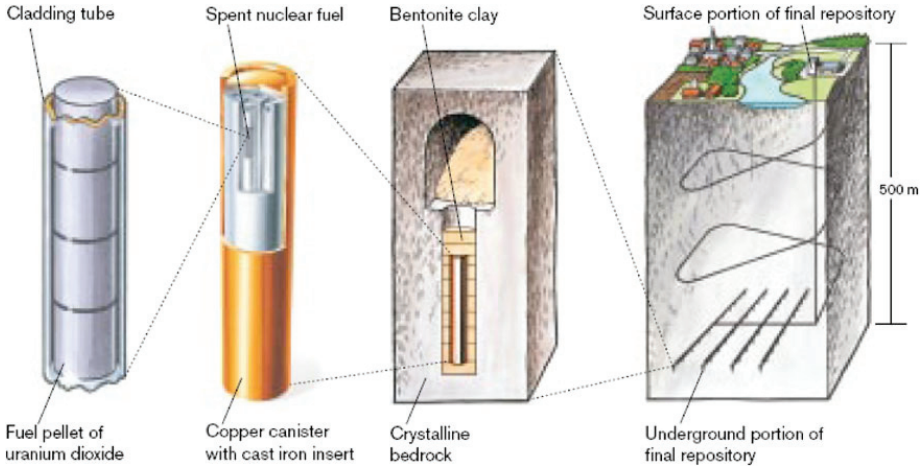

Fig. 1. The KBS-3V spent nuclear fuel final disposal concept.[1]

The first aim was to investigate the thermal (T), hydraulic (H), and chemical (C) phenomena affecting the bentonite. Comprehensive knowledge of the composition of bentonite after the thermal phase is crucial for estimating the long-term safety of the final disposal of spent nuclear fuel. The thermal phase will last a few thousand years, but most of the phenomena are assumed to occur during the first thousand years.[3]

In the first hundred years, there is a high temperature gradient in the bentonite. This gradient originates from the high activity spent fuel. In the A2 test there are more adverse conditions compared to the final repository site to accelerate the reactions and to compare the thermal load of the A2 test to the KBS-3V concept conditions for thousands of years.

TABLE I

Dimensions in LOT A2 Parcel Test*

Hole depth	4 m
Cylinder diameter	0.28 m
Cylinder height	0.1 m
Copper inner diameter	0.1 m
Copper wall thickness	0.004 m
Borehole diameter	0.3 + 0.01 m
Depth	450 m
Copper tube length	4.7 m
Hole height	8 m
Water Pressure	1.2 MPa

*Reference 2.

II. EXPERIMENT

The LOT test experiment A2 parcel test and its results were used in this model as reference data.[2] In the LOT tests, relatively small test parcels (see Table I) are exposed to field conditions at Äspö HRL. The LOT test series includes three test parcels with similar conditions to those expected in a KBS-3V repository and four test parcels with adverse conditions.

The A2 parcel is an adverse conditions parcel—adverse in this case referring to conditions that accelerate alteration processes (higher temperature and higher temperature gradient). The A2 parcel was placed in a vertical borehole in granitic rock. After ~5 to 6 yr of exposure, the test parcel was lifted and partitioned for examination. The results of these examinations were used as a reference. The test parcel dimensions were smaller compared to the KBS-3V deposition hole, in order to shorten the water saturation period, to achieve a higher temperature gradient over the buffer material, and to ease the uplift of the test parcel.[2]

The standard maximum temperature limit for final disposal repositories is 90°C. In the A2 test, the maximum temperature was set to 120 to 150°C. A 5-yr period in these conditions covers a significant proportion of the estimated thermal load in a KBS-3V repository. The higher-temperature conditions also accelerate kinetically controlled, slow processes.

II.A. Test Site Description

The test site depth was ~450 m from the surface. The rock consists mainly of Äspö diorite. The A2 hole

was 8 m deep and was situated 33 m from the tunnel entrance. The water pressure was kept higher than the vapor pressure at the test temperature and the water inflow rate kept low enough to prevent piping erosion. As this rate of water inflow was too low, it was decided to introduce external water via a supply hole. The water pressure into the hole was ~1.2 MPa. The water was injected into the test hole through titanium tubes. This pressure was kept constant throughout the test period. The test site dimensions are presented in Table I, and the test parcel is illustrated in Fig. 2 (Ref. 2).

III. MATERIAL

Research has shown that sodium bentonite is currently the most viable material for isolating radioactive materials because of its multiple beneficial characteristics[4]:

1. In the case of canister failure, the migration of the majority of contaminants (radionuclides) is retarded strongly, via sorption to the reactive clay surfaces.

2. Bentonite's ability to swell makes it an efficient barrier against contaminant migration.

3. Bentonite constitutes a mechanical and chemical zone of protection around the canister.

4. Bentonite has high thermal conductivity, thus serving to efficiently dissipate heat emitted by the waste.

Bentonites (montmorillonite clays) differ by mineralogical composition. The type chosen for final repository planning, MX-80, is extracted, for example, from Wyoming and is a commercial material supplied in powder form. The MX-80 material consists mainly of sodium montmorillonite clay with small amounts of quartz, tridymite, cristobalite, feldspars, sulfides, and other trace minerals.[2]

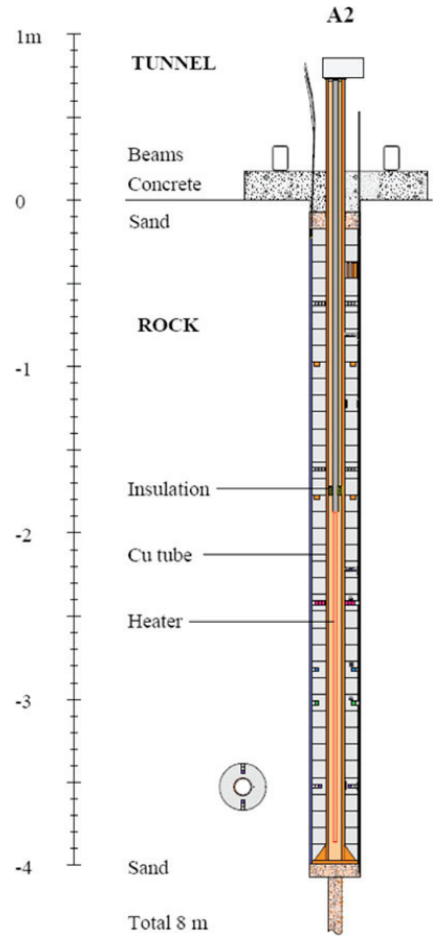

Fig. 2. Scaled schematic drawing of the A2 test parcel.[2]

IV. MODEL

IV.A. Modeling Concept

The chemical phenomena occurring in the bentonite barrier in a spent-fuel repository depend on numerous factors, such as the rate of iron corrosion, the reaction temperature, the composition of the incoming groundwater, the diffusion coefficients of the solutes, and the reactive surface area of minerals, etc. Owing to the complexity of their estimation and mutual couplings, consideration of all of these parameters within a single model remains highly challenging. Certain simplifications must therefore be made. The model presented in this paper is a simplified model, and its limitations as such must be recognized.

It is assumed that three phases (solid, liquid, and gas) are present in the modeled porous medium. The basic component of the solid montmorillonite is assumed to be insoluble but able to absorb ions and exchange them with solution. Precipitated minerals are assumed to be part of the solid phase. The gas phase consists of water vapor and air, while the liquid phase consists of water, dissolved air, and other dissolved species. Local equilibrium is assumed for all chemical reactions excluding mineral reactions with kinetics. Local chemical equilibrium is a limiting case for kinetics when mass transport is slow compared to reaction rates.

The model was created using the PetraSim user interface of the TOUGH2 and TOUGHREACT programs. The applied model is a coupled thermo-hydro-chemical

model, meaning no mechanical alterations and effects are considered. The purpose of the model was to match the results as closely to the experimental results as possible, and thus the time frame was limited to 10 yr (the LOT A2 parcel test duration was ~6 yr). After getting a sufficient match between the test and the model, the modeled results could be analyzed.

IV.B. Modeling Program

The TOUGHREACT EOS3 (equation of state 3) module was used to model the reactive unsaturated transport processes in one dimension, and the grid was pitched at uniform intervals. The model constructed was a simplified one. The idea was to simplify the real three-dimensional (3-D) model in which the copper canister producing heat is surrounded by bentonite and a rock matrix that contains a traversing water-conducting fracture. The model can be simplified to a one-dimensional (1-D) model because the changes in the bentonite are highest at the fracture location and diminish with increasing distance from it. Thus, the worst possible scenario is in the fracture position. Figure 3 shows the model grid.

Whereas the grid is simple, the phenomena at play within an actual system of this type are complex. Two cells on the left represent the heat source, i.e., the heat coming from the decay of spent fuel and the inert copper canister (1 cm). The right zone is granitic rock (29.5 cm) containing relatively free moving water. The dark zone in the middle is bentonite (9.5 cm), which is initially partially saturated or virtually dry. The rightmost cell is a magnified water source. As such, the chemistry and water concentration in that cell remains constant. The bentonite has an initial water-mineral content and cation exchange capacity, and it interacts with the granitic Äspö groundwater outside the bentonite block. The copper canister is inert, exclusive of its heat production.

PetraSim version 4.1.0219 was used. A newer version of the PetraSim (4.2.1118) user interface, which uses newer versions of TOUGH2 and TOUGHREACT, is also available, but we were unable to produce consistent results with this version. The newer version produced a number of anomalous results, and the cation exchanger compositions were also calculated apparently incorrectly. The reasons for this are being studied.

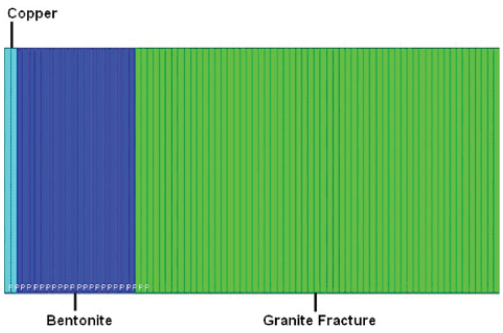

Fig. 3. 1-D grid with 80 pitched cells at uniform intervals.

IV.C. Model Parameters

The parameters for these models were taken from different sources.[2,4–9] Some of the parameters were approximated according to the data. Table II shows the material parameters, and Table III shows the water-retention parameters used. The water-retention parameters for the fracture were set for constant saturation of the rock.

Besides material parameters, chemical data were needed for the model. Table IV shows the bentonite mineral volume fractions in the model. The bolded minerals are inert.

The mineral kinetics were taken from Palandri and Kharaka[9] and can be seen in Table V, except for chalcedony, which was assumed to be at equilibrium. Also, groundwater, bentonite pore water, and ion exchanger composition were needed for the initial state and are shown in Table VI. The bentonite pore water was chosen so that the ion exchanger was initially calculated correctly.[10]

V. RESULTS

The results were fairly realistic. The obtained results were so numerous that they can be addressed here in part only. There are 12 different time steps taken from the 10-yr period. We should remember that the first 9.5 cm is bentonite, and after that the material is rock. The y letter in Figs. 4 through 18 means years, and d stands for days. The black line represents the value at the beginning of calculation. Even more thorough discussion of the results is presented in the thesis by Itälä.[11]

V.A. Properties

A number of key properties were given special attention. Figure 4 shows the temperature and temperature gradient in the bentonite and part of the rock matrix. As one can see, the temperature gradient is ~4.7°C/cm, and the temperature is 130 to 85°C in the bentonite. The temperature did not change after 200 days, and thus the latter time steps have been left out. Temperature profile is well matched with the experiment.[2] This is done for the later figures also. If time steps are missing, the results did not change after certain time step. Pressure of the gaseous species (air + water vapor) and capillary pressure are presented in Figs. 5 and 6. The gaseous pressure of bentonite with evolving capillary pressure generates suction

TABLE II

Material Parameters*

Parameter	Bentonite	Granitic Fracture	Copper
Pressure (Pa)	NTP[a]	1.20×10^{6}	NTP
Cation exchange capacity (meq/100 g)	75		
Rock grain density (kg/m^3)	2750	2650	8960
Diffusion coefficient (m^2/s)	2.00×10^{-9}		
Wet heat conductivity [W/(m C)]	1.3	2	2
Dry heat conductivity [W/(m C)]	0.3		
Porosity	0.43	0.14	0.01
Intrinsic permeability (m^2)	3.00×10^{-21}	5.00×10^{-11}	0
Tortuosity	0.124	0.2	
Specific heat [J/(kg C)]	2500	784	385

*References 2, 6, 7, and 8.
[a]NTP = normal temperature and pressure.

TABLE III

Water Retention Parameters: Van Genuchten for the Bentonite and Fatt and Klikoff for the Granitic Fracture*

	Bentonite	Granitic Fracture
λ	0.338	
S_{lr}	0.4	0.999
S_{ls}	1	
S_{gr}	0	
P_0	14.12 MPa	
P_{max}	140 MPa	

*Reference 7.

TABLE IV

Mineral Mass and Volume Fractions

Minerals	Mass Fraction (%)	Volume Fraction
Gypsum $CaSO_4 \cdot 2(H_2O)$	0.17	0.0012
Anhydrite $CaSO_4$	0.17	0.0009
Quartz SiO_2	15.00	0.0897
Montmorillonite $Na_{0.2}Ca_{0.1}Al_2Si_4O_{10}(OH)_2(H_2O)_{10}$	76.00	0.4236
K-Feldspar $KAlSi_3O_8$	7.00	0.0427
Calcite $CaCO_3$	0.70	0.0040
Chalcedony SiO_2 (crystalline)	0.96	0.0057
Sum	100	0.568

so that the bentonite remains saturated. As one can see, the pressure of the gaseous species and capillary pressure increase toward the heater. The bentonite was shown to saturate to 96% within ~1 yr (Fig. 7), which correlates closely with the LOT test report.[2] The initial saturation in bentonite is 40% of porosity and 100% in the granitic fracture part.

Other significant properties were pH and porosity. The change in porosity from 0.43 to 0.431 is so small that it does not affect the water flow or diffusion velocity. The pH in bentonite balances with the granitic water pH. The reduction in pH is due to lack of surface complexation and also to higher temperature, which increases the ionic product of OH^- and H^+ ions.

V.B. Minerals

Chalcedony is in equilibrium, and some equilibrium processes occur near the heater and rock surface (Fig. 8). Some calcite appears to dissolve near the copper (heat source) surface (Fig. 9), thus affecting the concentrations of calcium and carbonate ions. Gypsum dissolves within a couple of days.

Quartz and K-feldspar are almost stable during the whole test period. The kinetics of quartz and K-feldspar are slow, and thus, they would need a clearly longer time period to be dissolved/precipitated. The most interesting of the minerals, however, was anhydrite. Figure 10 shows the anhydrite profile. It appears that when sulfate is diffusing out and calcium is coming in, anhydrite precipitates near the rock surface. Anhydrite also starts to precipitate near the copper surface due to high temperature, which can also be seen in the experimental results.[12]

V.C. Primary Species

This section covers the concentration evolution of the main primary species in bentonite and part of the granitic rock during 10 yr. These concentrations are total aqueous component concentrations including all

TABLE V

Mineral Kinetics, Rate Parameters, and Activation Energies (kJ/mol) for Neutral, Acidic, and Alkaline Conditions*

Minerals	$K_{neutral}$	$E_a^{neutral}$	K_{acid}	E_a^{acid}	n_{acid}	$K_{alkaline}$	$E_a^{alkaline}$	$n_{alkaline}$
Gypsum	1.622×10^{-3}	0						
Anhydrite	6.457×10^{-4}	14.3						
Quartz	3.981×10^{-14}	90.9						
Chalcedony	Equilibrium							
K-Feldspar	3.890×10^{-13}	38	0	51.7	0.5	6.00×10^{-22}	94.1	−0.823
Calcite	1.549×10^{-6}	23.5	0.5	14.4	1	0.0003	35.4	1

*Reference 9.

TABLE VI

Groundwater, Bentonite Pore Water, and Cation Exchanger Composition

Variable	Groundwater Composition (mmol/ℓ)	Bentonite Pore Water Composition (mmol/ℓ)	Cation Exchanger Composition [equivalent fractions/ (meq/100 g)]
pH	6.9	8.62	
Na^+	100	9.972×10^{-4}	0.808/60.6
K^+	0.28	2.79×10^{-7}	0.009/0.675
Ca^{2+}	47.3	7.603×10^{-11}	0.128/9.6
Mg^{2+}	2.40	3.838×10^{-11}	0.055/4.125
Cl^-	178	1×10^{-3}	
SO_4^{2-}	4.60	Traces	
HCO_3^-	0.44	Traces	
Al^{3+}	Traces	Traces	
$H_4SiO_4(aq)$	Traces	Traces	
$O_2(aq)$	Traces	Traces	

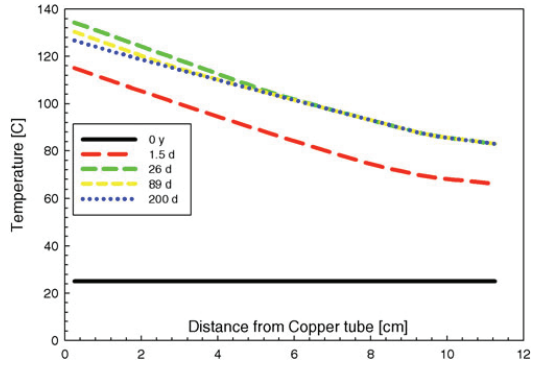

Fig. 4. Temperature evolution as a function of distance from the copper tube, over time.

the dissolved components like $CaCl_2(aq)$, $CaSO_4(aq)$, etc., where these primary species are included. The main primary species affecting the system were Na^+, Mg^{2+}, Ca^{2+}, K^+, Cl^-, and SO_4^{2-}. Other species present are not discussed here. The calcium profile (Fig. 11) shows calcium diffusing from the groundwater to the bentonite. However, the diffusion has not yet reached equilibrium and would continue even after 10 yr. After 5 yr the calcium concentration is ~5 mmol near the heater, which is in good agreement with the experimental results.[12]

Chloride concentration increases with saturation, and diffusion continues, although the diffusion profile is slightly anomalous compared to the boundary conditions (Fig. 12). The concentration is ~140 mmol/ℓ after 5 yr. The experimental chloride concentration—~80 mmol/ℓ and (~120 mmol/ℓ) (Refs. 12 and 2, respectively)—are however a bit lower. Based on these results, we could assume that more of the water is transported as water vapor in the experiment than in the model, because the chloride ion should be quite inert, and thus it should be carried along the liquid water. The experimental results are not from the fracture positions, which would also decrease the amount of diffused chloride.

Both sodium and sulfate ions diffuse out from the bentonite due to increasing sodium concentrations in the bentonite resulting from cation exchange reactions (Figs. 13 and 14) and an initial increase in sulfate concentrations caused by the dissolution of gypsum (Fig. 15). Sodium concentration in the model is from 130 mmol/ℓ near the heater and 100 mmol/ℓ near the rock surface and in the experimental analyses[12] corresponding values are 110 to 95 mmol/ℓ. The concentration profile is definitely affected by the fact that the measured block was not from the fracture position. Sulphate concentration is ~10 mmol/ℓ, which is in good agreement with the experimental values.[12]

Magnesium concentrations in the bentonite increase due to diffusion from groundwater and cation exchange reaction. Potassium concentrations increase initially due to diffusion, but later, the direction of diffusion turns outward to the rock matrix as the concentration in the bentonite exceeds that of the groundwater due to cation exchange.

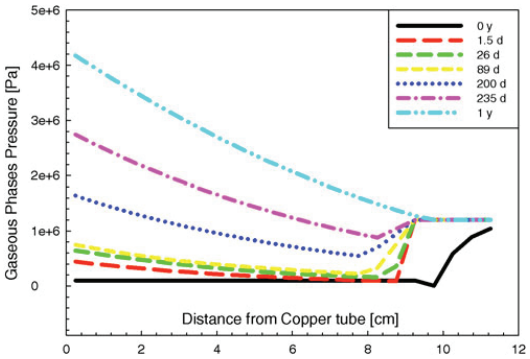

Fig. 5. Gaseous phases (air and water vapor) pressure as a function of distance from the copper tube, over time.

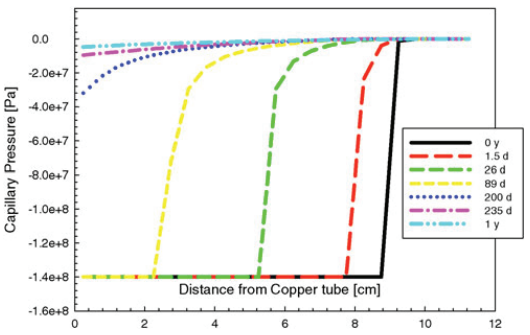

Fig. 6. Capillary pressure as a function of distance from the copper tube, over time.

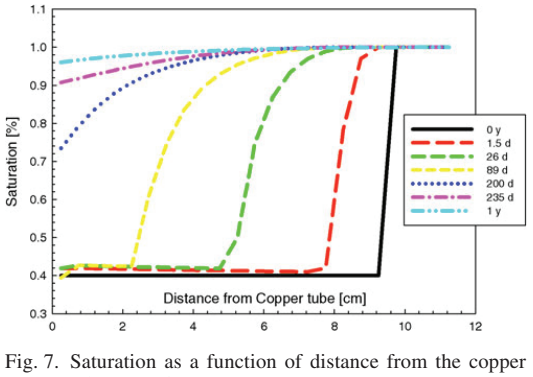

Fig. 7. Saturation as a function of distance from the copper tube, over time.

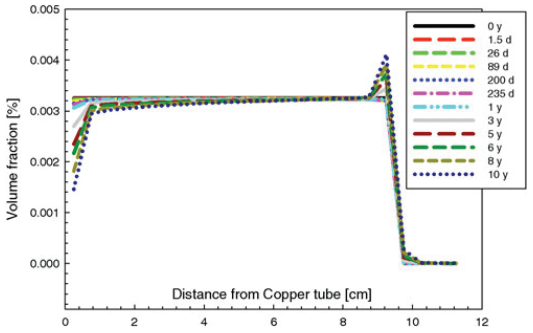

Fig. 8. Chalcedony volume fractions as a function of distance from the copper tube, over time.

V.D. Cation Exchanger

Because of numerical convergence problems, it was necessary to consider the aqueous sodium concentration as an adjustable parameter. Consequently, this procedure affected the initial cation exchange equilibria so that the amount of exchangeable sodium increased from its measured value of ~70% (equivalent fraction) (Ref. 2) to ~80%. An opposite effect resulted for the divalent cations. This obviously hampers a comparison of the model and experimental cation exchange results.

The cation exchanger composition changes are shown in Figs. 14, 16, 17, and 18 as meq/100 g. It appears that calcium enters the cation exchanger and sodium exits (Figs. 14 and 16). The calcium levels, however, are higher near the bentonite-rock interface owing to anhydrite precipitation near both interfaces (copper and rock) and incoming calcium from the groundwater. Thus, the concentrations are not balanced equally and equilibrium is not reached within the modeled time. The cation exchanger changes to calcium type, and because there is more calcium in incoming groundwater than in bentonite pore water the cation exchanger takes more calcium from the bentonite-rock interface. Consequently, not so much calcium reaches the other end, which is the main reason for the disequilibrium. The sodium content decreases with the changes highest near the rock surface (Fig. 14). Potassium and magnesium also exit the exchanger and are replaced by calcium (Figs. 17 and 18). The experimental values[2] show us a different kind of profile with only minor changes in the equivalent fractions of sodium and calcium.

VI. DISCUSSION (VALIDITY)

Whereas the majority of the results appear to be qualitatively correct, their validity is open to a number of questions. The following limitations were applied in the model:

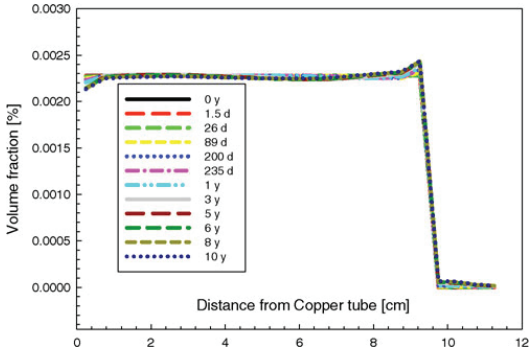

Fig. 9. Calcite volume fractions as a function of distance from the copper tube, over time.

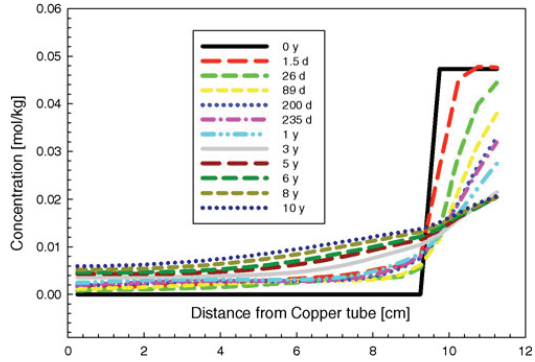

Fig. 11. Total aqueous calcium component concentrations as a function of distance from the copper tube, over time.

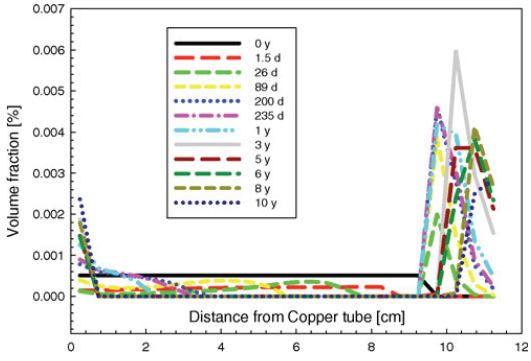

Fig. 10. Anhydrite volume fractions as a function of distance from the copper tube, over time.

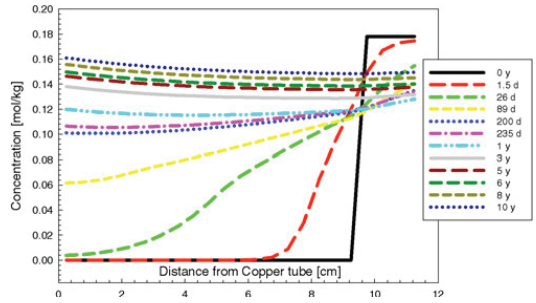

Fig. 12. Total aqueous chloride component concentrations as a function of distance from the copper tube, over time.

1. The calculation time of the model was limited to 10 yr since the principal aim was to obtain calculated results that were as close as possible to the measured values, and because the LOT-A2 parcel test duration was ~6 yr.

2. Montmorillonite was chosen as the insoluble solid phase with constant ion exchange capacity. Temperature might affect the ion exchange capacity of bentonite, but the experimental results do not give confirmation for this.[2] The hot blocks are more variable and have a little bit higher mean values than the cold part (~73.6 to 77 meq/100 g). If the montmorillonite would dissolve, the ion exchange capacity would change.

3. The calculations were carried out in one dimension to simplify the system. The grid was thus created with one cell only in the y and z directions and with multiple cells in the x direction.

4. It was assumed that the bentonite was already swelled to fill the hole completely at the beginning and that the saturation did not cause swelling anymore.

Topics 1 and 3 are planned to be improved by the present program versions, while topics 2 and 4 are more challenging and require updated program versions or application of a more advanced model, which possibly are new combinations of present programs of the TOUGH family.

The model itself also contained the following limitations:

1. A major source of uncertainty is the fact that the model does not take into account the three different water types present in bentonite: the interlayer water, double layer water, and free water. The model assumes that all water content is accessible to solutes for transport and geochemical reactions.

2. THC predicted concentrations systematically overestimate measured values near the heater and show

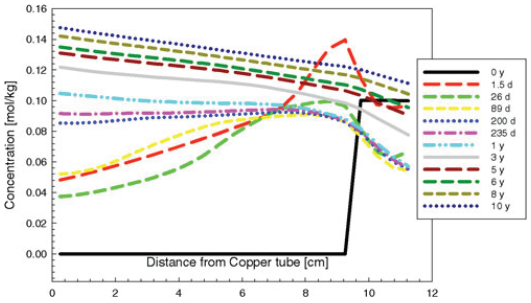

Fig. 13. Total aqueous sodium component concentrations as a function of distance from the copper tube, over time.

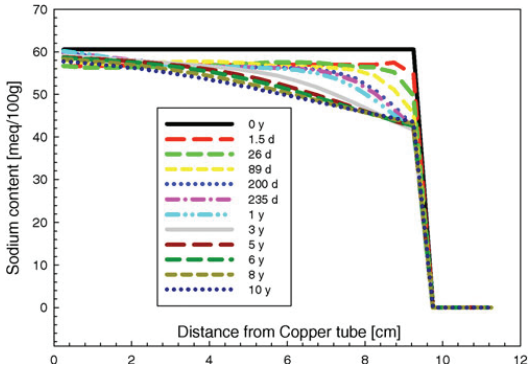

Fig. 14. Sodium content (meq/100 g) in the cation exchanger as a function of distance from the copper tube, over time.

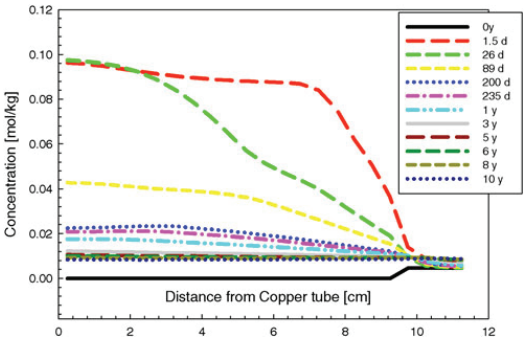

Fig. 15. Total aqueous sulfate component concentrations as a function of distance from the copper tube, over time.

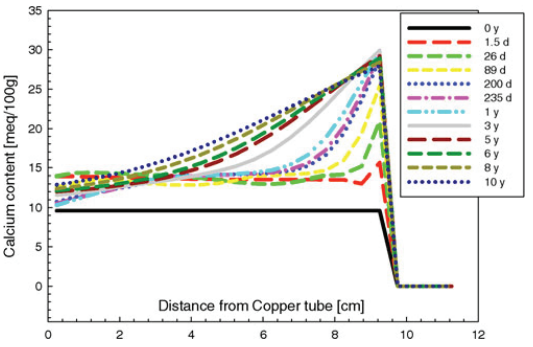

Fig. 16. Calcium content (meq/100 g) in the cation exchanger as a function of distance from the copper tube, over time.

probably sharper gradients than those of measured data. This is because the model does not take into account bentonite swelling/shrinkage (or water evaporation near the copper-bentonite interface).

3. TOUGHREACT does not include surface complexation, i.e., protonation/deprotonation of surface edge sites.

4. Even though THC processes are expected to alter the capillary strength parameter $(1/\alpha)$, this effect has not been included in these models.

5. The diffusion coefficient is assumed constant for all ions and neutral molecules. This is closely coupled to topic 1.

6. All material parameters are constant, and functions such as temperature cannot be added.

7. The model was 1-D, whereas a realistic model should be 3-D.

Again, some topics—such as topic 7—are more easily corrected, but topics 1 and 5 are really solved only when a good microstructural model of bentonite is available. Surface complexation (topic 3) is quickly becoming a part of most common modeling programs and will be in the next version of TOUGHREACT. Models including both THC and THM (where M = mechanical) capabilities are under construction (topic 2). The lack of suitable data, such as in topics 4 and 6, is not solved by modeling but instead needs additional experimental work to be carried out.

Furthermore, data limitations of THC modeling include:

1. General lack of kinetic data for environmental and geochemical processes is a major drawback.

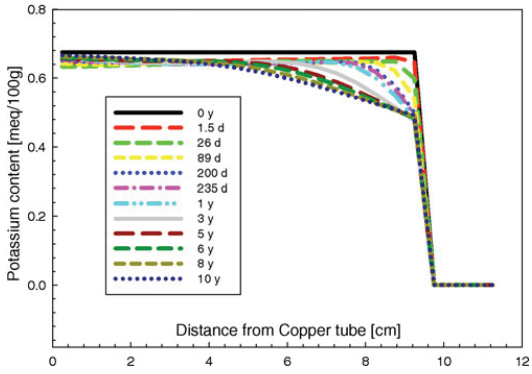

Fig. 17. Potassium content (meq/100 g) in the cation exchanger as a function of distance from the copper tube, over time.

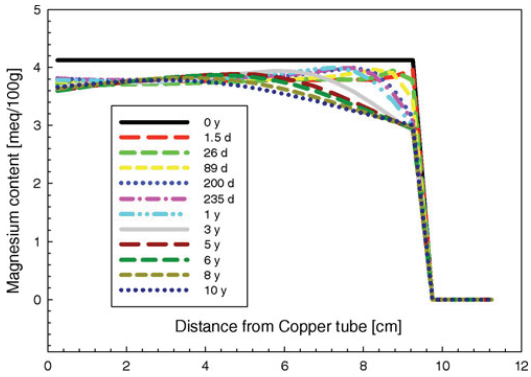

Fig. 18. Magnesium content (meq/100 g) in the cation exchanger as a function of distance from the copper tube, over time.

Laboratory-based values are not necessarily applicable to the field situation.

2. It is not well understood how to handle a lack of equilibrium among redox couples.

3. Reactive surface areas and grain radii of minerals are highly uncertain.

4. Uncertainties in thermodynamic data, especially at higher temperatures, may exist.

5. Van Genuchten function parameters for partial saturation in rock and bentonite are not well known, and no data are given for different temperatures.

VII. CONCLUSIONS

LOT parcel test A2 has been modeled. The results show similarity with experimental data. However, the results are open to question, and further study is needed to confirm their validity. The parameters used should be applied to other modeling programs (e.g., PHREEQC) and the results compared with those of TOUGHREACT.

However, even the experimental results can be questioned. There are different methods to measure, for example, cation exchange, which yields different results. There could be many factors that cause uncertainty in the experiments, such as calibration of sensors, transportation of bentonite block, air affecting the bentonite after lifting, etc. The differences between model and experiment can, for example, be parameters, the in-built model formulas, or the difference between the model and the real system. Thus, the experimental system should be thoroughly planned and documented, and the model boundaries made as realistic as possible.

The bentonite structure and waters affecting the system are under large uncertainty, for example, because the bentonite microstructure and behavior are not well known. Our model also assumes that the bentonite is swelled at the beginning, which is not the case in a real experiment. When water contacts bentonite, the bentonite near the waterfront starts to swell and loses its density. Thus, there will be a soft mass (at the water-bentonite boundary) at the beginning where different behavior can occur. This can affect the bentonite saturation and accelerate it. When the bentonite is saturated enough and swells, this soft mass comes to contact the rock interface and the exterior of the bentonite block starts to tighten again. If we would like to take this into account, we would need to include mechanical phenomena in the model. Our THC model could be improved by incorporating mechanical and geochemical coupling to account for porosity changes caused by swelling phenomena. This would lead to fully coupled THMC models, which is our goal for the coming years.

Additionally, based on the results of chloride compared to experimental results,[12] we could assume that more of the water is transported as water vapor in the experiment than in the model because the chloride ion should be quite inert and thus should be carried along the liquid water. The experimental results are not necessarily from the fracture positions, which would decrease the amount of diffused chloride. The sulfate concentrations, however, in the experiment[2] and in the model seem to indicate that anhydrite precipitates somewhere near the heater, which also means calcium precipitation. According to these results, one could say precipitation of anhydrite is going to happen, but on the other hand it is hard to say if this precipitation is irreversible or reversible during longer time periods.

According to the modeling results, the bentonite changes more to the calcium form. When this happens, it

means that the stability of bentonite improves, but the swelling pressure decreases. This means that in dilute waters, bentonite does not dissolve so easily, which is a good property when it happens in the outer parts of the bentonite near the bentonite-rock interface.

The cation exchanger acts differently than in the experiment.[2] In the model, the cation exchanger has the tendency to change to calcium form, contrary to the experimental observations, which show no change in exchangeable cations except for the hot end where lowering of exchangeable sodium takes place. The mismatch between model and observed results may be attributable to the definition of the model boundary conditions, to the fact that the temperature dependence of cation exchange selectivities is unknown, and also to the initial chemical composition of the cation exchanger in the model, which deviates 10% from the reported experimental composition.

The model is designed so that the water in the bentonite is very dilute, and the ion exchanger is filled according to that.[10] This is not, however, the case in real bentonite pore water, where there is, for example, more sulphate in bentonite pore water than in groundwater. This can cause some difference in the results in short-time calculations when the equilibrium is not fully reached. In this model the time period was 10 yr and the system did not yet reach chemical equilibrium.

We have to also remember that the changes in bentonite in a real repository would take longer because the changes in the bentonite are lesser elsewhere than in the fracture position after the swelling seals the deposition hole. This is probably the case in the experimental results, where there is not much change in cation exchanger,[2] which may affect all the results. Thus, we are going to create a two-dimensional model where the fracture position and the changes elsewhere can be seen and compared better with the experiment.

Finally, dramatic changes in bentonite do not occur, but there is still need for further modeling and more thorough research of partially saturated bentonite (more experimental data are needed), especially since very little is known about this topic and the model will be applied to Olkiluoto conditions later on. It can take several years to develop a model accurate enough to model the partial saturation of the final repository, and this project will be a long-term one.

ACKNOWLEDGMENTS

The study is jointly funded by the Finnish Research Program on Nuclear Waste Management (KYT2010) and VTT Technical Research Centre of Finland. The reference material is provided courtesy of Clay Technology AB. Many thanks to our colleague M. Tanhua-Tyrkkö for our many fruitful discussions.

REFERENCES

1. "Long-Term Safety for KBS-3 Repositories at Forsmark and Laxemar—A First Evaluation. Main Report of the SR-Can Project," SKB-TR-06-09, p. 620, SKB—Swedish Nuclear Fuel and Waste Management Company (2006).

2. O. KARNLAND et al., "LOT Project—Long Term Test of Buffer Material. Parcel A2 Field and Laboratory Draft Report," p. 117, Clay Technology AB (2008).

3. B. PASTINA and P. HELLÄ, "Expected Evolution of a Spent Nuclear Fuel Repository at Olkiluoto," Posiva-2006-05, p. 405, Posiva Oy (2008).

4. P. WERSIN, "Geochemical Modelling of Bentonite Porewater in High-Level Waste Repositories," *J. Contam. Hydrol.*, **61**, 405 (2003).

5. O. KARNLAND, S. OLSSON, and U. NILSSON, "Mineralogy and Sealing Properties of Various Bentonites and Smectite-Rich Clay Materials," TR-06-30, p. 117, SKB (2006).

6. R. ARTHUR and W. ZHOU, "Reactive-Transport Model of Buffer Cementation," 2005:59, p. 36, SKI (2005).

7. A. C. JACINTO, M. V. VILLAR, R. GÓMEZ-ESPINA, and A. LEDESMA, "Adaptation of the Van Genuchten Expression to the Effects of Temperature and Density for Compacted Bentonites," *Appl. Clay. Sci.*, **42**, 575 (2009).

8. "PetraSim User Manual," Thunderhead Engineering (2005).

9. J. L. PALANDRI and Y. K. KHARAKA, "A Compilation of Rate Parameters of Water-Mineral Interaction Kinetics for Application to Geochemical Modeling," Open File Report 2004-1068, p. 64, U.S. Geological Survey (2004).

10. C. TOURNASSAT et al., "Two Cation Exchange Models for Direct and Inverse Modelling of Solution Major Cation Composition in Equilibrium with Illite Surfaces," *Geochim. Cosmochim. Acta*, **71**, 1098 (2007).

11. A. ITÄLÄ, "Chemical Evolution of Bentonite Buffer in a Final Repository of Spent Nuclear Fuel During the Thermal Phase," MS Thesis, Tampere University of Technology (2009).

12. A. MUURINEN, "Chemical Conditions in the A2 Parcel of the Long-Term Test of Buffer Material in Äspö (LOT)," Working Report 2006-83, p. 23, Posiva Oy (2006).

PUBLICATION II

Lot A2 test, THC modelling of the bentonite buffer

In: Physics and Chemistry of the Earth (2011), Part A/B/C 2011, Vol. 36, Issues 17-18, pp. 1830–1837.

https://doi.org/10.1016/j.pce.2011.10.020

Physics and Chemistry of the Earth 36 (2011) 1830–1837

Contents lists available at SciVerse ScienceDirect

Physics and Chemistry of the Earth

journal homepage: www.elsevier.com/locate/pce

Lot A2 test, THC modelling of the bentonite buffer

Aku Itälä *, Markus Olin, Jarmo Lehikoinen

VTT Technical Research Centre of Finland, P.O. Box 1000, FI-02044 VTT, Finland

ARTICLE INFO

Article history:
Available online 13 October 2011

Keywords:
THC
Modelling
Cation exchange
Nuclear waste
Heat transport
Bentonite

ABSTRACT

Finnish spent nuclear fuel is planned to be disposed of deep in the crystalline bedrock of the Olkiluoto island. In such a repository, the role of the bentonite buffer is considered to be central. The initially unsaturated bentonite emplaced around a spent-fuel canister will become fully saturated by the groundwater from the host rock. In order to assess the long-term safety of a deep repository, it is essential to determine how temperature influences the chemical stability of bentonite. The aim of this study was to achieve an improved understanding of the factors governing the thermo-hydro-chemical evolution of the bentonite buffer subject to heat generation from the disposed fuel and in contact with a highly permeable rock fracture intersecting a canister deposition hole.

TOUGHREACT was used to model a test known as the long-term test of buffer material adverse-2, which was conducted at the Äspö hard rock laboratory in Sweden. The results on the evolution of cation-exchange equilibria, bentonite porewater chemistry, mineralogy, and saturation of the buffer are presented and discussed. The calculated model results show similarity to the experimental results. In particular, the spatial differences in the saturation and porewater chemistry of the bentonite buffer were clearly visible in the model.

1. Introduction

Finnish spent nuclear fuel is planned to be disposed of according to the KBS-3 (KärnBränsle Säkerhet) concept in a deep repository planned to be constructed at a depth of 420 m in the crystalline bedrock of the Olkiluoto island (Fig. 1). In the KBS-3 concept, the spent nuclear fuel bundles are contained in copper-covered cast iron canisters, which are surrounded by a compacted bentonite buffer. Compacted bentonite clay is considered a suitable material for limiting the migration of radionuclides in case of canister breach, for providing a mechanical and chemical zone of protection around the canister and high enough thermal conductivity to efficiently dissipate heat emitted by the spent fuel.

Upon saturation with groundwater, bentonite swells and seals the deposition hole. However, thermal, hydrological, mechanical and chemical processes taking place in the bentonite buffer over thousands of years may change the properties of the bentonite to the extent that long-term safety is compromised. Therefore, sufficient long-term stability of this material must be demonstrated. Due to inaccessible time scales for relevant experiments, the assessment of material stability in a repository needs to be based on numerical modelling.

In this work, we concentrated on the modelling of the effects of temperature on the chemistry and hydrology of initially partially saturated bentonite using an integrated thermo-hydro-chemical (THC) model.

The Long Term Test of Buffer Materials (LOT) A2 parcel experiment at the Äspö hard rock laboratory (HRL) in Sweden was considered (Karnland et al., 2009) in this work. Thermal and hydraulic gradients are known to generally promote mineral dissolution/precipitation reactions in the bentonite. For example, anhydrite is found to precipitate at elevated temperatures. Also, the incoming groundwater affects the bentonite porewater, which may, in turn, influence the mechanical properties of the bentonite. Consequently, this has to be taken into consideration in a performance assessment of the buffer.

The expected thermal phase in a KBS-3 repository will last for a few thousand years. The most significant mineral alterations are expected during the first one thousand years (Pastina and Hellä, 2008). The A2 test was carried out under more extreme temperature conditions than to be expected in an actual KBS-3 repository to accelerate the kinetically controlled mineral reactions and to compare the thermal load of the test to the expected KBS-3 conditions over several thousand years.

The aim of this study was to investigate thermal, hydraulic and chemical processes affecting the bentonite buffer. For this purpose, a computational model was designed to simulate the THC processes in the A2 test.

* Corresponding author. Tel.: +358 20 722 4673; fax: +358 20 722 6390.
E-mail address: aku.itala@vtt.fi (A. Itälä).

1474-7065/$ - see front matter © 2011 Elsevier Ltd. All rights reserved.
doi:10.1016/j.pce.2011.10.020

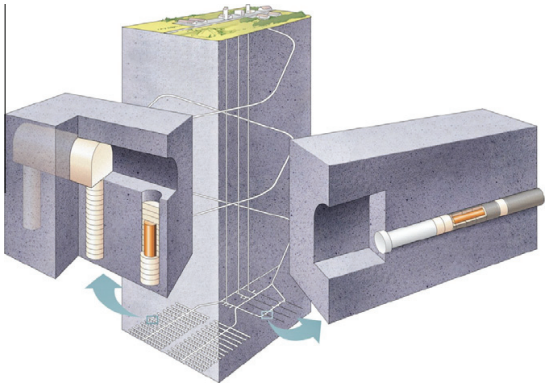

Fig. 1. The KBS-3 disposal concept displaying both the vertical (left) and horizontal (right) option (courtesy of Posiva Oy). The repository is located at a depth of 420 m. A deposition hole is 6–8 m deep depending on the type of spent fuel (Posiva, 2010).

2. Experimental

The A2 test at Äspö was carried out in crystalline rock at the depth of approximately 450 m from the ground surface. The water pressure was kept higher than the vapour pressure and the water inflow rate low enough to prevent piping erosion. However, the rate of water inflow was found too low and, consequently, it was decided to introduce external water via a supply hole to accelerate the progress of the experiment. The water pressure in the hole was about 1.2 MPa and the water supply was connected to the borehole through titanium tubes. The water pressure was kept constant throughout the test period (Karnland et al., 2009). The dimensions of the parcel test, illustrated in Fig. 2, are presented in Table 1. An internal heater was placed inside the lower parts of the copper tube with a maximum power of 2 kW (Fig. 2).

Table 1
Dimensions in LOT A2 parcel test (Karnland et al., 2009).

Borehole depth	4 m
Borehole diameter (nominal)	0.3 m
Emplaced parcel diameter	0.28 m
Copper tube height	4.7 m
Heater diameter	0.108 m

The results from the parcel test were used as reference data for comparison with model results (Karnland et al., 2009). In the test, relatively small parcels (see Table 1 for the dimensions) were exposed to field conditions at Äspö HRL. The test series included three parcels with similar conditions to those expected in a vertical variant of the KBS-3 repository (KBS-3 V) and additional four parcels, which were exposed to more extreme temperature conditions. For the horizontal disposal option (KBS-3H), see Fig. 1.

The A2 parcel was placed in a vertical borehole, which was drilled into excavated, horizontal tunnels in granitic bedrock. In the parcel, MX-80 bentonite, considered by Posiva as the reference buffer material, was exposed to elevated temperatures (120–150 °C) and very high temperature gradients (4.5–5.0 °C/

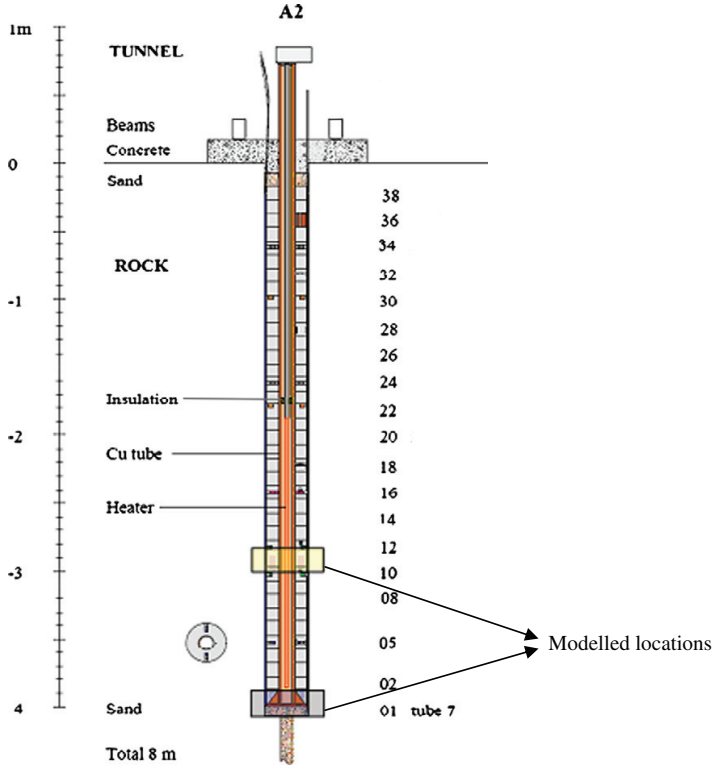

Fig. 2. Schematic drawing of the A2 test parcel (Karnland et al., 2009). Modelled locations are indicated by rectangles (the lower denotes the fracture and the upper is 1.1 m above the fracture). The numbers refer to the respective bentonite blocks. The water-supply hole was situated at the position "01".

cm) (considered to be extreme test conditions). The parcel diameter was smaller than that in a planned KBS-3 V spent-fuel repository to shorten the water-saturation period, to achieve a higher temperature gradient over the buffer material, to accelerate kinetically controlled processes, and to ease the uplift of the test parcel (Karnland et al., 2009). After approximately five to six years of exposure to extreme conditions, the test parcel was lifted and sectioned for examination.

According to Posiva (2010), the entire KBS-3 repository must be designed in such a manner that the maximum temperature allowed for the buffer remains below 100 °C (controlled by the cooling time of the fuel elements). In the A2 test, the maximum temperature was set to 120–150 °C. A five-year period in these conditions covers a significant portion of the estimated thermal load per canister in a KBS-3 V repository. However, the problem in estimating the implications of a thermal load is that the higher temperatures will lead to chemical reactions completely different from those at lower, actual temperatures in the repository. In addition, the modified chemical reaction rates are not balanced by respective changes in solute transport rate, which will eventually change the fluid-rock dynamics to differ clearly from those in real systems. Although the results from the experiments may not represent a realistic scenario, by modelling it is possible to increase our understanding of the coupled processes taking place in a repository system.

The main observations from the test included sulphate redistribution along the thermal gradient in heated blocks. Anhydrite was accumulated about 3–5 cm from the heater, whereas the peripheral parts were depleted in sulphates. The carbonate content decreased with increasing temperature in the heated parts. Dissolution/precipitation reactions had influenced the porewater composition and the cation-exchange equilibria. Some sodium had been replaced by calcium and magnesium in the inner parts of the heated blocks. The source of Mg was not identified. XRD data did not show evidence of a structural change of montmorillonite (Karnland et al., 2009). Detailed results from the experiment can be found in Muurinen (2006) and Karnland et al. (2009).

3. Model

3.1. Description

Processes occurring in the bentonite buffer in a spent-fuel repository depend on several factors, the complexity and couplings of which make their consideration in a single computational model highly challenging. Certain simplifications are, therefore, necessary. The aim was to develop a realistic model of the test, in which the heat-producing canister is surrounded by bentonite and a rock matrix, which contains a permeable fracture that intersects the deposition hole (Fig. 3). The model was axisymmetric with one symmetry axis located in the vertical midplane of the canister. Consequently, only one half of the canister was needed to be taken into account explicitly in the model (i.e., the hot part of the parcel).

The materials considered were the host rock, heater (with copper cover), fracture and bentonite (Fig. 3). The main component of the MX-80 bentonite is montmorillonite, which was assumed to act as an insoluble cation exchanger. The mineral precipitation and dissolution reactions were taken to contribute to changes in porosity and permeability. The gas phase consisted of water vapour and air, while the liquid phase consisted of water and dissolved aqueous species. Local equilibrium was assumed for all chemical reactions, except for mineral reactions, which were kinetically controlled.

The model grid was fairly coarse due to the complexity of the system and the significantly increased computational times required by finer grids (Fig. 3).

The properties of the host rock and fracture were defined such that they remain fully saturated at all times (no capillary pressure). The heater was considered chemically inert and was assigned a constant heat production rate of 780 W to simulate the temperature profile in the experiment. Initially, the bentonite had a gravimetric water content of 0.11 and a saturation of 0.40. It was allowed to interact with the granitic Äspö groundwater for ten years. The rightmost boundary cells in Fig. 3 were defined as having a constant chemical composition (i.e., Dirichlet boundary condition) from the borehole analyses reported in Karnland et al. (2009) at all times. The water pressure in the rock matrix and fracture was initially 1.2 MPa, and in the bentonite 101.3 kPa. For more detailed information about the boundary conditions, see Itälä (2009).

The model couples thermo-hydro-chemical processes, but no mechanical effects were considered. The aim was to match the model results as closely as possible to the experimental ones after up to six years of interaction without the use of any adjustable model parameters (except for the initial concentration of sodium in the bentonite porewater, cf. Section 3.3). The location of the water supply, which was realized using titanium tubes and valves, was changed during the experiment (after having reached the block 32 (Fig. 3)) (Karnland et al., 2009), which may have affected the experimental results. However, this was not taken into account in the model. The model was applied to obtain the spatio-temporal THC evolution of the bentonite.

3.2. Software

The model was created using the PetraSim v. 4.1.119 user interface of the TOUGHREACT v. 1.0 (Xu et al., 2004) program. The EOS3 equation of state of water was applied to calculate the two-phase flow in bentonite.

In TOUGHREACT, all flow and transport equations have the form of a generalized continuity equation. For more detailed information about the program, see Pruess et al. (1999) and Xu et al. (2004).

3.3. Parameters

The model parameters were taken from Bradbury and Baeyens (2002), Thunderhead Engineering (2005), Itälä (2009), Karnland et al. (2009) and Jacinto et al. (2009), except for the specific heat capacity of bentonite and the rock properties (Table 2). Some of the parameters, like the initial chemical composition of bentonite porewater, were calculated from the data in Itälä (2009).

The specific heat capacity (C_p) for each mineral, (taken from the background information for the THERMODDEM thermodynamic database (Blanc et al., 2007) adopted in this study), was used to calculate the C_p for anhydrous bentonite according to Gailhanou et al. (2007) considering an average temperature of 110 °C.

The mineralogical composition of the MX-80 bentonite is depicted in Table 3. No other mineral phases for the buffer were considered. Montmorillonite in the bentonite was taken to be a chemically insoluble cation exchanger (cation-exchange capacity 0.75 meq/g) due to the short experimental time and to the fact that no structural changes in montmorillonite were observed in the experiment (Karnland et al., 2009). Minerals in the rock were not taken into consideration in the model.

The mineral reaction kinetic data were taken from Palandri and Kharaka (2004), except for chalcedony, which was assumed to be at equilibrium at all times. The chemical compositions of the groundwater and cation exchanger are shown in Table 4.

The water-retention parameters used in the model can be found from Table 5 and the selectivity coefficients used for the cation-exchange reactions from Table 6.

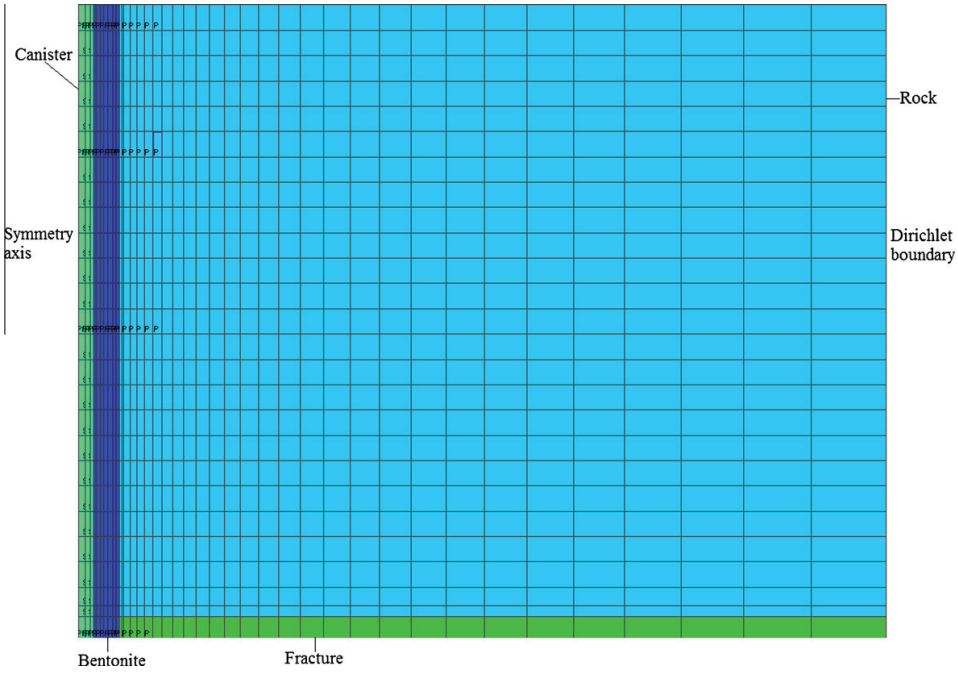

Fig. 3. Model grid. The computational cells on the left (light green) represent the simulated heat source of the experiment. The middle zone (dark blue) is bentonite. The horizontal part at the bottom is the fracture (dark green) and the rest is host rock (light blue). The radius and height of the axisymmetric model was 3.00 m and 2.35 m, respectively. The number of computational cells in the model was 962. (For interpretation of the references to colour in this figure legend, the reader is referred to the web version of this article.)

Table 2
Material parameters.

Parameter	Bentonite	Fracture	Heater[a]	Rock
Initial pressure (MPa)	0.1	1.2	NTP	1.2
Grain density (kg/m^3)	2750	2650	8960	2650
Molecular diffusion coefficient (m^2/s)	$2{\cdot}10^{-9}$			
Wet thermal conductivity (W/(m·C))	1.3	2.61	391.1	2.61
Dry thermal conductivity (W/(m C))	0.3			
Porosity	0.43	0.14	1×10^{-10}	0.01
Intrinsic permeability (m^2)	$3.0{\cdot}10^{-21}$	5.0×10^{-11}	0	1×10^{-19}
Specific heat (J/(kg C))	969	784	385	811
Initial saturation	0.4	1.0		1.0

[a] Assumed to have the properties of copper.

4. Results

The results are reported for two vertical locations: at the fracture level (0 m) and at 1.1 m above the fracture (see Fig. 2). Water intake to the bentonite occurs from the fracture and the rock matrix, the latter being significantly slower as mass transfer in the intact rock is governed by diffusion as opposed to advection in the fracture (see Table 2 for the 5-order-of-magnitude difference in permeability). The results are reported as a function of distance from the heater. In the figures, the first 9.6 cm on the abscissa is bentonite and the rest being either the host rock or the fracture.

4.1. Thermo-hydraulics

Some of the key physical model parameters, such as the temperature and water saturation, are briefly discussed. Fig. 4 shows the temperature and temperature gradient in the bentonite and in part of the rock matrix. It can be seen that the temperature is between 130 °C and 85 °C in the bentonite after only a few days. The radial temperature profile was almost constant at every distance from the fracture and after one year, the system attained a thermal steady state (Fig. 4). The initial degree of saturation in

Table 3
Initial mineral mass and volume fractions for MX-80 bentonite (simplified from Arcos et al. (2003)).

Minerals	Mass fraction (%)	Volume fraction (%)
Anhydrite/gypsum ($CaSO_4/CaSO_4{\cdot}2H_2O$)	0.34	0.23
Quartz (SiO_2)	15.00	8.97
Montmorillonite $((Na, Ca)_{0.3}(Al, Mg)_2Si_4O_{10}(OH)_2{\cdot}nH_2O)$	75.00	42.36
K-Feldspar ($KAlSi_3O_8$)	7.00	4.27
Calcite ($CaCO_3$)	0.70	0.40
Chalcedony (SiO_2)	0.96	0.57
Sum	100	56.7

Table 4
Groundwater (Karnland et al., 2009) and initial cation exchanger composition.

Variable	Groundwater (mmol/l)	Cation exchanger (equivalent fraction)
Na^+	100	0.87
K^+	0.28	0.02
Ca^{2+}	47.3	0.08
Mg^{2+}	2.4	0.03
Cl^-	178	
$SO4_2^-$	4.6	
HCO_3^-	0.44	
Al^{3+}	Traces	
H_4SiO_4(aq)	Traces	
pH	6.9	

Table 5
Water-retention parameters. The van Genuchten model was selected for the bentonite (Jacinto et al., 2009) and the Fatt-Klikoff model for the rock/fracture. See Pruess et al. (1999) for model details.

Variable	Bentonite	Fracture/Rock
λ	0.338	
S_{lr}	0	0.999
S_{ls}	1.0	
S_{gr}	0.0	
P_0	14.1 MPa	
P_{max}	140 MPa	

Table 6
Cation-exchange selectivity coefficients for MX-80 bentonite (Bradbury and Baeyens, 2002).

Selectivity	Value
$K_{Na/K}$	4.0
$K_{Na/Ca}$	2.6
$K_{Na/Mg}$	2.2

bentonite was 40%, and in the granitic fracture and rock 100%. The bentonite was calculated to saturate fully within 200 days next to the fracture and to over 93% within 1.5 years at a distance of 1.1 m above the fracture (Fig. 5). This is in agreement with the experimental observations. Porosity changes (not shown in the graphs) were practically negligible.

4.2. Mineralogy

Chalcedony was found to dissolve near the heater and precipitate close to the rock surface (Fig. 6) due to the difference in solubility at different temperatures. The changes are slightly faster next to the fracture. Fig. 7 shows the anhydrite concentration profile. It appears that when sulphate is diffusing out from the bentonite and calcium is coming in from the rock, anhydrite precipitates near the bentonite-rock interface on the rock side. Also, anhydrite starts to precipitate near the heater due to the high temperature. Precipitation occurs more slowly with increasing vertical distance from the fracture. Some calcite appears to dissolve near the heater, more with increasing distance from the fracture (Fig. 8), which affects the concentration of calcium and carbonate ions. Gypsum was calculated to dissolve within a couple of days, whereas quartz and K-feldspar were virtually non-reactive during the whole model period (10 a) and would clearly need a longer time to dissolve or precipitate.

4.3. Aqueous chemistry

This section presents the calculated evolution for the total aqueous concentration of some of the primary species in bentonite

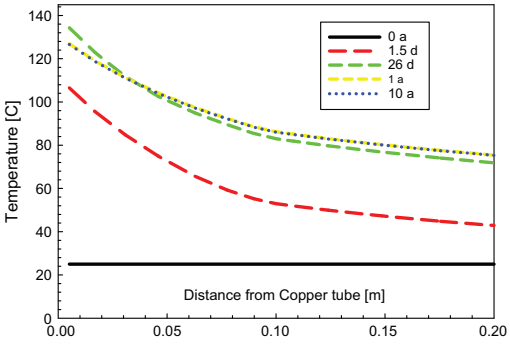

Fig. 4. Temperature evolution as a function of distance from the heater at various times. The final profile is obtained soon after 26 days.

porewater and in part of the granitic rock. The species reported are Na^+, Ca^{2+}, Cl^- and SO_4^{2-} as they are responsible for the greatest changes in mineralogy and cation-exchange equilibria in the bentonite. The calcium concentration in the bentonite, shown in Fig. 9, is seen to increase with time next to the fracture, but remains constant at 1.1 m above the fracture. This is due to cation exchange and lesser ingress of groundwater from the low-permeability rock. The chloride concentration increases with saturation and its diffusion continues even after ten years (Fig. 10). The chloride concentration becomes lower with increased distance from the fracture, which is due to the slower water supply from the rock.

Both sodium and sulphate ions diffuse out from the bentonite (Figs. 11 and 12) due to the increasing sodium concentration in the bentonite resulting from cation exchange (Figs. 13 and 14) and increase in sulphate concentration caused by the dissolution of gypsum. Increased calcium ingress next to the fracture changes bentonite progressively to calcium form due to cation exchange. The different permeability for the rock and fracture seems to affect the rate of depletion of sulphate in bentonite, since the sulphate concentration appears to increase as a function of distance from the fracture. The magnesium and potassium concentrations in bentonite increase due to diffusion from groundwater and subsequent cation exchange. The potassium concentration in the bentonite porewater is found to exceed that in the groundwater (not shown). The pH of the porewater tends towards a slightly alkaline value (7.3) due to the high temperature and lowered ion product of

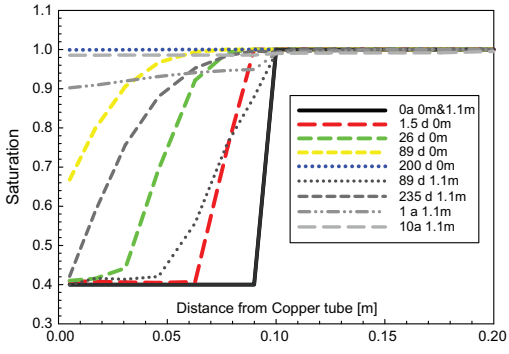

Fig. 5. Saturation as a function of distance from the heater at various times. The two positions (0 m and 1.1 m) differ clearly from each other at early times due to significantly different rock permeabilities.

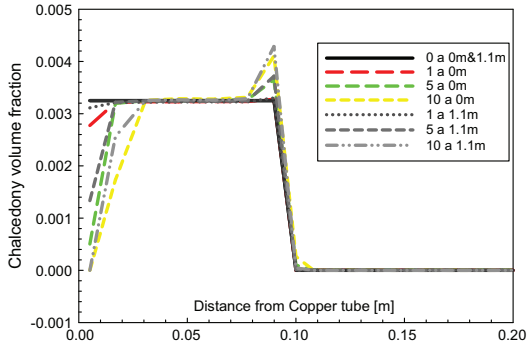

Fig. 6. Chalcedony volume fraction as a function of distance from the heater at various times. The vertical position is observed to cause only minor differences. The main factors governing the dissolution rate are the temperature and the rate of mass exchange with the surrounding rock, the latter being significantly faster near the fracture.

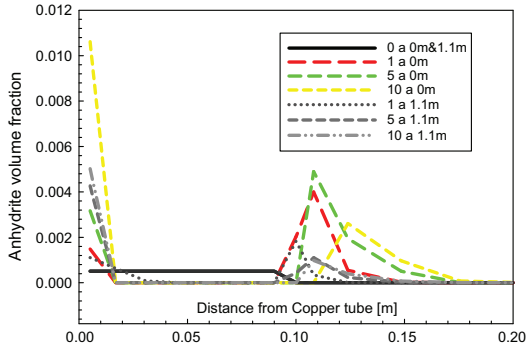

Fig. 7. Anhydrite volume fraction as a function of distance from heater at various times. The vertical position is seen to cause notable differences. At the fracture plane, the changes are much more significant due to faster mass transfer.

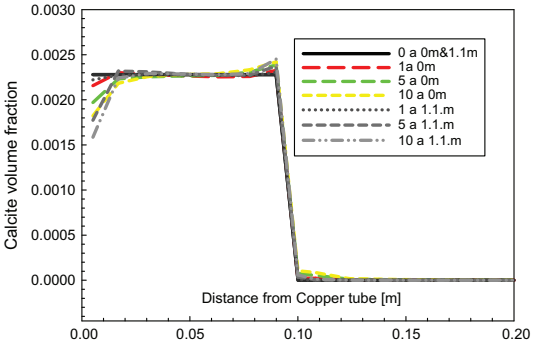

Fig. 8. Calcite volume fraction as a function of distance from the heater at various times. The vertical position is seen to cause but minor differences. Calcite dissolution is driven by reaction kinetics, on which the vertical position has only a small effect.

water (neutral pH at the elevated temperatures considered here would be around 6). This pH is not considered hazardous to the chemical stability of bentonite *per se*.

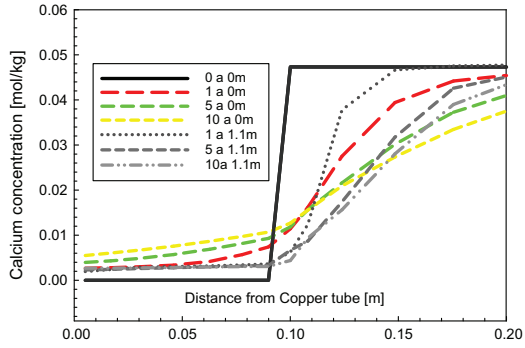

Fig. 9. Total aqueous calcium concentration as a function of distance from the heater at various times. Close to the fracture, the calcium profile extends farther into the rock due to faster mass transfer.

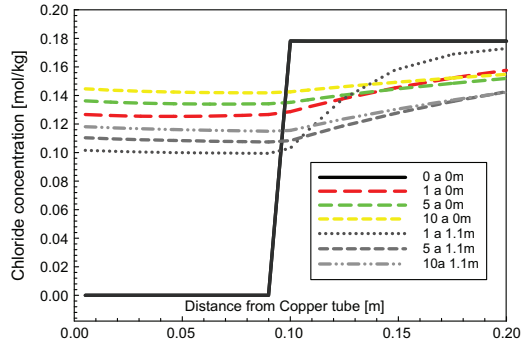

Fig. 10. Total aqueous chloride concentration as a function of distance from the heater at various times. The chloride concentration is seen to increase towards the fracture due to faster mass transfer.

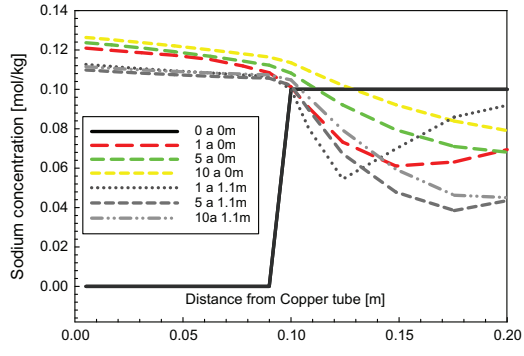

Fig. 11. Total aqueous sodium concentration as a function of distance from the heater at various times.

4.4. Cation exchange

Due to numerical convergence problems, it was necessary to consider the aqueous sodium concentration in the bentonite pore-water as an adjustable parameter. This affected the initial cation-exchange equilibria so that the amount of exchangeable sodium

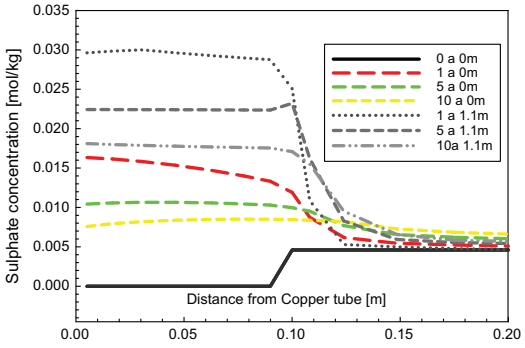

Fig. 12. Total aqueous sulphate concentration as a function of distance from the heater at various times. The distance from the fracture has a pronounced effect on the sulphate concentration, which is much lower close to the fracture due to higher fracture permeability. Sulphate from dissolved anhydrite/gypsum equilibrates faster near the fracture.

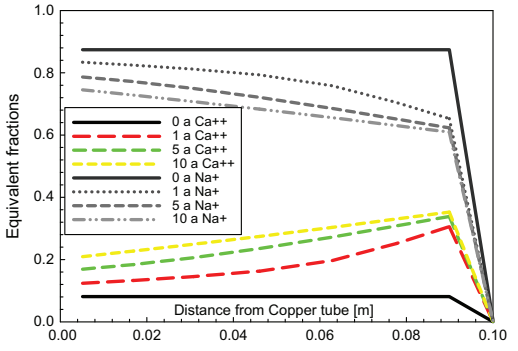

Fig. 13. Exchangeable sodium and calcium as a function of distance from the heater at the fracture level at various times. The calcium content is seen to decrease, while that of sodium to increase. The steady state is yet to be attained.

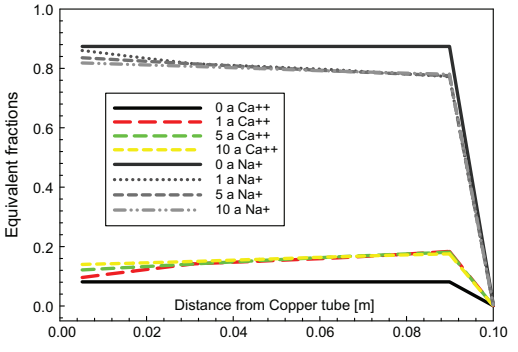

Fig. 14. Exchangeable sodium and calcium as a function of distance from the heater at 1.1 m above the fracture at various times. The changes are observed to be smaller than at the fracture level.

increased from its observed value of about 70% (equivalent fraction) (Karnland et al., 2009) to about 87%. An opposite effect resulted for the divalent cations. This obviously hampers a quantitative comparison of the model and experimental results.

In bentonite, sodium, potassium and magnesium are found to exchange for calcium (see Figs. 13 and 14 for exchangeable sodium and calcium). The concentration changes for potassium and magnesium are very small (not shown) compared to sodium and calcium. Anhydrite precipitation near the heater affects cation exchange, but the main reason for the difference between the heater-bentonite and bentonite-rock interfaces is the incoming calcium from the groundwater. Consequently, a lower aqueous calcium concentration is calculated near the heater in comparison to the bentonite-rock interface, which is the reason for the concentration gradient. The extent of cation exchange lessens as a function of distance from the fracture.

In the model, the cation exchanger has the tendency to change to calcium form, contrary to the experimental observations, which show no change in exchangeable cations, except for the hot end, where a slight lowering of exchangeable sodium takes place. This difference between observed and model results could be attributable to the above-mentioned adjustment of the sodium concentration in the bentonite porewater. The chemical changes in the experiment also indicate that mineral alterations were very slow after the bentonite was saturated. Also, the cation-exchange selectivity coefficients for compacted bentonite may have differed from those determined for uncompacted bentonite, which were used in this work (Bradbury and Baeyens, 2002).

5. Conclusions

In this work, an attempt was made to interpret the experimental results from the LOT A2 parcel test at the Äspö HRL in Sweden using the integrated thermo-hydro-chemical model, TOUGHREACT.

The initially unsaturated bentonite was calculated to saturate to over 93% within 1.5 years up to 1.1 m from the hydrating rock fracture, which is in line with experimental observations. The most prominent mineral reactions were calculated to be total depletion of gypsum, and enrichment of anhydrite near the heater. However, this probably cannot be directly compared to the expected repository conditions, in which the temperature stays below 100 °C, and which may give rise to different mineral reactions. The chemical composition of the bentonite porewater was found to reflect changes in mineralogy and cation exchange. However, the model results for cation exchange in bentonite did not agree with the experimental results. In the model, the cation exchanger has the tendency to change to calcium form, contrary to the experimental observations, which show no change in exchangeable cations except for the hot end, where decrease of exchangeable sodium takes place. The mismatch between model and observed results may be attributable to the definition of the model boundary conditions, to the initial chemical composition of the cation exchanger in the model, which deviates markedly from the reported experimental composition, and to the fact that the cation-exchange selectivities used in this work may have been unfit for compacted bentonite. Future attempts to model the present system would benefit from, for example, the consideration of selectivity coefficients determined for compacted material and use of alternate water-retention models for bentonite.

The model results are similar to the experimental results presented in Muurinen (2006) and Karnland et al. (2009). They are also consistent with the model results in Itälä (2009). Overall, no dramatic changes in bentonite chemistry were calculated to occur in ten years of simulation time. However, there is a definite need for further modelling to improve the agreement with experimental results and, ultimately, to be able to predict the THC evolution of the KBS-3 repository near field over time scales relevant to long-term safety.

A remaining challenge is also to implement mechanical material response for compacted bentonite into an existing THC model to take into account potential deformation and decrease in material density due, for example, to expansion to fill buffer emplacement gaps and to material loss by an extremely dilute post-glacial melt water (Posiva, 2010). The latter threat may become reality, should the level of exchangeable divalent cations in bentonite not be high enough at the onset of the post-glacial phase.

Acknowledgments

This study was jointly funded by the Finnish Research Programme on Nuclear Waste Management (KYT2010) and VTT (Technical Research Centre of Finland). The reference material was provided courtesy of Clay Technology AB. Many thanks to our colleagues Dr. Kari Rasilainen and Ms. Merja Tanhua-Tyrkkö for many discussions that helped to improve the manuscript.

References

Arcos, D., Bruno, J., Karnland, O., 2003. Geochemical model of the granite-bentonite groundwater interaction at Äspö HRL (LOT experiment). Applied Clay Science 23 (1–4), 219–228.

Blanc, P., Lassin, A., Piantone, P., 2007. THERMODDEM – A database devoted to waste minerals ⟨http://thermoddem.brgm.fr⟩.

Bradbury, M.H., Baeyens, B., 2002. Porewater chemistry in compacted re-saturated MX-80 bentonite: physico-chemical characterisation and geochemical modelling. PSI Berich Nr. 02–10. Villigen, Switzerland.

Gailhanou, H., van Miltenburg, J.C., Roges, J., Olives, J., Amouric, M., Gaucher, E.C., Blanc, P., 2007. Thermodynamic properties of anhydrous smectite MX-80, illite IMt-2 and mixed-layer illite-smectite ISCz-1 as determined by calorimetric methods. Part I: Heat capacities, heat contents and entropies. Geochimica et Cosmochimica Acta 71, 5463–5473.

Itälä, A., 2009. Chemical evolution of bentonite buffer in a final repository of spent nuclear fuel during the thermal phase. VTT Publications No. 721. Helsinki: VTT ⟨http://www.vtt.fi/inf/pdf/publications/2009/P721.pdf⟩.

Jacinto, A.C., Villar, M.V., Gómez-Espina, R., Ledesma, A., 2009. Adaptation of the van Genuchten expression to the effects of temperature and density for compacted bentonites. Applied Clay Science 42 (3–4), 575–582.

Karnland, O., Olsson, S., Dueck, A., Birgersson, M., Nilsson, U., Hernan-Håkansson, T., 2009. Long term test of buffer material at the Äspö hard rock laboratory. LOT Project. Final Report on the A2 Test Parcel. TR-09-29. Stockholm, Sweden: SKB.

Muurinen, A., 2006. Chemical conditions in the A2 parcel of the long-term test of buffer material in Äspö (LOT). Working Report 2006-83. Olkiluoto, Finland: Posiva Oy.

Palandri, J.L., Kharaka, Y.K., 2004. A compilation of rate parameters of water-mineral interaction kinetics for application to geochemical modeling. Open File Report 2004-1068. Menlo Park, California, USA: US Geological Survey.

Pastina, B., Hellä, P., 2008. Expected evolution of a spent nuclear fuel repository at Olkiluoto. Posiva-2006-05. Olkiluoto, Finland: Posiva Oy.

Posiva, 2010. TKS-2009. Nuclear waste management at Olkiluoto and Loviisa power plants review of current status and future plans for 2010–2012. Olkiluoto, Eurajoki, Finland: Posiva Oy.

Pruess, K., Olderburg, C., Moridis, M., 1999. TOUGH2 User's Guide. Version 2.0. Berkeley, Earth Sciences Division, Lawrence Berkeley National Laboratory, University of California.

Thunderhead Engineering., 2005. PetraSim User Manual. Manhattan, Kansas, USA.

Xu, T., Sonnenthal, E., Spycher, N., Pruess, K., 2004. TOUGHREACT User's Guide: A simulation program for nonisothermal multiphase reactive geochemical transport in variably saturated geologic media. Berkeley, California, USA: Lawrence Berkeley National Laboratory.

PUBLICATION III

Na/Ca selectivity coefficients of montmorillonite in perchlorate solution at different temperatures.

In: MRS Symposium Proceedings (2012), Vol 1475, pp. 335-340.

Na/Ca selectivity coefficients of montmorillonite in perchlorate solution at different temperatures.

Aku Itälä and Arto Muurinen
VTT Technical Research Centre of Finland, Otakaari 3 K, Espoo, FI-02044 VTT, Finland

ABSTRACT

The Finnish spent nuclear fuel disposal is based on the Swedish KBS-3 concept in crystalline bedrock. The concept aims at long-term isolation and containment of spent fuel in copper canisters surrounded by bentonite buffer which mostly consists of montmorillonite. For the long-term modelling of the chemical processes in the buffer, the cation-exchange selectivity coefficients have to be known at different temperatures. In this work, the cation-exchange selectivity coefficients and cation-exchange isotherms were determined in batch experiments for montmorillonite at three different temperatures (25 ^{o}C, 50 ^{o}C and 75 ^{o}C). Five different ratios of $NaClO_4$/$Ca(ClO_4)_2$ were used in the experimental solutions. After equilibration the solution and montmorillonite were separated and the solution analysed to get the desired exchange parameters. The experiments were modelled with a computational model capable of taking into account the physicochemical processes that take place in the experiment.

INTRODUCTION

The Finnish plan for the disposal of spent nuclear fuel is based on the Swedish KBS-3 concept in crystalline bedrock. The concept aims at long-term isolation and containment of spent fuel assemblies in copper canisters with a nodular cast iron insert. The canisters are emplaced several hundred metres deep into the bedrock. Each canister will be separated from the bedrock by a bentonite clay layer (the buffer). The purpose of the buffer material is to maintain the integrity of the canisters by protecting them from detrimental THMBC (thermo-hydro-mechanical-biological-chemical) processes and to limit and retard the release of any radionuclides from the canisters, should any be damaged [1].

The MX-80 bentonite used in the experiments consists mainly of sodium montmorillonite and small amounts of other minerals [2]. The beneficial properties of bentonite are due to the properties of montmorillonite mineral. The Tetrahedral-Octahedral-Tetrahedral (TOT) layer structure of montmorillonite has a permanent negative charge, which is compensated by the exchangeable cations on the surfaces. In aqueous solutions these cations can exchange with those in a solution. The total permanent negative charge is called cation-exchange capacity (*CEC*). There are also surface edge sites which can protonate/deprotonate according to the pH in the surrounding solution. Those sites were not investigated in these experiments, however.

The cation form affects many essential properties of montmorillonite. In the KBS-3 concept, the maximum temperature limit has been decided to be 90 ^{o}C [3]. However, the selectivities for montmorillonite have mostly been studied at room temperatures. Therefore, it is essential to study how the temperature affects the cation-exchange selectivities.

EXPERIMENT

Na-Montmorillonite

MX-80 bentonite obtained from Wyoming (USA) in the powdered form was first purified to Na-montmorillonite form using a method described in Tributh and Lagaly [4] and Bergaya et al. [5]. The purification comprised the removal of large particles, dissolution of carbonates by acid treatment, dissolution of iron oxides, removal of organic material, changing to the sodium form and removal of the excess salt by washing and finally by dialysis. After the purification the montmorillonite was dried in the oven at 60 ^{o}C and finally placed in a vacuum freeze dryer. This purification is needed to enable accurate experimental results and to exclude any unnecessary complexes and mineral reactions in the montmorillonite.

Cation-exchange experiments

The cation-exchange experiments were carried out with the purified sodium montmorillonite powder in centrifugal tubes. The test series were carried out at the temperatures of 25 ^{o}C, 50 ^{o}C and 75 ^{o}C. Every test series included five Na/Ca concentration ratios with two parallel samples. Perchlorate background was chosen because it does not form complexes with ions [6]. In earlier studies [7-9] complexing has appeared to affect the cation-exchange selectivities.

In the tests, 1g ± 0.005g of sodium montmorillonite powder was allowed to react with approximately 30 ml of $NaClO_4/Ca(ClO_4)_2$ solution. The pH of the solution was 6.2±0.3 and total cation normality 0.1 ± 0.005 eq/l. In the tests at 25^{o}C, the tubes were shaken with rotation for five days. In the tests at 50 ^{o}C and 75 ^{o}C, the tubes were placed horizontally in a digital incubator with a shaker and left there for five days to equilibrate. At the end of the tests, the centrifugal tubes were centrifuged and the separated solution was ultra filtered with 10kDa filters for the analysis.

Analyses

The concentration of sodium and calcium were determined from the filtered solution using ICP-AES (Inductively Coupled Plasma Atomic Emission Spectrometry). It was estimated that the maximum analytical errors were ± 10 % for the sodium and calcium analyses. The *CEC* for Na-montmorillonite was determined using the copper-triethylenetetramine method [10]. The measured *CEC* was 0.96meq/g.

After the analyses, it was found that the amount of cations in the solutions was higher than in the original solutions. It was concluded that this is due to the Donnan exclusion effect [11] caused by the negatively charged montmorillonite layers which moves ions from the clay pores to the supernatant. Thus, the original solution had a larger volume where the dissolved ions could be than the final solution after centrifugation. This phenomenon had to be considered in the calculations.

RESULTS AND DISCUSSION

The Donnan exclusion effect [11] which caused the increase of cation concentration in the supernatant was taken into account by using an effective volume for the solution after centrifugation. The effective volume was set so that the cation charge [eq] in the solution at the beginning was equal to the cation charge [eq] at the equilibrium, as stated below.

$$\left(2c^{\mathrm{i}}_{\mathrm{Ca}} + c^{\mathrm{i}}_{\mathrm{Na}}\right)V_{\mathrm{total}} = \left(2c^{\mathrm{e}}_{\mathrm{Ca}} + c^{\mathrm{e}}_{\mathrm{Na}}\right)V_{\mathrm{effective}} \quad (1)$$

where i refers to the known initial value and e to the measured equilibrium condition, V_{total} is the total liquid volume at the beginning, $V_{\mathrm{effective}}$ is the used effective volume, and c refers to concentration.

The amount of sodium and calcium in the montmorillonite was calculated from the mass balance (equation 2 and 3). The decrease in calcium concentration indicates how much calcium had gone inside the exchanger. The original amount of sodium in the exchanger was known to be 0.96meq/g (*CEC*).

$$2\left(c^{\mathrm{i}}_{\mathrm{Ca}}V_{\mathrm{total}} - c^{\mathrm{e}}_{\mathrm{Ca}}V_{effective}\right) = \beta_{Ca}(CEC \cdot m_{montmorillonite}) \quad (2)$$

$$\beta_{Ca} + \beta_{Na} = 1 \quad (3)$$

where β is the equivalent fraction in the exchanger.

Table I shows the different concentrations of $NaClO_4$ and $Ca(ClO_4)_2$ used in the original solutions and the cation concentrations in the solution and montmorillonite at the equilibrium. The values were calculated as an average from the two parallel tests.

Table I. Experimental data on Na^+/Ca^{2+} exchange at 25 °C, 50 °C and 75 °C on Na-montmorillonite in 0.1M perchlorate solution.

Temp	Initial c_{Na} [mmol/l]	Initial c_{Ca} [mmol/l]	Analyzed c_{Na} [mmol/l]	Analyzed c_{Ca} [mmol/l]	q_{Na} [eq/kg]	q_{Ca} [eq/kg]	$K_{\mathrm{Ca/Na}}$
25	88.24	5.26	104.39	1.62	0.736	0.227	4.48
25	67.84	15.02	91.34	6.36	0.420	0.543	6.46
25	48.55	25.23	73.95	14.22	0.273	0.690	5.73
25	28.82	35.94	56.55	24.08	0.195	0.767	4.35
25	9.94	45.50	39.36	32.44	0.116	0.847	4.95
50	86.97	5.16	100.04	1.58	0.739	0.223	4.19
50	68.17	16.18	91.34	7.24	0.404	0.559	6.51
50	48.83	25.60	73.95	14.47	0.270	0.692	5.91
50	29.18	35.81	56.55	23.95	0.199	0.763	4.31
50	9.79	46.07	40.23	34.93	0.139	0.824	3.38
75	87.61	5.14	100.04	1.57	0.744	0.219	4.22
75	68.20	15.34	91.34	6.49	0.412	0.551	7.05
75	48.72	25.62	78.29	14.72	0.245	0.718	8.55
75	29.41	35.84	60.90	24.08	0.151	0.811	9.50
75	9.73	46.11	40.89	34.93	0.125	0.837	4.49

In Table I above, *c* refers to the concentration in the aqueous solution phase, and q refers to the amount as equivalents per kg montmorillonite. The $K_{Ca/Na}$ values in the table are the selectivity coefficients calculated as below.

The cation-exchange reaction during the test was as follows:

$$2NaX+Ca^{2+} \rightleftharpoons 2Na^{+}+CaX_2 \tag{3}$$

The selectivity coefficients for this reaction were calculated according to the Gaines-Thomas convention [12]:

$$K_{Ca/Na} = \frac{\beta_{Ca}\gamma^2_{Na^+} m^2_{Na^+}}{\beta^2_{Na}\gamma_{Ca^{2+}} m_{Ca^{2+}}} \tag{4}$$

where β is the equivalent fraction of the exchangeable cation in the montmorillonite, γ refers to activity coefficient of the species i, and m refers to molality [mol/kg H_2O] at the equilibrium. The density of liquid was assumed to be 1 in these calculations and concentration was assumed to be equivalent to molality. The activity coefficients were calculated according to the Davies equation [12,13]:

$$\log \gamma_i = -Az_i^2 \left(\frac{\sqrt{I}}{1+\sqrt{I}} - 0.3I \right) \tag{5}$$

where, A is a temperature-dependent coefficient [14], z_i is the charge number of ion i, and I is the ionic strength.

The total absorbed metal charge in the montmorillonite was assumed to remain constant. The values show higher selectivity towards calcium at 75 ^{o}C.

The exchange isotherms for the sodium are presented in Figure 1, where the experimental results are indicated with symbols. The variables here are equivalent fractions of sodium in the exchanger phase and in the solution from the total cation equivalence. There are slight differences to earlier results by Sposito [9] in the figure, but the earlier experiments were done with a total cation normality of 0.05N while these were done with an initial solution of 0.1N cation normality.

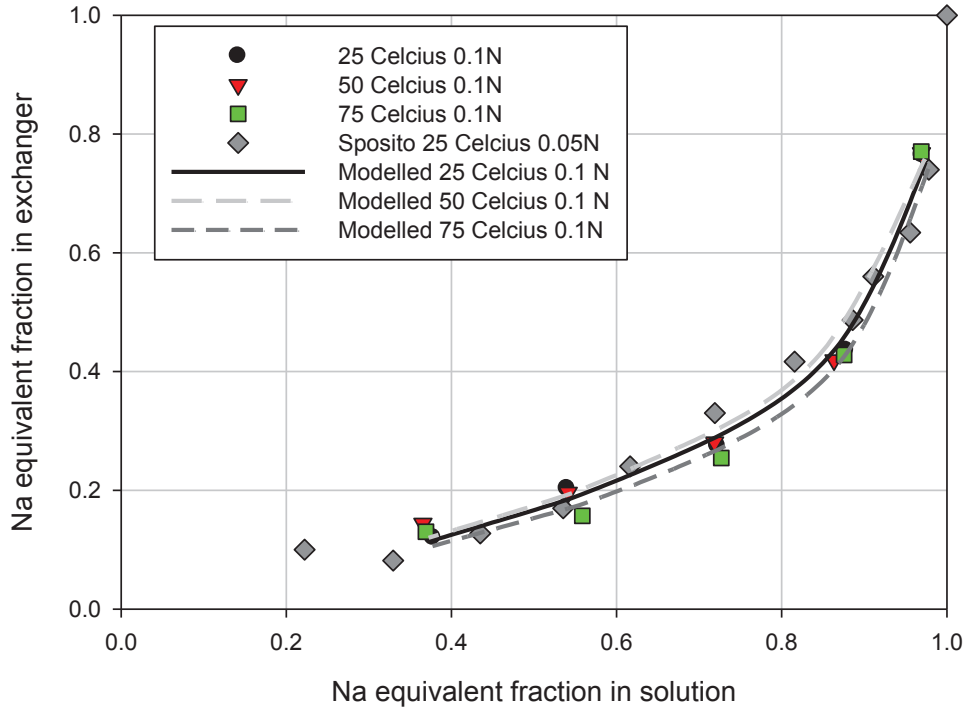

Figure 1. Exchange isotherm of Na^+ on Na-montmorillonite in perchlorate background for Na-Ca exchange.

The results were also modelled using PHREEQC, which is a computer program capable of calculating different kinds of chemical reactions [12]. The average values of the $K_{Ca/Na}$ from Table I (5.19 for 25 ^oC, 4.86 for 50 ^oC and 6.76 for 75 ^oC) were used in the modelling. The modelled results are shown in Figure 1 as lines. Earlier experiments have shown for $K_{Ca/Na}$ values 2.6 [15] for MX-80 and 2-11 [9,12,16] for Na-montmorillonite. Therefore, these experiments were in agreement with earlier studies. From the modelled exchange isotherm we can see that they match well with the experiments.

CONCLUSIONS

The exchange of Na^+ for Ca^{2+} on Na-montmorillonite at 25, 50 and 75 ^oC in a 0.1N perchlorate background medium can be characterised by Gaines-Thomas selectivity coefficients that are independent of the exchanger composition. When the mean values of the exchange coefficients were inserted into PHREEQC, the produced theoretical curve agreed well with the experimental adsorption data.

The experimental results showed a tendency to take slightly more calcium inside the exchanger at the highest temperature (75 ^oC). Thus temperature seems to affect on the behavior

of the cation exchanger. The selectivity coefficients were in agreement with earlier experiments done with MX-80 and montmorillonite.

ACKNOWLEDGMENTS

This study was jointly funded by the Finnish Research Programme on Nuclear Waste Management (KYT2014) and VTT (Technical Research Centre of Finland). The authors would also like to thank Prof. Markus Olin for his comments on this work and Eeva-Liisa Kotilahti and Markku Honkala for the sodium and calcium analyses.

REFERENCES

1. B. Pastina and P. Hellä. *Expected evolution of a spent nuclear fuel repository at Olkiluoto.* (Posiva Oy, Olkiluoto, Finland, 2006, Posiva Report 2006-05) p. 405.
2. O. Karnland, S. Olsson, U. Nilsson, *Mineralogy and sealing properties of various bentonites and smectite-rich clay materials.* (Swedish Nuclear Fuel and Waste Management Company, Stockholm, Sweden, 2006) p. 117.
3. TKS-2009. *Nuclear Waste Management at Olkiluoto and Loviisa Power Plants. Review of Current Status and Future Plans for 2010-2012*. (Posiva Oy, Finland, 2010) p. 563.
4. H. Tributh and G.A. Lagaly, "Aufbereitung und Identifizierung von Boden- und Lagerstättentonen. I. Aufbereitung der Proben im Labor". (GIT-Fachzeitzschrift für das Laboratorium 30, 1986) pp. 524-529.
5. F. Bergaya, B.K.G. Theng, G. Lagaly, *Handbook of Clay Science.* (Elsevier, Oxford, United Kingdom, 2006) p. 1125.
6. R.E. Hester and R.A. Plane, Inorg. Chem. 3, 769-770 (1964).
7. A. Maes, P. Peigneur, and A. Cremers, Proc. Int. Clay Conf. 1975, 319-329.
8. G. Sposito, *The thermodynamics of soil solution.* (Oxford Univ. Press, Oxford, U.K., 1981) p. 223.
9. G. Sposito, K.M. Holtzclaw, L. Charlet, C. Jouany, and A.L. Page, Soil Sci. Soc. Am. J. 47, 51-56 (1983).
10. L. Meier, G. Kahr. Clays and Clay Minerals, Vol. 47, No. 3, 368-388,1999.
11. F. G. Donnan, *Z. Elektrochemie* 17, 572 (1911).
12. C. A. J. Appelo, D. *Postma, Geochemistry, groundwater and pollution*, 2nd ed. (A.A. Balkema Publishers, Leiden, Netherlands, 2007) p. 649.
13. C.W. Davies, *Ion association.* (Butterworth & Co. (Publishers) Ltd. London, 1962) p. 190.
14. R.A.Robinson, R.H. Stokes, Electrolyte solution. The measurement and interpretation of concuctance, chemical potential and diffusion in solution of simple electrolytes, 2nd ed. (London Butterworths Scientific Publications, 1959) p. 559.
15. M.H. Bradbury, B. Baeyens, Porewater chemistry in compacted re-saturated MX-80 bentonite: Physico-chemical characterisation and geochemical modelling. (PSI Berich Nr. 02-10, Villigen, 2002) p. 42.
16. M.G.M. Bruggenwert, A. Kamphorst, in *Developments in Soil Science*, edited by G.H. Bolt (Elsevier Ltd, 1979, Vol 5, Part B) pp. 141-203.

PUBLICATION IV

CO_2 effect on the pH of compacted bentonite buffer on the laboratory scale

In: Clay Minerals (2013), Vol. 48, No. 2, pp. 277–283.

Clay Minerals, (2013) **48**, 277–284

CO_2 effect on the pH of compacted bentonite buffer on the laboratory scale

A. ITÄLÄ*, J. JÄRVINEN AND A. MUURINEN

VTT Technical Research Centre of Finland, P.O. Box 1000, FI-02044 VTT, Finland

(*Received 4 December 2012; revised 25 March 2013; Editor: John Adams*)

ABSTRACT: Disposal of Finnish spent nuclear fuel is planned to be based on the KBS-3 repository concept. The role of the bentonite buffer in this concept is essential, and thus the behaviour of the bentonite has to be known. The experiments in this paper concentrated on providing information about the effects of carbon dioxide CO_2(g) partial pressure on compacted sodium bentonite, giving an insight into the buffering capacity. The experimental setup consisted of a hermetic box which had a CO_2-adjusted atmosphere, and the bentonite was in contact with this atmosphere through water reservoirs. The results indicated that it is possible to measure online the changing pH in the porewater inside compacted bentonite using IrOx electrodes. It was found that the pH fell if the CO_2 partial pressure increased above atmospheric conditions. The experimental results indicated a greater fall in pH than in our model in the test cases where CO_2 was present. The pH in the experiment with 0 P_{CO_2} remained nearly constant throughout the 5 month period. On the other hand, the pH dropped to near 6 with 0.3 P_{CO_2} and to 5.5 with 1 P_{CO_2}.

KEYWORDS: bentonite, pH, carbon dioxide, buffer, alteration, compaction.

Many countries, including Finland, are planning to use bentonite as a buffer material around the waste canisters in their high-level radioactive waste disposal concept. The Finnish plan follows the KBS-3 (KärnBränsle Säkerhet) concept, which aims at long-term isolation and containment of the spent fuel assemblies in copper canisters with a nodular cast iron insert. The canisters are emplaced over 400 m deep into the crystalline bedrock. Each canister is separated from the bedrock by bentonite (the buffer) rings and placed in a drilled borehole. The purpose of the buffer material is to maintain the integrity of the canisters by protecting them from detrimental Thermal-Hydraulic-Mechanical-Chemical-Biological (THMCB) processes and to limit and retard the release of any radionuclides in the case of a damaged canister (Pastina & Hellä, 2006).

* E-mail: aku.itala@vtt.fi
DOI: 10.1180/claymin.2013.048.2.09

The knowledge of pH conditions is essential for performance assessment (PA) since pH strongly affects the mobility of most relevant radionuclides (see e.g. Kohlicková & Jedináková-Krizová 1998). The subject has been studied earlier by Wersin (2003). In these studies he used the approach of Bradbury & Baeyens (1997, 1998) to model the results of Muurinen & Lehikoinen (1999), who studied the changes in porewater chemistry in compacted bentonite in different ionic strengths and in different solid/liquid ratios. Wersin (2003) made a sensitivity analysis of different parameters affecting the bentonite porewater and found that the main reactions controlling major ion chemistry were calcite and gypsum equilibrium, Na-Ca exchange reactions and de-protonation of functional surface groups. The uncertainty in pH was found to be mainly affected by the P_{CO_2} of the surrounding host rock. In the paper by Wersin (2003) it was clearly suggested that diffusion experiments on compacted samples should be performed, focusing only on the identification and quantification of surface exchange and sorption reactions.

The electrodes used in this paper were tested previously by Muurinen & Carlsson (2007, 2010) who measured the pH and Eh inside the compacted bentonite and in pore water that had been squeezed out during the compaction of the clay. The performance of electrodes was tested at different compaction densities and by saturating the bentonite with deionized water, with 1 M NaOH conditions remaining constant. The results indicated the usefulness of IrO_x electrodes for measuring the pH of the porewater inside the compacted bentonite (Muurinen & Carlsson, 2007).

In the paper of Muurinen & Carlsson (2010) the model of Bradbury & Baeyens (2002, 2003) was tested for the pH measurements with IrO_x electrodes with different bentonite/external water ratios (chloride porosity). The model assumes that the initial state of the edge site in the bentonite is in equilibrium with the atmospheric carbon dioxide. The results showed that the model of Bradbury & Baeyens (2002, 2003) is quite capable of modelling the results from the compacted samples and it is possible to use IrO_x electrodes for diffusion experiments also (Muurinen & Carlsson 2010).

The aim of the experiments reported here was to study how carbon dioxide $CO_2(g)$ partial pressure affects both the pH in the compacted MX-80 bentonite and the buffering capacity of bentonite.

EXPERIMENTAL

Materials

The Wyoming MX-80 bentonite used in these experiments consists mainly of sodium montmorillonite and smaller amounts of other minerals (quartz, calcite, feldspar, etc.) (Kiviranta & Kumpulainen, 2011). The beneficial properties of bentonite are mainly determined by this montmorillonite mineral (see, e.g. Grauer, 1986). These properties include the sorption capability during canister failure, the ability to swell upon saturation with water, the mechanical and chemical protection around the canister, and good enough thermal conductivity to dissipate the heat emitted by the waste.

The Tetrahedral-Octahedral-Tetrahedral (TOT) layer structure of montmorillonite has a permanent negative charge, which is compensated by the exchangeable cations within the area of the interlayer space. In aqueous solutions, these cations can undergo a stoichiometric exchange with cations in a solution. The total amount of exchangeable cations is called the cation-exchange capacity (CEC) (see, e.g. Kaufhold & Dohrmann, 2013). According to Kaufhold *et al*. (2008) the form of these cations can affect the pH at small solid/liquid ratios which is not the case in highly compacted bentonites (Muurinen & Carlsson, 2010). There is also a second category of reactive sites related to montmorillonite. These are called surface hydroxyl groups and they are located along the edges of the TOT layers. These sites can protonate/deprotonate according to the pH in the surrounding solution, which means that the hydroxyl groups can function as a powerful pH buffer (Bradbury & Baeyens, 2002).

Concept

The experimental setup consisted of a hermetic box with a CO_2-adjusted atmosphere, diffusion cell, pH electrodes, compacted bentonite sample, and water reservoirs (Fig. 1). The gas in the hermetic box was in contact with the external solution of the diffusion cell. The geometry of the bentonite was cylindrical, the diameter of the sample was 20 mm, and the length 20 mm. The samples were compacted to a dry density of 1.57 g/cm^3. The volume of each external water reservoir was 50 ml, and these were filled with 0.1 M NaCl at the beginning of the test. The bentonite samples were fully saturated by the deionized water mixed into the bentonite before compaction. The CO_2 partial pressures were kept constant through the experiment by changing the gas in the hermetic box twice a month. The temperature was 25^{o}C in all four experiments. All of the experiments were carried out with unpurified MX-80 bentonite.

Test cases

The experiment was conducted under three different conditions with the same apparatus. The only parameter that was varied in these experiments was the partial pressure of CO_2. All the three experiments, which are listed in Table 1, were sustained at atmospheric pressure, and in two cases the other gas besides CO_2 was argon. The reservoir water pH was evaluated through modelling before the experiment with the Geochemist's Workbench (GWB). The water reservoir pH under test case atmosphere means that there is no buffer present.

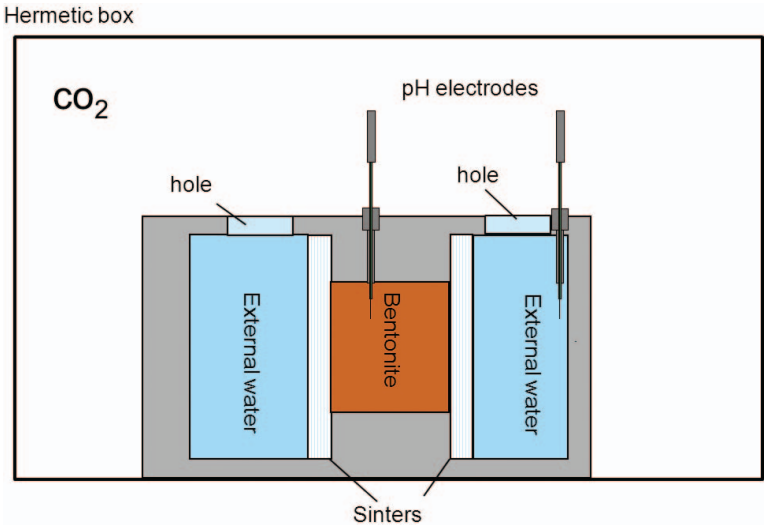

FIG. 1. Schematic picture from the experimental setup.

Analyses

The pH was measured online from the porewater of the bentonite and water reservoir with calibrated pH-electrodes (Muurinen & Carlsson, 2009). However, during the experiment, leakage-free single-junction reference electrodes were observed to shift during the experiments under acidic conditions. Therefore, the external water pH values were measured by a commercial Ross electrode about once a month. These values were used to calculate theoretical values for the reference electrodes to match the online measurements and the Ross electrode measurements from the external water. The same calculated reference electrode values were used for the IrOx electrodes which were employed to measure the pH inside the bentonite. Some uncertainties lie in this method and therefore more research will be undertaken to verify these results.

Modelling

The pre-modelling of the experiment was performed using GWB to approximate the pH changes and the time needed to reach constant conditions. After the experiment, the model and the experimental results were compared. The model was arranged as a column model, where there was 2 cm of bentonite in the middle, and 50 ml water cells at both ends with inlets at the ends of the water cells. These inlets kept the outer CO_2 (g) partial pressure constant. The model included cation exchange, surface complexation and mineral equilibrium of calcite and gypsum. The relevant reactions in this experiment should be the surface complexation reactions, which can work as a pH buffer. According to Bradbury & Baeyens (2002) there are two different kinds of weak sites SOH (in MX-80) which can both protonate and deprotonate, according to the equations below:

TABLE 1. Test cases and evaluated water reservoir pH before the experiment.

Test	Bentonite type	Solution type	Partial pressure of CO_2 (atm)	Water reservoir pH under test case atmosphere	Evaluated water reservoir pH	Experimental time (months)
1	MX-80	NaCl (0.1 M)	0 (Argon)	7	~7	6
2	MX-80	NaCl (0.1 M)	0.3 (Argon)	5.7	6.2	6
3	MX-80	NaCl (0.1 M)	1	3.92	5.9	6

TABLE 2. Water and mineral composition in the model.

Ion/mineral	Bentonite water molality (mol/kg)	Water cell molality (mol/kg)	Mineral volume fraction in bentonite (%)
Na^+	0.127	0.1	
K^+	0.0031	traces	
Mg^{2+}	0.0041	traces	
Ca^{2+}	0.0103	traces	
SO_4^{2-}	charge balanced	traces	
H_4SiO_4(aq)	traces	traces	
Cl^-	traces	0.1	
Gypsum			0.36
Calcite			0.72
Na-montmorillonite			55.62

$$SOH + H^+ = SOH_2^+ \quad (1)$$
$$SOH = SO^- + H^+ \quad (2)$$

Parameters

The diffusion coefficient used for all ions was 10^{-10} m^2/s (the porosity 0.43 and tortuosity 0.12 of bentonite were included in the diffusion coefficient). GWB calculates porosity according to given volume fractions of the minerals and the fluids, and takes this into account when calculating the permeability of the material. The water composition and mineral volume fractions used in the modelling are listed in Table 2. The bentonite porewater was calculated such that the ion exchange and sorption sites were filled according to the experimental results of Kiviranta & Kumpulainen (2011). Mineral volume fraction and cation exchange composition were also taken from Kiviranta & Kumpulainen (2011) such that the gypsum and calcite amounts were from this report and the rest of the mineral volume fraction was supposed to be montmorillonite. The material in the report is called Wy−VT0002-BT1-3-Sa-R (Kiviranta & Kumpulainen, 2011).

The cation-exchange capacity used was 93 meq/100 g (Kiviranta & Kumpulainen, 2011) The selectivity coefficients and cation exchange reactions can be found in Table 3.

The protolysis constants as well as surface areas of bentonite can be found in Table 4. The Thermoddem database was used in the calculations for the water chemistry part (Blanc *et al.*, 2007).

TABLE 3. Selectivity coefficients and reaction for cation exchange on MX-80 (Bradbury & Baeyens, 2002).

Exchange reaction	Selectivity coefficient
$NaX + K^+ <=> KX + Na^+$	4
$2NaX + Mg^{2+} <=> MgX_2 + 2Na^+$	2.2
$2NaX + Ca^{2+} <=> CaX_2 + 2Na^+$	2.6

TABLE 4. Site types, capacities and protolysis constants (Bradbury & Baeyens, 2002).

Site types:	Site capacity (mol/kg)
Sw1OH	0.04
Sw2OH	0.04
Surface complexation reaction	log K_{int}
$Sw1OH + H^+ <=> Sw1OH^{2+}$	4.5
$Sw1OH <=> Sw1O- + H^+$	−7.9
$Sw2OH + H^+ <=> Sw2OH^{2+}$	6
$Sw2OH <=> Sw2O- + H^+$	−10.5

RESULTS AND DISCUSSION

At the beginning of the test the bentonite was in equilibrium with 390 ppm CO_2(g) volume fraction of ambient air (partial pressure was about 39 Pa). The first test case shows that the pH rises slightly when the CO_2 (g) partial pressure decreases (Fig. 2). The pH results shown in the figures are

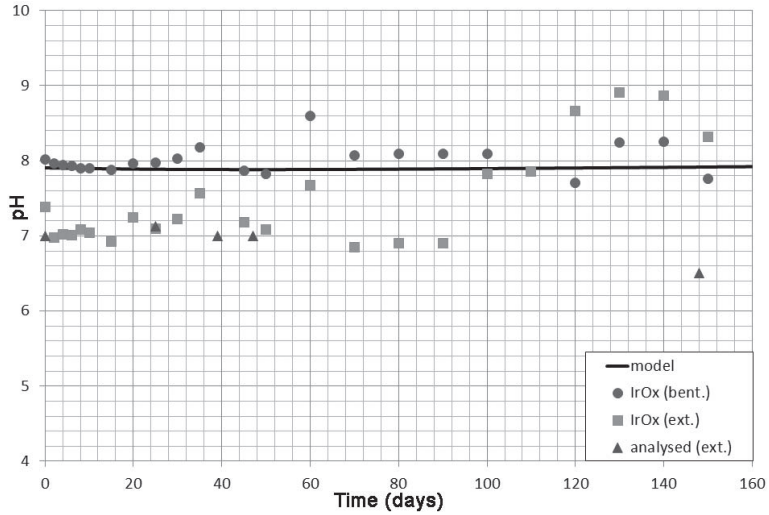

FIG. 2. Results of test case 1, CO_2 (g) partial pressure 0.

from the middle of the bentonite and from the external water solution. The results were analysed over 160 days. The pH of the external solution according to the modelling can be seen in Table 1. The meanings of the legends are ext.= external water measured with normal pH electrode and with our own handmade iridium-oxide (IrOx) electrode and the model legends refer to our calculated model. IrOx(bent.) means that the electrode was in the middle of the bentonite tablet. As can be seen from the figure, bentonite buffers the changes as the CO_2 (g) volume fraction decreases from 390 ppm towards zero. The differences in the external water results of the two different electrodes are related to the reference electrode calibration.

In the latter two tests, the pH falls as the CO_2 (g) partial pressure increases (Figs 3 and 4). Our model clearly gives a smaller decrease in pH than in the experiment. In test case two (Fig. 3), the pH in the experiment drops down from 9 to approximately 6,

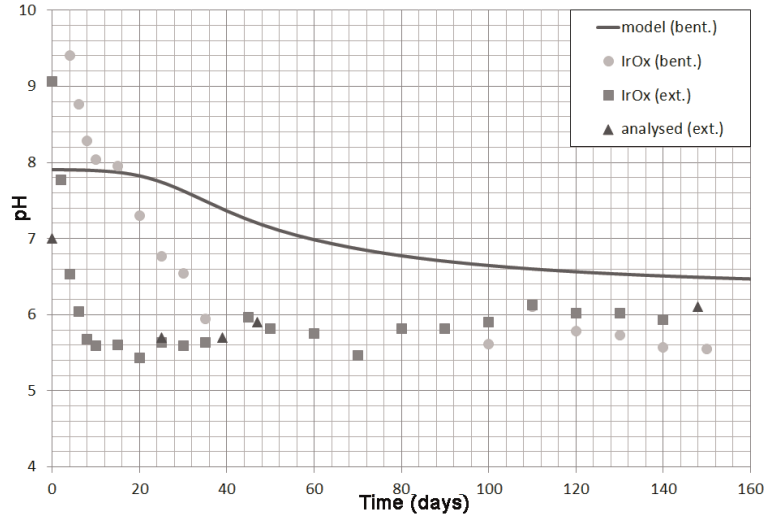

FIG. 3. Results of test case 2, CO_2 (g) partial pressure 0.3.

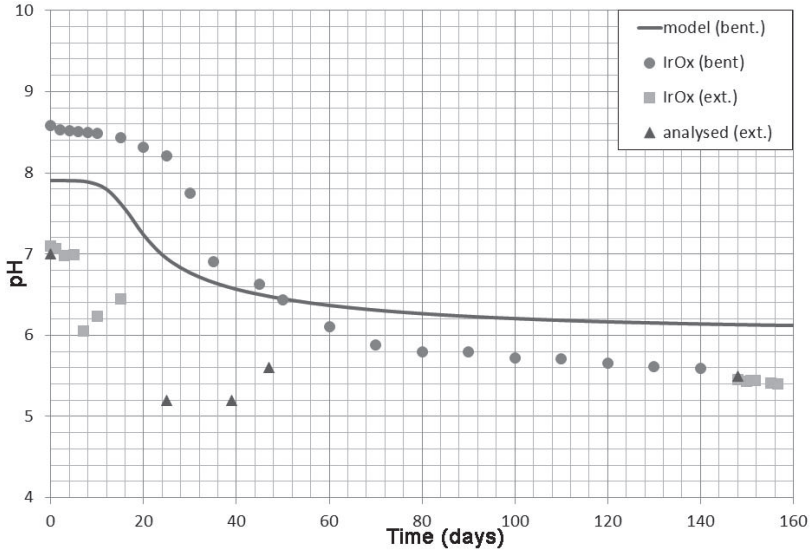

FIG. 4. Results of test case 3, partial pressure 1.

while the model shows only a drop to 6.5. The higher values for the IrOx(bent) electrode at the beginning could be related to the fact that it takes time for the electrode to find the equilibrium potential at the beginning of the test. The fact that test case 2 does not show a buffering trend at the beginning of the test is probably related to the fact that there were some problems with the reference electrode during the test.

In test case 3 (Fig. 4), the model shows a drop from 8 to 6.1, but the experimental results clearly show a bigger drop in pH from 8.6 to approximately 5.5. In this figure, it is clearly visible that the bentonite buffers the pH change at the beginning of the test before the pH starts to fall. However, again the pH can be seen to exhibit a greater drop than in the model.

The differences between the modelling and experimental results is mainly related to the fact that GWB calculates some kind of equilibrium state (with model minerals) in water cells even if those cells do not include minerals. This leads to higher pH in water cells than in the experiment. The starting values in the outside water cells in the model was 6.2 for 0.3 P_{CO_2} (Fig. 3) and 5.9 for 1 P_{CO_2} (Fig. 4). In the experiment the starting points were respectively 5.6 and 5.2 at the beginning and the pH rose slightly during the test when the water cells were equilibrating with the bentonite pore water.

The Bradbury & Baeyens (2002) model does not take into account the electrostatic phenomena in the bentonite (see, e.g. Bourg *et al.*, 2007), which could also affect the modelling results. Bourg *et al.* (2007) also showed that none of the available surface complexation models work over the entire set of experimental conditions, which in our case are extended to high CO_2 fugacity. Additionally, in the experiment, some complexes can form, for example with CO_2 (g), which can interact with the surface complexation sites and could induce some effects on the results. The calibration, due to the fact that the reference electrodes did not work very well in acidic conditions, could affect the experimental results. Thus, additional experiments are needed to confirm these measurements and to understand the phenomena in bentonite better.

As can be seen, it is not possible to get the modelling results to match the experimental results perfectly. We tried to change the number of surface sites, but this just changed the point at which the pH starts to decrease from the original value. Changing the diffusion coefficient also affected this point, but the pH does not fall lower in the model owing to the external water in the model not having as low a value as in the experiment. The effect of calcite and gypsum minerals were also tested and it seems that in the compacted system the only feature buffering the pH changes is the surface protonation sites (as the water amount compared to the surface site

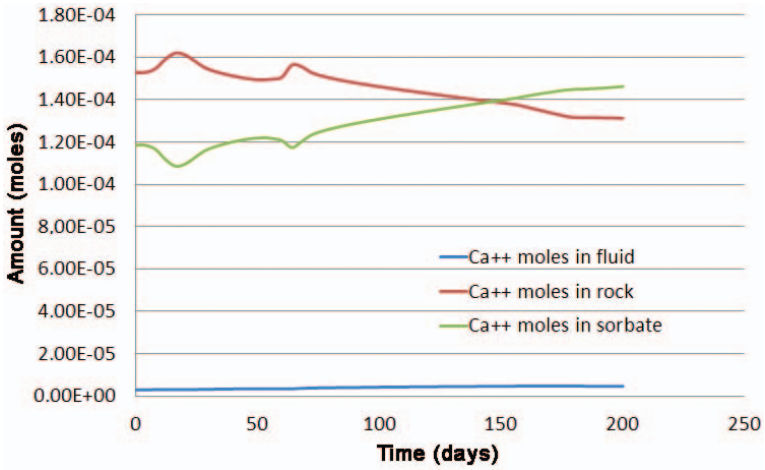

FIG. 5. Calcium amounts from the middle of the bentonite in the model (1 P_{CO_2} case).

amounts is very small). Gypsum dissolves after 50 days in the model and calcite is first precipitated but starts to dissolve after the gypsum is dissolved; however, the total amount is the same as the original amount at the end of the test time. The calcium fraction increases in the exchanger phase due to dissolving gypsum from 28% to 31%. The modelled calcium amounts in fluid, rock (minerals) and sorbate (cation exchanger) can be seen from Fig. 5.

CONCLUSIONS

We can see that the bentonite buffering capacity in the kind of conditions where the water/bentonite ratio is high does not prevent pH changes which happen rapidly after 20 days. The only feature buffering the pH changes inside compacted bentonite seems to be the surface protonation sites which can buffer the changes at about 0.3 pH units. However, reactions which have not been previously identified and contribute to the pH drop in addition to CO_2 equilibrium might also occur. Thus, we propose that more results are needed to conclude which kinds of phenomena occur inside the bentonite and whether the electrode calibration was the only reason for such low pH values.

ACKNOWLEDGMENTS

The research leading to these results has received funding from the Finnish Research Programme on Nuclear Waste Management (KYT) 2011-2014 (BOA project).

REFERENCES

Blanc P., Lassin A. & Piantone P. (2007) *Thermoddem: a Database Devoted to Waste Minerals.* BRGM (Orléans, France). http://thermoddem.brgm.fr

Bourg I.C., Sposito G. & Bourg A.C.M. (2007) Modeling the acid-base surface chemistry of montmorillonite. *Journal of Colloid and Interface Science*, **312**, 297–310, doi: 10.1016/j.jcis.2007.03.062.

Bradbury M.H. & Baeyens B. (1997) A mechanistic description of Ni and Zn sorption on Na-montmorillonite. *Journal of Contaminant Hydrology*, **27**, 223–248, doi: 10.1016/S0169-7722(97)00007-7.

Bradbury M.H. & Baeyens B. (1998) A physicochemical characterisation and geochemical modelling approach for determining porewater chemistries in argillaceous rocks. *Goechimica et Cosmochimica Acta*, **62**, 783–795, doi: 10.1016/S0016-7037(97)00387-6.

Bradbury M.H. & Baeyens B. (2002) *Porewater Chemistry in Compacted Re-saturated MX-80 Bentonite: Physico-Chemical Characterisation and Geochemical Modelling.* PSI Bericht Nr. 02-10, Villigen, 42 pp.

Grauer R. (1986) *Bentonite as a Backfill Material in the High Level Waste Repository: Chemical Aspects.* Nagra Technical Report NTB 86-12E, Villigen, 130 pp.

Kaufhold S. & Dohrmann R. (2013) The variable charge of dioctahedral clay minerals. *Journal of Colloid and Interface Science*, **390**, 225–233.

Kaufhold S., Dohrmann R., Koch D. & Houben G. (2008) The pH of aqueous bentonite suspensions. *Clays and Clay Minerals*, **56**, 338–343.

Kiviranta L. & Kumpulainen S. (2011) *Quality Control*

and Characterization of Bentonite Materials. Posiva Oy, Olkiluoto, Finland, Working Report 2011-84.

Kohličková M. & Jedináková-Křižová V. (1998) Effect of pH and Eh on the sorption of selected radionuclides. *Journal of Radioanalytical and Nuclear Chemistry*, **229**, 43–48, doi: 10.1007/BF02389444.

Kumpulainen S. & Kiviranta L. (2010) *Mineralogical and chemical characterization of various bentonite and smectite-rich clay materials. Part A. Comparison and development of mineralogical characterization methods Part B: Mineralogical and chemical characterization of clay materials.* Posiva Oy, Olkiluoto, Finland, Working Report 2010-52, 74 pp.

Muurinen A. & Carlsson T. (2007) Development of methods for on-line measurements of chemical conditions in compacted bentonite. *Physics and Chemistry of Earth*, **32**, 241–246, doi: 10.1016/j.pce.2006.02.059.

Muurinen A. & Carlsson T. (2010) Experiences of pH and Eh measurements in compacted MX-80 bentonite. *Applied Clay Science*, **40**, 23–27, doi: 10.1016/j.clay.2008.05.007.

Muurinen A. & Lehikoinen J. (1999) *Porewater Chemistry in Compacted Bentonite.* Posiva Report.

Pastina B. & Hellä P. (2006) *Expected Evolution of a Spent Nuclear Fuel Repository at Olkiluoto.* Posiva Oy, Olkiluoto, Finland, Posiva Report 2006-05, 405 pp.

Wersin P. (2003) Geochemical modelling of bentonite porewater in high-level waste repositories. *Journal of Contaminant Hydrology*, **61**, 405–422.

PUBLICATION V

Modeling Transport of Water, Ions, and Chemical Reactions in Compacted Bentonite: Comparison Among Toughreact, Numerrin, and Comsol Multiphysics.

In: Nuclear Technology (2014), Vol. 18, No. 2, pp. 169–174.

MODELING TRANSPORT OF WATER, IONS, AND CHEMICAL REACTIONS IN COMPACTED BENTONITE: COMPARISON AMONG TOUGHREACT, NUMERRIN, AND COMSOL MULTIPHYSICS

RADIOACTIVE WASTE MANAGEMENT AND DISPOSAL

KEYWORDS: *cation exchange, modeling, transport*

AKU ITÄLÄ,[a]* MIKA LAITINEN,[b] MERJA TANHUA-TYRKKÖ,[a] and MARKUS OLIN[a]

[a]*VTT Technical Research Centre of Finland, P.O. Box 1000, FI-02044 VTT, Finland*
[b]*Numerola Oy, P.O. Box 126, FI-40101 Jyväskylä, Finland*

Received May 15, 2013
Accepted for Publication February 6, 2014
http://dx.doi.org/10.13182/NT13-79

The bentonite barrier is an essential part of a safe spent fuel repository in granitic bedrock. One of the most important safety functions of bentonite buffer is to limit groundwater flow so that all mass transport takes place by diffusion. In this work a new mathematical model was developed to define the transport of ions inside the bentonite, where there are bound interlayer water and free extra layer water and sorption capability. This model is tested in a specified geometry and calculated by two numerical platforms—Numerrin and COMSOL Multiphysics—and compared to the original TOUGHREACT model. The model comparison was not a straightforward task because of different approaches in the model setup. Therefore, all the equations are written down, and parameterization is done to create model descriptions near each other. The developed model adapts easily, and there are many new ideas to be tested in bridging the gap between performance assessment and real systems.

Note: Some figures in this paper may be in color only in the electronic version.

I. INTRODUCTION

Many phenomena and processes have to be understood when considering the safety of the engineering barrier system (EBS) of a spent fuel repository. Our main interest is in the bentonite buffer part of the EBS. Bentonite is a kind of natural composite material with

1. smectite layers and charge-compensating cations
2. water, part of which is free in large pores and part of which is bound on smectite layers
3. salts and minerals dissolved into pore water and in solid state.

Therefore, a composite material having interaction between its components already at nanolevel can behave in quite a complex and nonlinear way. Bentonite buffer must survive under changing conditions, and in many cases the conditions may change far into the future with reactions taking thousands of years to be completed. Thus, modeling is the only option to study these systems

*E-mail: aku.itala@vtt.fi

to guarantee the proper functioning of bentonite buffer over a planned period of more than 100 thousand years. Our approach is based on segregation of modeling steps to enable more flexibility:

1. conceptualization, which is at least partially free of the limitations in the code to be applied
2. collection of data needed; creation of a mathematical model, having hopefully bigger freedom concerning the code
3. implementation of the model on the TOUGH2 code[1] and/or the TOUGHREACT code,[2] which are specifically designed for earth science applications
4. implementation of the model on two other platforms: COMSOL Multiphysics and Numerrin,[3] which are not bound on any application area and are therefore flexible
5. solution of the models by the selected approach
6. evaluation of differences in these approaches: Basically, COMSOL and Numerrin should be able to use exactly the same equations while TOUGH family codes use state of the art in earth science applications
7. comparison of the results.

We present a new version of our transport and chemical reaction model (RFT: Reactions, Fluxes, Temperature), which will be validated against experimental data to be produced in VTT's (Technical Research Centre of Finland) other projects. The wetting processes are studied by tomographical methods, and models based on those experiments are planned to be implemented in Numerrin and COMSOL and, if possible, in TOUGH family codes, too. Our model is aimed to be a kind of benchmark for testing new ideas, which typically are possible to implement both onto Numerrin and COMSOL platforms, thus enabling verification of these implementations. The TOUGH family code on the other hand enables verification on commercially available software, whenever models are possible to be implemented on all three platforms. Therefore, our approach makes it possible to test new innovative ideas for supporting performance assessment (PA) purposes while having verified solutions and links to TOUGH modeling. A class of issues in bentonite is connected to pore water and fractioning of it into free and bound waters, and even more fractions. Our model approach allows almost any combination to be applied in Numerrin and COMSOL implementations and, therefore, makes it possible to test consequences of different approaches and show differences to be tested experimentally.

In the present work, only a very limited set chemical reactions is applied, mainly aiming to show the basic ideas of our modeling approach.

II. MODEL FOR CATION EXCHANGE AND DIFFUSION

Compacted bentonite is a composite material; the main component montmorillonite belongs to swelling clay minerals, which may be considered more accurately as a very dense solution of colloidal particles than traditional porous material. However, in most transport models and in all PA models known to the authors, bentonite is considered to be porous material; the porosity is given by total water content ($>40\%$ for the targeted 1600 kg/m^3 density of the KBS-3 method). However, many transport properties of bentonite are quite different compared to typical porous materials of such high porosity like sand or nonswelling clays. For example, the anion diffusivity is quite low, while diffusion conductivity (often called effective diffusivity) is comparably high: Anions appear to occupy much less porosity than 40%, but cations diffuse in the whole pore volume. Therefore, bentonite transport modeling is much more complicated than in powderlike porous materials.

The models that are used globally assume that the whole porosity is available for water transport, and we wanted to change this. The main idea in our model was to take into account the different kinds of waters inside bentonite where there is free water on pores and intellamellar water between clay platelets.[4] We have not yet implemented all chemical reactions and processes needed for a complete description, but there is an option for those in the future. For example, both bulk and surface reactions (cation exchange and surface complexation) are strongly affected by the amount of free pore water. In many cases, it is possible to include these effects in the fitted parameter data, at least in fixed conditions: high density and fully saturated system at room temperature. However, in many cases of interest for PA, the density can be very small and bentonite gel-like or even approaching a colloidal state, and in analyzing the initial state of bentonite, the system is only partially wetted. In all those and many other situations, the bentonite model should be based on real physical-chemical understanding of bentonite, which hopefully will be applicable in many conditions with almost constant parameter values. Our work aims to that, and in our approach, mechanical and hydrological behavior (for example, wetting and swelling) is relatively straightforward to couple in chemical and thermal behavior.

II.A. Definitions

Compacted bentonite consists of dry bentonite (montmorillonite and accessory minerals), water, and air, which together fill all the available space (see Fig. 1).

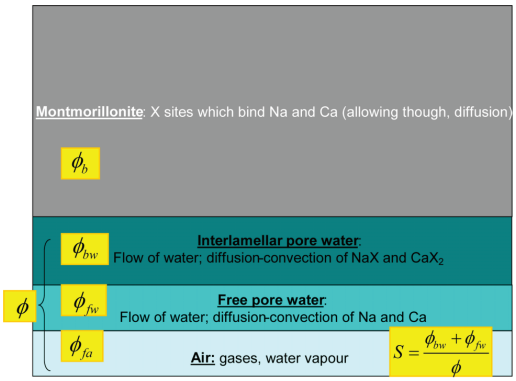

Fig. 1. Basic concept of montmorillonite pore structure.

The total mass of bentonite in volume V is therefore

$$\begin{aligned} M &= M_b + M_{bw} + M_{fw} + M_{fa} \\ &= \rho_b \phi_b V + \rho_w \left(\phi_{bw} V + \phi_{fw} V\right) + \rho_a \phi_{fa} V \\ &\cong \left[\rho_b \phi_b + \rho_w \phi_{bw} + \rho_w \frac{\chi}{1-\chi} \phi_{bw}\right] V, \end{aligned} \tag{1}$$

which gives the following for the density of the bentonite:

$$\rho \cong \phi_b \rho_b + \frac{\phi_{bw} \rho_w}{1-\chi} , \tag{2}$$

where

M_i = mass of dry bentonite, b; water bound on bentonite, bw; free water, fw; or air, fa

ρ_b = specific dry density of bentonite (2760 kg/m^3)

ρ_w = density of water, both bound on bentonite and free ($\cong$1000 kg/m^3), though bound water may have higher density

ρ_a = density of air ($\cong$1.3 kg/m^3)

ϕ_i = volume fraction of component i, where $\sum_{i=b,bw,fw,fa} \phi_i = 1 = \phi_b + \phi$

ϕ = volume fraction of all fluids, where $\phi = \phi_{bw} + \phi_{fw} + \phi_{fa}$

χ = ratio of volume fractions of free and total water volume, where $\chi = \phi_{fw} / \left(\phi_{bw} + \phi_{fw}\right)$.

The mass of bentonite per total volume

$$\rho_d = M_b / V = (1-\phi)\rho_b \tag{3}$$

is called the dry density. The total porosity ϕ and the dry and specific densities are conveniently coupled by

$$\phi = 1 - \rho_d / \rho_b . \tag{4}$$

The cation exchange capacity (CEC) (equivalent per kilogram) is the fixed charge content (negatively charged sites X occupied by cations) of the solid bentonite. The concentration of CEC per bound water volume is given by

$$c_X = \frac{M_{CEC}}{\phi_{bw} V} = \frac{\phi_b}{\phi_{bw}} \text{CEC} \cdot \rho_b . \tag{5}$$

Any other quantity given as content (moles per kilogram of bentonite) will be transformed similarly to concentration per bound water. For example,

$$c_{NaX} = \frac{M_{NaX}}{\phi_{bw} V} = \frac{\phi_b}{\phi_{bw}} \text{CEC} \cdot \rho_b \beta_{NaX} . \tag{6}$$

II.B. Cation Exchange Reactions

The chemical model is extremely simple: two sodium isotopes (^{s}Na and ^{r}Na), two chloride isotopes (^{s}Cl and ^{r}Cl), and cation exchange site (X). ^{s}Na and ^{r}Na form complexes ^{s}NaX and ^{r}NaX with X:

$$^s\text{NaX} + {}^r\text{Na}^+ \underset{k}{\overset{k}{\rightleftarrows}} {}^r\text{NaX} + {}^s\text{Na}^+ , \tag{7}$$

where k is the kinetic constant, which in this case is the same in both directions. No other complexes were considered in this study, and extensions to more realistic chemistry is straightforward. Possible stable (s) and radioactive (r) sodium isotopes are ^{23}Na and ^{22}Na, respectively; the half-life of beta-active ^{22}Na is $\sim$2.6 yr. Chlorine has two stable isotopes: ^{35}Cl and ^{37}Cl. The half-life of beta-active ^{36}Cl is $\sim$300 000 yr.

At equilibrium, reaction (7) gives

$$\frac{\beta_{r\text{NaX}}}{\beta_{s\text{NaX}}} = \frac{c_{r\text{Na}}}{c_{s\text{Na}}} , \tag{8}$$

where

$c_{i\text{Na}}$ = concentration (mol/m^3)

β_i = equivalent fraction of cation isotope i.

For implementation in COMSOL or Numerrin, the cation exchange reaction is reformulated for aqueous concentrations, which are the applied variables in transport equations instead of equivalent fractions ($\beta_i = z_i c_{Xi} / c_X$):

$$\beta_{i\text{NaX}} = \frac{\phi_{bw}}{\phi_b} \frac{1}{\text{CEC} \cdot \rho_b} c_{i\text{NaX}} . \tag{9}$$

The equilibrium equation (8) is then rewritten

$$\frac{c_{r\mathrm{NaX}}}{c_{s\mathrm{NaX}}} = \frac{c_{r\mathrm{Na}}}{c_{s\mathrm{Na}}} \ . \tag{10}$$

The total mass of each element is conserved:

$$\overline{c_{s\mathrm{Na}}} = \phi_{fw} c_{s\mathrm{Na}} + \phi_{bw} c_{s\mathrm{NaX}} \ ,$$

$$\overline{c_{r\mathrm{Na}}} = \phi_{fw} c_{r\mathrm{Na}} + \phi_{bw} c_{r\mathrm{NaX}} \ ,$$

$$\overline{c_{s\mathrm{Cl}}} = \phi_{fw} c_{s\mathrm{Cl}} \ ,$$

and

$$\overline{c_{r\mathrm{Cl}}} = \phi_{fw} c_{r\mathrm{Cl}} \ , \tag{11}$$

where $\overline{c_i}$ is the total concentration of element i.

The charge balance must be kept in the bound and free aqueous phase:

$$c_{\mathrm{X}} = c_{s\mathrm{NaX}} + c_{r\mathrm{NaX}}$$

and

$$c_{s\mathrm{Cl}} + c_{r\mathrm{Cl}} = c_{s\mathrm{Na}} + c_{r\mathrm{Na}} \ . \tag{12}$$

II.C. Chemical Kinetics

For the reaction (8) it is possible to write forward and reverse rates:

$$r_f = k \cdot c_{s\mathrm{NaX}} c_{r\mathrm{Na}} \tag{13}$$

and

$$r_r = k \cdot c_{r\mathrm{NaX}} c_{s\mathrm{Na}} \ , \tag{14}$$

which gives for total reaction rate

$$r = r_f - r_r = k_c \left(c_{s\mathrm{NaX}} c_{r\mathrm{Na}} - c_{r\mathrm{NaX}} c_{s\mathrm{Na}} \right) \ , \tag{15}$$

which at equilibrium is zero, giving properly Eq. (9).

II.D. Mass Transport by Molecular Diffusion

The mass transport problem is as follows: Find $c = c(\boldsymbol{x},t)$ such that

$$\frac{\partial}{\partial t} \left(\phi_j c_i \right) = \nabla \cdot \left(\mathbf{j}_{ij} - \mathbf{u} c_i \right) + R_{ij} \ . \tag{16}$$

Diffusion in porous media is often described by modified Fickian laws of diffusion. Instead of Fick's first law, the diffusion flux j is given in the form

$$\mathbf{j}_{ij} = -\phi_j G\left(\phi_j, S\right) D_j \nabla c_i \ , \tag{17}$$

where

i = species

j = bw or fw for bound or free water species, respectively

G = geometric factor, which takes account of the longer diffusion path in a porous medium compared to free space and other geometric processes. It may depend both on volume fraction and saturation.

Free and bound water diffusion constants have traditionally been named pore D_p and surface diffusion D_s constants, respectively.[5]

It is clarifying to write out the complete set of transport equations:

$$\partial_t c_{s\mathrm{Cl}} = D_p \nabla^2 c_{s\mathrm{Cl}} \ ,$$

$$\partial_t c_{r\mathrm{Cl}} = D_p \nabla^2 c_{r\mathrm{Cl}} - \lambda_{\mathrm{Cl}} c_{r\mathrm{Cl}} \ ,$$

$$\partial_t c_{s\mathrm{Na}} = D_p \nabla^2 c_{r\mathrm{Na}} + \phi_{fw} r \ ,$$

$$\partial_t c_{s\mathrm{NaX}} = D_s \nabla^2 c_{s\mathrm{NaX}} - \frac{\phi_{fw}}{\phi_{bw}} r \ ,$$

$$\partial_t c_{r\mathrm{Na}} = D_p \nabla^2 c_{r\mathrm{Na}} - r - \lambda_{\mathrm{Na}} c_{r\mathrm{Na}} \ ,$$

and

$$\partial_t c_{r\mathrm{NaX}} = D_s \nabla^2 c_{r\mathrm{NaX}} + \frac{\phi_{fw}}{\phi_{bw}} \left[r - \lambda_{\mathrm{Na}} c_{r\mathrm{NaX}} \right] \ , \tag{18}$$

where $\lambda_i \, (i = \mathrm{Cl}, \mathrm{Na})$ is the linear reaction rate, e.g., radioactive decay.

II.E. With and Without Surface Diffusion

Both Numerrin and COMSOL apply surface diffusion and exchange kinetics, but TOUGHREACT applies traditional porous media diffusion and assumes exchange equilibrium, which means that the K_d value is needed.

Assuming equilibrium to be already obtained, the effective diffusivity formulas for the two approaches are given by[6]

$$D_e^t = \phi^t D_p^t$$

and

$$D_e^s = \phi^s D_p^s + (1 - \phi^s) K_d^s \rho_d D_s \ , \tag{19}$$

where t and s stand for traditional and surface diffusion, respectively, and similarly for apparent diffusivities, we have

$$D_a^t = \frac{D_e^t}{\alpha^t} = \frac{\phi^t D_p^t}{\phi^t + (1 - \phi^t) K_d^t \rho_d}$$

and

$$D_a^s = \frac{D_e^s}{\alpha^s} = \frac{\phi^s D_p^s + (1 - \phi^s) K_d^s \rho_d D_s}{\phi^s + (1 - \phi^s) K_d^s \rho_d} \ . \tag{20}$$

In order to compare the models, the effective and apparent diffusivities should have similar values:

$$\phi^t D_p^t = \phi^s D_p^s + (1-\phi^s) K_d^s \rho_d D_s$$

and

$$\phi^t + (1-\phi^t) K_d^t \rho_d = \phi^s + (1-\phi^s) K_d^s \rho_d \,, \qquad (21)$$

where in the latter formula the equality of effective diffusivity values has been utilized. Finally, parameter values to be applied in traditional modeling given by surface diffusion parameters are

$$D_p^t = \chi D_p^s + \left(\frac{1}{\phi} - \chi\right) K_d^s \rho_d D_s$$

and

$$K_d^t = \frac{(\chi-1)\phi + (1-\chi\phi) K_d^s \rho_d}{(1-\phi)\rho_d} \,. \qquad (22)$$

III. CASES

In all test cases simple one-dimensional geometry of 0.1-m length is applied. The right boundary is closed for mass transport, like the left side is only closed for bound water species. However, a concentration boundary condition is applied for free water species on the left boundary. The parameters that we used can be found in Table I.

The needed bentonite parameters are given in Table I. The initial state is given by assuming that all bound sites are occupied by stable sodium and in free water there is the concentration 100 mol/m^3 of stable sodium and chloride. At the left boundary there is the same total concentration, but the fraction of "radioactive" NaCl is varied.

The goal is to model the evolution of the system, varying also the kinetics in COMSOL and Numerrin.

TABLE I

Parameter Values for Test Cases

Symbol	Value
ρ_d	1600 kg/m^3
ϕ	0.4
χ	0.25
$\chi\phi$	0.1
S	1
D_p^s	1E−10 m^2/s[a]
D_s	1E−12 m^2/s
D_p^t	6.1E−11 m^2/s
K_d^s	0.010 m^3/kg
K_d^t	0.015 m^3/kg
CEC	1 eq/kg

[a]Read as 1×10^{-10} m^2/s.

IV. RESULTS

Figure 2 shows the results of the comparison among the three models (COMSOL, Numerrin, and TOUGHREACT) (fraction of radioactive NaCl is 0.001). Because of relatively high kinetic rates, all the approaches give rather similar results. If the kinetic rates on Numerrin and COMSOL were slower, the results would differ because TOUGHREACT uses the equilibrium approach.

V. CONCLUSIONS

Two of our test models, COMSOL and Numerrin, are more easily suitable for kinetic surface reactions, while the third one, TOUGHREACT, accepts equilibrium models in a rather straightforward manner. Another difference is in the implementation of surface diffusion models, which is straightforward for COMSOL and Numerrin, while in TOUGHREACT, we applied traditional porous medium diffusion with modified parameter values.

Our aim in this and future work is to model thermal-hydraulic mechanical-chemical reactions using the same numerical implementation and apply the best knowledge of bentonite's microstructure and transport properties. The work has appeared difficult to carry out mainly because of limited understanding of basic physical and chemical reactions and phenomena and not so much because of limitations in the actual implementations of the models. However, computational problems may still be difficult when all the needed physics and chemistry are implemented.

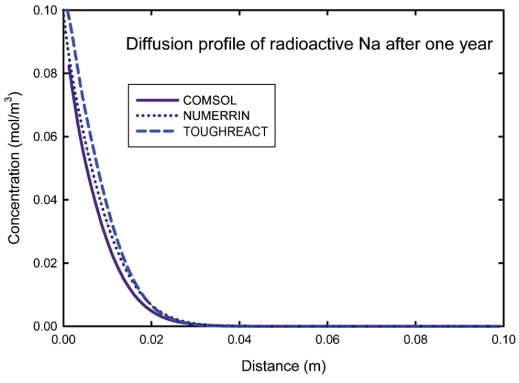

Fig. 2. Comparison of the models applied.

ACKNOWLEDGMENTS

The study is jointly funded by the Finnish Research Program on Nuclear Waste Management (KYT2010) and VTT.

REFERENCES

1. K. PRUESS, C. OLDENBURG, and G. MORIDIS, "TOUGH2 User's Guide, Version 2.0," LBNL-43134, Lawrence Berkeley National Laboratory (1999).

2. T. XU et al., "TOUGHREACT User's Guide: A Simulation Program for Nonisothermal Multiphase Reactive Geochemical Transport in Variably Saturated Geologic Media, Version 1.2.1," LBNL-55460, Lawrence Berkeley National Laboratory (2004).

3. A. ITÄLÄ et al., "Comsol Multiphysics, TOUGHREACT and Numerrin Comparison in Some Modelling Task of Spent Nuclear Fuel Disposal," presented at Comsol Conference 2010, Paris, France, 2010; www.comsol.com/papers/8807/ (current as of May 15, 2013).

4. A. MUURINEN, T. CARLSSON, and A. ROOT, "Bentonite Pore Distribution Based on SAXS, Chloride Exclusion and NMR Studies," *Clay Minerals*, **48**, 251 (2013); http://dx.doi.org/10.1180/claymin.2013.048.2.07.

5. A. RASMUSON and I. NERETNIEKS, "Surface Migration in Sorption Processes," TR 83-87, SKBF/KBS (1983).

6. M. OLIN, "Diffusion in Crushed Rock and in Bentonite Clay," VTT Publication 175, VTT Technical Research Centre of Finland (1994).

PUBLICATION VI

Methodology for studying the composition of non-interlamellar pore water in compacted bentonite

In: Clay Minerals (2016), Vol. 51, No. 2, pp. 173–187.

Clay Minerals, (2016) **51**, 173–187

Methodology for studying the composition of non-interlamellar pore water in compacted bentonite

JOONAS JÄRVINEN*, MICHAŁ MATUSEWICZ AND AKU ITÄLÄ

VTT Technical Research Centre of Finland Ltd, P.O. Box 1000, FI-02044 VTT, FINLAND

(*Received 31 May 2015; revised 07 February 2016; Guest Editor: Maarten Van Geet*)

ABSTRACT: Many safety functions required of the compacted bentonite buffer in the KBS-3 concept rely on processes influenced by the composition of the pore water. Important safety-relevant processes are related to the bentonite buffer, *e.g.* swelling, precipitation and dissolution reactions, and transport of water, colloids and ions. One of the methods used in analysing pore water in compacted bentonite is the 'squeezing technique'. Various possible artefacts which can occur during squeezing, such as mixing of different pore-water types, dissolution of accessory minerals and cation exchange, need special attention.

The present work describes the methodology for studying the composition of the non-interlamellar pore water by combining squeezing methods, chemical analyses, microstructure measurements and geochemical modelling. Four different maximum pressures were used to squeeze the compacted bentonite pore water. The origin of the pore water was studied by analysing the bentonite microstructure both before and after squeezing using SAXS and NMR, the cation exchange and dissolution reactions were studied by chemical analyses and geochemical modelling.

The pore-water yield increased from 32 to 48 wt.% from the initial amount of pore water in the samples when the maximum squeezing pressure was increased from 60 MPa to 120 MPa. About 35 wt.% of the water collected originated from the interlamellar (IL) pores. The ratio between IL and non-IL pore waters as well as the composition of the squeezed pore water was constant in the squeezing-pressure range used. The results of microstructural measurements by SAXS were in perfect agreement with previous studies (*e.g.* Muurinen & Carlsson, 2013). The dissolving accessory minerals have an effect on the ratio of the cations in the squeezed solution while the migration of anions in bentonite seems to be diffusion limited. According to geochemical modelling the chloride concentration of the non-IL pore water in compacted bentonite before squeezing was 0.34 M greater than in the squeezed pore water due to the mixing of two main water types.

KEYWORDS: bentonite, pore water, squeezing, microstructure.

The Finnish and Swedish plans for disposal of spent nuclear fuel are based on the KBS-3 concept (KärnBränsleSäkerhet, nuclear fuel safety). The spent nuclear fuel will be contained in copper canisters which will be emplaced several hundred metres deep into bedrock and surrounded by a compacted bentonite barrier (Posiva, 2010; SKB, 2011). The purpose of the bentonite buffer is to maintain the integrity of the canisters and to limit and retard the release of radionuclides from the canisters. Many of the safety functions of the bentonite buffer are determined by montmorillonite and based on processes which are related to the composition of the buffer pore water. Important safety-relevant processes are, *inter alia*, swelling, precipitation and dissolution reactions, and transport of the water, colloids and ions (Posiva, 2010). The Wyoming MX-80 bentonite used in

*E-mail: joonas.jarvinen@vtt.fi
DOI: 10.1180/claymin.2016.051.2.05

the experiments consists mainly of sodium/calcium montmorillonite, smaller amounts of other minerals (quartz, calcite, feldspar, *etc*.) and pore water (Muurinen, 2010; Kiviranta and Kumpulainen, 2011).

The pore water in compacted bentonite consists of interlamellar water (IL-water) and non-interlamellar water (non-IL water) (Pusch *et al.*, 1999; Bradbury & Baeyens, 2002; Wersin, 2003; Fernández *et al.*, 2004; Muurinen *et al.*, 2007; Holmboe *et al.*, 2012; Muurinen & Carlsson, 2013). The fraction of non-IL water in compacted bentonite changes as a function of the dry density, the salinity of the non-IL water and exchangeable cations in montmorillonite (Van Loon *et al.*, 2007; Muurinen & Carlsson, 2013). The exchangeable cations, external conditions, the dissolving components in montmorillonite and accessory minerals determine the composition of the non-IL water, and thereby the amounts of major ions in the non-IL water: Ca, Na, sulfate, bicarbonate, chloride, Mg and K. In addition to simplified distribution of the pore water into two water types, the negative charge of the unit layers should also be taken into account when non-IL water composition is evaluated. Repulsion of the anions by the negatively charged surfaces (exclusion) restricts the anion-accessible space in the pore water which varies according to ionic strength and dry density. In the present study the anion-accessible space is referred to as chloride-accessible porosity (Cl-porosity) according to the anion used to evaluate the volume proportion (Bolt & Warkentin, 1958; Van Loon *et al.*, 2007; Muurinen, 2009; Muurinen & Carlsson, 2013). The composition of the pore water in the compacted bentonite can be studied by, among other methods, the squeezing technique (Muurinen & Lehikoinen, 1999; Sacchi *et al.*, 2001; Fernández *et al.*, 2014). Although this technique has been used successfully on highly consolidated clayrocks in many studies, the effects of squeezing on bentonites are still under study (Muurinen, 2001; Fernández *et al.*, 2004, 2014, 2015). Due to the high pressure used in squeezing bentonite for extracting pore water, different pore-water types may mix together and cause a new chemical balance between montmorillonite, IL-water, non-IL water and the anion-accessible water. This may cause dissolution of the easily dissolving minerals in non-IL water, changes in the composition of exchangeable cations and dilution of the anion concentrations. The rate at which pore water can be squeezed from bentonite depends on the hydraulic conductivity, and the force needed in squeezing depends on the swelling pressure (Muurinen, 2006; Muurinen & Järvinen, 2013; Fernández *et al.*, 2014).

The aim of the present study is to develop a squeezing methodology to analyse the chemical composition of non-IL water from compacted bentonite by combining chemical analyses, measurements of microstructure and geochemical modelling. The methodology used here is a combination of techniques tested by Muurinen (2001) for squeezing tests, by Karnland *et al.* (2006), Muurinen (2006) and Kumpulainen & Kiviranta (2011) for chemical analyses, and by Muurinen & Carlsson (2013) and Matusewicz *et al.* (2013) for microstructure studies.

Block 1 (MX-80) from package 2 of the Alternative Buffer Material (ABM) project was used in the present study. More detailed information about the ABM project at Äspö in Sweden can be found in Svensson *et al.* (2011). Four fully saturated parallel samples were squeezed under anoxic conditions. The squeezing pressure was increased stepwise to a maximum value. Four maximum pressures were used: 60, 80, 100 and 120 MPa. To estimate the origin of the squeezed pore waters and to reverse calculate the initial chemical composition of non-IL pore water in the compacted bentonite, several analyses were performed. The ratios of the IL and non-IL water were determined by SAXS and NMR measurements before and after squeezing. The squeezed pore-water concentration, water content before and after squeezing, as well as the exchangeable cations, carbonates, chloride and sulfate content in oven-dried bentonite at 105°C were determined. A simplified conceptual model was used in geochemical modelling, where the pore water was divided into two water types, IL and non-IL waters. The exclusion effect was not included in the geochemical modelling.

EXPERIMENTAL

Background of the samples

To study the behaviour of the alternative buffer materials (ABM) in field conditions, three packages were assembled in the Äspö Hard Rock Laboratory (HRL) at the end of 2006. The packages contained a central steel tube with a heater, and 11 different compacted clay rings. The heater target temperature was 130°C. The clay rings had a diameter of 30 cm and a height of 10 cm. The whole test package was ∼3 m high. Two of the packages were saturated artificially and the third was saturated naturally (Svensson *et al.*, 2011). Package 2 was dismantled in 2013. Part of the lower block 1 (MX-80) of package 2 was used in these experiments. The sample studied was altered by heat and Ca-rich solution during the 7 y of underground

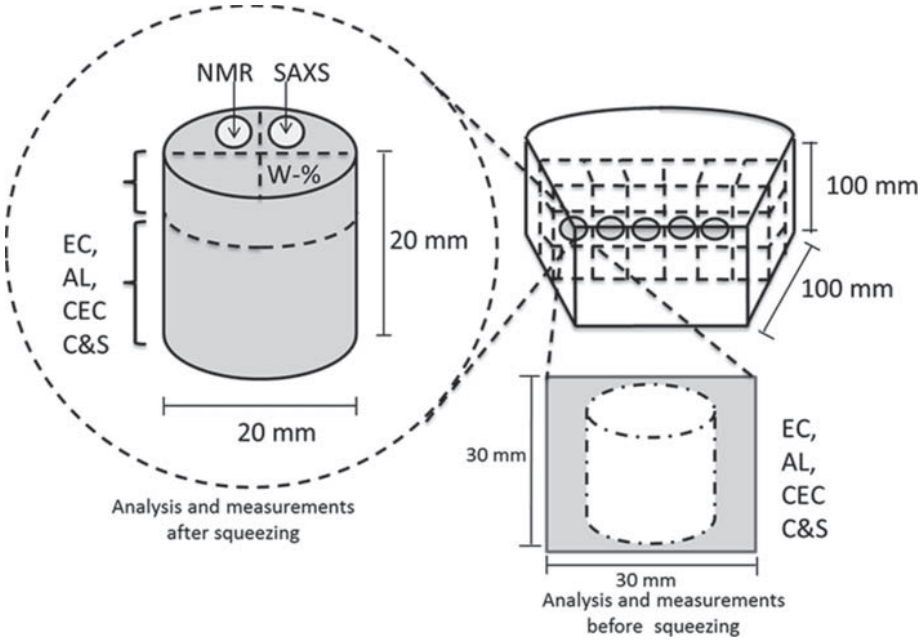

FIG. 1. Schematic representation of the cutting of block 1 into subsamples for squeezing experiments (on the upper right), and for analyses before (on the lower right) and after (on the left) squeezing. The samples for SAXS, NMR and water-content measurements were cut from the wet sample before and after squeezing and the rest of the sample was dried at 105°C. EC = exchangeable cations, AL = aqueous leachates, CEC = cation exchange capacity, C&S = total carbon + sulfur + carbonates. The grey-coloured areas are used for analyses.

experiment. Thus, the composition of the sample no longer corresponded to MX-80 bentonite. The dominant exchangeable cation was Ca rather than Na, and the chloride content was greater.

Sampling

After uplift, a third of block 1 was cut by Clay Technology AB and enclosed in a gas-tight vacuum bag. The part of the block to be used for squeezing studies was enclosed in metal transportation vessels in inert gas and transported to VTT's laboratory where it was further cut into smaller subsamples with a band saw under anoxic conditions: (1) A 1 cm-thick slab was cut from one side of the block to prepare 1 cm^3 (1 cm × 1 cm × 1 cm) sub-samples for water content measurements. A 1–2 mm slice in contact with the rock surface was cut from these subsamples to remove sand. (2) 3 cm-thick slabs were cut from the block to prepare ~27 cm^3 (3 cm × 3 cm × 3 cm) blanks for the squeezing studies. The blanks were further cut into cylindrical sub-samples (diameter: 2 cm, height: 2 cm) with a cutting knife. Four parallel sub-samples were chosen for the squeezing experiments and one for a reference sample for microstructural and water content measurements. Leftovers from the blanks were dried at 105°C and used for chemical analyses to represent the state before squeezing.

The cutting scheme of block 1 is presented in Fig. 1. The cutting and shaping of the subsamples were carried out under anoxic conditions in an argon-flushed glove-box. The oxygen concentration in the glove-box atmosphere during cutting of the sub-samples with a band saw varied from 10 to 300 ppm and from 1 to 10 ppm during final preparation of the cylindrical samples. After the analyses and measurements, each sample was dried at 105°C for 24 h and enclosed in an individual vessel to await chemical analysis.

Squeezing

Pore water was squeezed from the four parallel bentonite samples (diameter: 20 mm and height: 20 mm) with a squeezing apparatus as depicted in Fig. 2. A strong spring maintained the pressure during squeezing. The length of the frame to which the squeezing cell was fixed was adjusted with a hydraulic

pump in order to increase the pressure. The pressure was increased stepwise to the chosen maximum pressures: 60, 80, 100 and 120 MPa. The lowest maximum pressure value was set at 60 MPa in order to reach an adequate yield of pore water for chemical analyses (0.8 mL) and the upper limit (120 MPa) was the maximum force possible with the equipment used. All the bentonite samples were squeezed at the same time with a similar procedure. The sample preparation, squeezing, pH measurements and HCO_3^- titration were performed under anoxic conditions. The squeezed pore water was collected using a 2 mL syringe.

Analysis of the clay matrix

After squeezing, the wet clay samples were cut into pieces, and microstructure and water-content measurements were performed. The rest of the sample was dried at 105°C for chemical analyses. Reference samples were taken from the blanks used to prepare cylindrical squeezing samples. (Fig. 1)

The water content, weight of the water per weight of the solids, was determined by gravimetric measurement of weight loss at 105°C for a period of 24 h. The cation exchange capacity (CEC) was determined by dispersing 0.3 g of dry clay in 16 mL of 10 mmol/L Cu(II)-triethylenetetramine solution. The copper adsorption was measured at 577 nm using a Shimadzu UV-180 spectrophotometer (Meier & Kahr, 1999; Amman *et al.*, 2005). The exchangeable cations were analysed by dispersing 1 g of dried clay in 20 mL of NH_4Cl in 80% ethanol. Then the solution was evaporated and the solids dissolved into water, and the Fe, Ca, K, Mg and Na cations were analysed by Inductively Coupled Plasma-Optical emission spectrometry (ICP-OES). The uncertainty of the ICP-OES analyses was ±10% according to the accredited laboratory, 'Ramboll Analytics' (Vantaa, Finland). Aqueous leachates were prepared by dispersing the bentonite sample in deionized water (0.3 g/30 mL) and left to soak for a week. Then the solid phases were separated by centrifuging at 8000 rpm for 5 h, the solution phase was ultra-filtered by 10kD ultra-filters and analysed using Ion Chromatography (IC). The estimated uncertainty in the IC measurements of Cl^- and SO_4^{2-} was ±20% and ±15%, respectively, according to Ramboll Analytics. The total carbon and sulfur were determined by combustion (up to 1400°C) measuring the evolved S and C compounds by infrared detector. To determine carbonates, a dry sample was treated with HCl and the amount of total carbon was determined by an ELTRA CS 2000 device, with a detection limit of the detector at 0.05%. The uncertainty of the carbonate analysis was ±25% according to the accredited laboratory Labtium Oy (Kuopio, Finland). The amounts of bentonite and water that remained in the sinters were determined by gravimetric measurement of weight loss at 105°C, before and after ultrasonic cleaning.

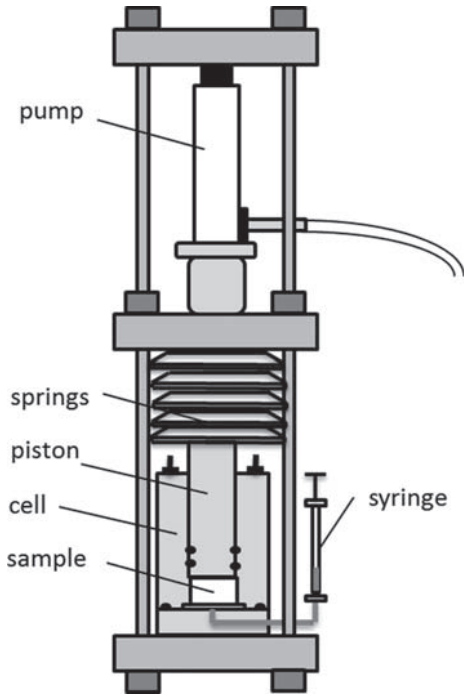

FIG. 2. Squeezing apparatus with the compaction cell (6 cm × 10 cm) made of stainless steel for the bentonite sample (2 cm × 2 cm) allocation and the syringe for collecting squeezed pore water (Muurinen, 2001).

ANALYSES OF SQUEEZED PORE WATER

After completion of the squeezing test, the syringe was decoupled from the device and the exact amount of squeezed pore water in the syringe was determined gravimetrically. The squeezed pore-water samples were analysed by ICP-OES to determine Ca, Na, K, Mg and Fe concentrations, by IC to determine sulfate and chloride concentrations, and by titration to determine bicarbonate according to the Gran method (Gran, 1950), and the pH value by an IrOx electrode (Muurinen, 2009; Itälä *et al.*, 2013). The pore-water samples were kept in air-tight syringes before the bicarbonate and pH determinations. These last

measurements were carried out inside an anoxic glovebox in closed vessels to minimize contact with the argon atmosphere (CO_2 content of <0.04 ppm). The gas volume in the titration vessel was 100 mL and the sample size was 3 mL. The pH change before titration was ~1 pH unit, which corresponds to a change of <0.01 mM in bicarbonate concentration. The estimated uncertainty for the IC and ICP-OES analyses was ±20% and ±10%, respectively, according to the accredited laboratory ALS Finland Oy (Helsinki, Finland).

Small angle X-ray scattering (SAXS)

Samples for SAXS measurements were probed with a stainless steel cylindrical cutter 4 mm in diameter. The samples obtained were further cut into 0.3 mm slices. The slices were enclosed in metal rings and sealed tightly with thin polypropylene film to prevent drying during the measurement. All the preparations were carried out in a chamber with controlled relative humidity of ~80%. Reference samples were cut from the clay blocks, and the squeezed samples were probed directly in the squeezing cells.

The X-rays were generated with an X-ray tube with a Cu-anode (PANalytical, Almelo, the Netherlands). The X-ray beam was collimated and monochromated to Cu-*K*α radiation (1.54 Å) using a Montel-multilayer mirror. The scattered X-rays were collected using a Bruker Hi-Star area detector. Based on the scattering patterns, the average interlamellar distance was calculated and the mean stack size was estimated. Along with the specific surface area (Kumpulainen & Kiviranta, 2011), these values were used to calculate the volume of the interlamellar pores (Matusewicz *et al.*, 2013; Muurinen & Carlsson, 2013).

Nuclear magnetic resonance (NMR)

The stainless steel cylindrical cutter (Ø 4 mm) was also used to probe the reference samples from the clay blocks, and the squeezed samples from the squeezing cells. The clay sample from inside the cutter was pushed into a glass NMR tube (4 mm inner Ø) (Wilmad, USA) and closed tightly at both ends with polytetrafluoroethylene (PTFE) caps. The measurements of the samples were carried out using a high-field Chemagnetics CMX Infinity 270 MHz NMR spectrometer with a 5 mm static ^{1}H NMR probe using a spin-locking Carr-Purcell-Meiboom-Gill (CPMG) technique (refocusing delay of 22 µs). The experiments were carried out at room temperature. The signal obtained from the method is the relaxation curve of the hydrogen nuclei in water molecules. The more confined the pore space is, the shorter is the relaxation time. A cut-off time of 510 µs was used here to separate the signal from the pore water in the nanopores, including the interlamellar pores, and remaining water (Ohkubo *et al.*, 2008; Matusewicz *et al.*, 2013).

Geochemical modelling

Geochemical modelling was based on the assumption that cations stay in the interlamellar space during squeezing and the deionized water from the IL space will mix with the non-IL pore water.

The modelling was performed using the *PHREEQC* code as a batch model (Parkhurst & Appelo, 2013). In the first phase, calcite, gypsum, cation exchange and surface complexation sites were equilibrated with the assumed pore water composition in the bentonite. After that, in the second phase, the pore water was mixed with the assumed deionized IL water in the ratio determined by the NMR and SAXS measurements for bound and free water. Then in the third phase, the mixed water was equilibrated with bentonite to obtain the composition of the squeezed pore water in the syringe. The geochemical modelling was performed as a target calculation, where the composition of mixed water in the third phase was iterated to respond to the squeezed pore water by changing the pore-water composition in the first phase.

The surface complexation parameters were taken from Bradbury & Baeyens (2002). The cation exchange parameters needed to be adjusted because after the ABM test in Äspö the bentonite was no longer the same as the initial MX-80. The initial Na-bentonite had equilibrated with various different bentonite materials and at the end of the ABM test was in a Ca form. Relevant cation exchange data, therefore, could not be found for these conditions in the literature. Thus, the cation exchange selectivity values were fixed so that the modelling results corresponded to experimental results. The cation-exchange parameters used are

TABLE 1. Cation exchange selectivity coefficients

Reaction	Selectivity coefficient
$^{K/Na}K_c$	8.51
$^{Mg/Na}K_c$	4.46
$^{Ca/Na}K_c$	8.32

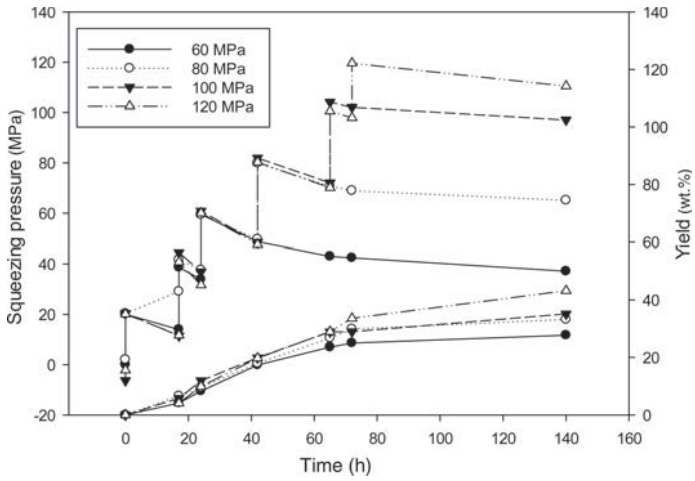

FIG. 3. Squeezing pressure and pore-water yield during the squeezing experiments as a function of time. The water yields were 32, 38, 41 and 45 wt.% for maximum squeezing pressures of 60, 80, 100 and 120 MPa, respectively.

presented in Table 1. The Thermoddem database was used for the modelling (Blanc *et al.*, 2007).

RESULTS

Squeezing

Six days (144 h) was the time for squeezing the samples to reach an adequate yield of pore water but to minimize back diffusion of ions if the squeezed porewater was not in equilibrium with the bentonite. The initial dry density of the samples was 1.45 g/cm^3 and the maximum squeezing pressures 60, 80, 100 and 120 MPa. The development of the squeezing pressures and yield of the pore water by squeezing are shown in Fig. 3.

The pore-water yield was calculated according to equation 1, where, m_{syr}, m_{sinter} and m_{tubes} are balanced amounts of the water in the syringe, sinter and tubes, respectively, and m_{H_2O} the total amount of water in the sample before squeezing, according to the water content measurements.

$$\text{Yield} = \frac{m_{syr} + m_{sinter} + m_{tubes}}{m_{H_2O}} \times 100\% \quad (1)$$

The recovery efficiency (RE %) is the amount of squeezed pore water in the syringe divided by the loss of water from the clay sample during the squeezing according to water-content measurements before and after squeezing. The recovery efficiency is calculated according to equation 2, where m_{dry} is the dry weight of the sample, and wt.%$_{initial}$ and wt.%$_{end}$ are the water contents before and after squeezing, respectively.

$$\text{RE} = \frac{m_{syr}}{m_{dry} \times (\text{wt.\%}_{initial} - \text{wt.\%}_{end})} \times 100\% \quad (2)$$

The dry densities (ρ_{dry}) were calculated according to equation 3, whereby the water density $\rho_{H_2O} = 1.00$ g/cm^3, grain density $\rho_g = 2.76$ g/cm^3, and wt.% is the water mass per dry sample mass at 105°C (Karnland *et al.*, 2006).

$$\rho_{dry} = \frac{\rho_{H_2O} \times \rho_g}{\rho_g \times \frac{\text{wt.\%}}{100\%} + \rho_{H_2O}} \quad (3)$$

The samples' total weight and water content were determined before squeezing. The mass of the squeezed pore water in the syringe, the final sample water content and water in the sinters were determined after squeezing. The average water volume of the connecting pipe and the sinter was 0.085 mL. The calculated and measured values are presented in Table 2.

Squeezing of all of the samples was started at the same time. The pressure was increased stepwise in 20 MPa steps until the maximum pressure was reached. Before the samples were dismantled the pore water was collected for at least 60 h after reaching the maximum pressure. All the samples were dismantled at the same time.

There was a clear difference in the amount of the squeezed pore water obtained at the various squeezing pressures. The yield increased from 32 to 48 wt.% when

TABLE 2. Results from the squeezing experiments at different maximum pressures. The average initial values for dry density and water content were 1.45 g/cm^3 and 33.0 wt.%, respectively.

Maximum squeezing pressure	Before squeezing sample wet mass	After squeezing		Water in		Yield	
		Dry density	Water content	Squeezed pore water	Sinter and tubes	From pore water	Recovery ratio
(MPa)	(g)	(g/cm^3)	(wt.%)	(mL)	(g)	(wt.%)	(wt.%)
60	11.659	1.76	20.71	0.848	0.0881	32.4	78.7
80	11.043	1.79	19.69	0.956	0.0819	37.9	86.6
100	11.190	1.82	18.71	1.057	0.0852	41.2	88.0
120	11.870	1.88	16.87	1.340	0.0846	48.4	93.1

the maximum squeezing pressure increased from 60 to 120 MPa. The recovery ratio was better for samples with a higher squeezing pressure, obviously caused by the larger amount of water collected in the syringe.

Pore-water analyses

The chemical compositions of the squeezed and modelled pore waters are presented in Table 3. The Charge Balance Error (CBE, %) was calculated based on the species in the Thermoddem database when using the *PHREEQC* code.

The CBE is clearly below the acceptable limit of ±5%. The variation in pH between samples was <0.05 pH units. No significant drop in ion concentrations as a function of the squeezing pressure was observed between the maximum pressures from 60 to 100 MPa. A slight reduction in chloride, Na, K and Ca contents was detected when the maximum squeezing pressure was increased from 100 to 120 MPa. These changes are below the uncertainty limit of the chemical analyses, however.

Analytical results from the clay matrix

The samples were dismantled after squeezing as indicated in Fig. 1. The four sub-samples selected for the squeezing tests were cut at an identical distance from the heater and height from the bottom of block 1, and thus were parallel. The concentrations of chlorides and sulfates in the bentonite for each sample before and after squeezing are listed in Table 4. The exchangeable cations and CEC results for each sample before and after squeezing are shown in

TABLE 3. Chemical composition of the squeezed (60–120 MPa) and modelled (0 MPa = non-IL water before squeezing) pore waters.

Phase	Unit	Modelled	Squeezing pressure (MPa)			
		0	60	80	100	120
pH	(–)	7.7	7.7	7.7	7.7	7.7
Na	(mmol/L)	425	239	240	237	217
K	(mmol/L)	3.9	2.1	2.2	1.8	1.6
Ca	(mmol/L)	110	62	62	67	59
Mg	(mmol/L)	46	25	24	25	25
Cl^-	(mmol/L)	712	381	375	384	355
SO_4^{2-}	(mmol/L)	13	7	7	6	7
Alkalinity	(meq/L)	0.7	3.6	3.9	3.3	3.4
Ionic strength	(M)	0.84	0.47	0.47	0.48	0.44
Charge balance error	(%)	–	2.1	2.6	2.9	2.0

The uncertainty for anion and cation analyses was ±20% and ±10%, respectively.

TABLE 4. Concentrations of carbonates, water-dissolving chloride and sulfate from samples before and after squeezing.

Max. S.P. (MPa)	Before squeezing (0 MPa)				After squeezing			
	C_org (mg/g)	C_carb (mg/g)	Cl^- (mg/g)	SO_4^{2-} (mg/g)	C_org (mg/g)	C_carb (mg/g)	Cl^- (mg/g)	SO_4^{2-} (mg/g)
60	1.85	1.96	2.87	4.39	2.17	1.37	0.66	3.08
80	1.61	2.18	2.39	3.86	2.44	1.58	0.58	2.90
100	1.84	2.18	2.74	3.68	2.07	1.82	0.57	3.37
120	1.95	2.80	2.4	4.02	2.88	0.77	0.47	3.40
Avg.	1.81	2.28	2.60	3.99	2.39	1.39	0.57	3.19
SD	0.14	0.36	0.24	0.30	0.36	0.45	0.08	0.24

Max. S.P. = maximum squeezing pressure, SD = standard deviation.

Table 5. Standard deviation (SD) was calculated from four parallel samples for ion content, exchangeable cations and CEC analyses. Twice the value of SD (2 × SD) from each of the four parallel samples was used as the limit of error analyses, representing a 95% confidence level.

The 2 × SD value between parallel samples was ±0.7 mg/g, ±0.5 mg/g and ±0.6 mg/g for carbonates, chloride and sulfate, respectively. A clear decrease in the chloride content and slight reductions in the carbonate and sulfate contents were observed after the squeezing experiments but not as a function of the squeezing pressure. The carbonate content in the samples was calculated by subtracting the amount of organic carbon from total carbon. A decrease in total carbon content was not observed before or after

TABLE 5. Cation exchange capacity (CEC) and exchangeable cations before and after squeezing.

Max. S.P. (MPa)	CEC (meq/100 g)	Exchangeable cations			
		Ca (meq %)	K (meq %)	Mg (meq %)	Na (meq %)
Before squeezing					
60	86.0	52.2	1.7	11.5	34.7
80	86.9	53.6	1.8	10.8	33.8
100	85.9	53.6	1.7	10.2	34.4
120	86.5	52.8	1.9	11.5	33.9
Average	86.3	53.1	1.8	11.0	34.2
SD	0.46	0.69	0.09	0.63	0.42
After squeezing					
60	85.7	53.6	1.8	10.8	33.8
80	87.1	52.3	1.9	10.6	34.2
100	87.2	54.0	1.8	11.0	33.2
120	OL	53.1	1.7	11.1	34.1
Average	86.7	53.3	1.8	10.9	33.8
SD	0.84	0.73	0.08	0.22	0.45

OL: excluded as an outlier (83.8).
SD = standard deviation.
Max S.P. = Maximum squeezing pressure.

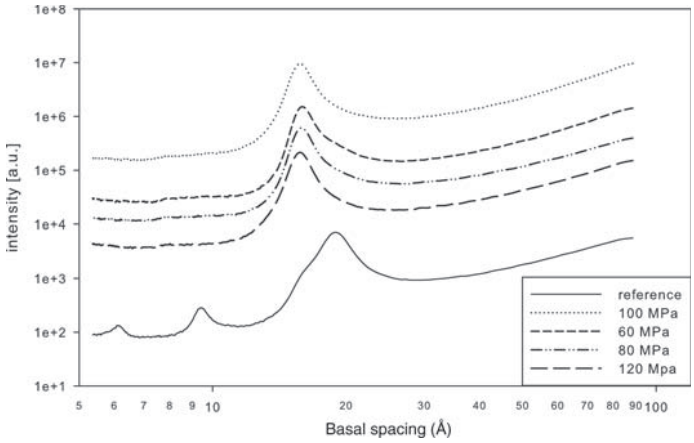

FIG. 4. Scattering intensities of montmorillonite in the reference sample and squeezed samples as a function of basal spacing.

squeezing. Thus, changes in the carbonate content before and after squeezing seem to be more dependent on the analytical method than due to a real decrease in carbonate content; these data were therefore excluded from interpretations of the results.

The chloride-accessible porosity was calculated according to equation 4, where m_{Cl} is the chloride mass in the sample (g), m_b is sample dry mass (g), ρ_g is grain density of the clay (g/cm^3), V_w is the water volume in the sample (cm^3) and C^o_{Cl} is the chloride concentration (g/cm^3) in the external solution (Muurinen & Carlsson, 2013).

$$\varepsilon_{Cl} = \frac{m_{Cl}}{\left(\frac{m_b}{\rho_g} + V_w\right) C^0_{Cl}} \quad (4)$$

The chloride-accessible porosities were 23, 7.9, 7.2, 7.1 and 6.6 vol.% for samples with maximum squeezing pressures of 0, 60, 80, 100 and 120 MPa, respectively, when squeezed pore-water chloride concentrations were C^o_{Cl}.

The 2 × SD value between the parallel samples was <1.0 meq/100 g and 1.4 meq % for the CEC and exchangeable cations, respectively. The CEC and exchangeable cation compositions were similar for the different squeezing pressures and the samples before and after squeezing. The CEC for the samples after 120 MPa squeezing differs by >∼3 times the SD value. Such a big difference in CEC value would mean structural changes in montmorillonite, and thus the value is expected to be an outlier and is excluded from the interpretation of the results.

SAXS AND NMR

The X-ray scattering curves show a clear difference between the reference sample and the squeezed samples (Fig. 4). For the reference sample, the position of the main peak is at 18.6 Å which corresponds to three water layers in the interlamellar space. A clear shoulder is visible at ∼16 Å which suggests that some of the interlamellar pores have two water layers. For the squeezed samples, a single peak close to 16 Å is observed, suggesting that most of the interlamellar spaces are filled with two water layers. Small differences were also observed between the squeezed samples. The position of the peak shifts slightly towards smaller distances with an increase in the squeezing pressure (Fig. 5).

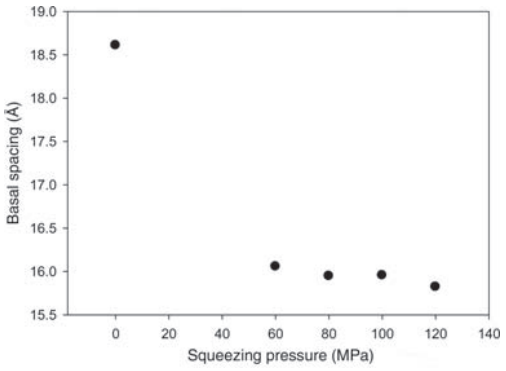

FIG. 5. Variation of basal spacing of montmorillonite as a function of squeezing pressure.

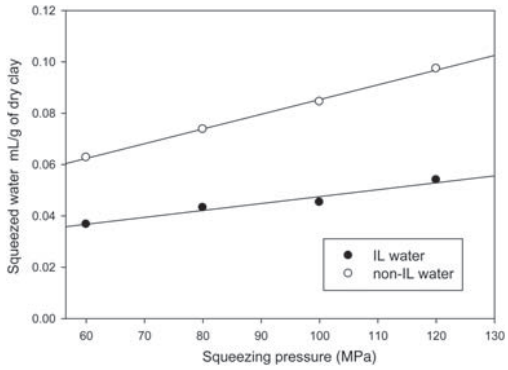

FIG. 6. IL and non-IL water squeezed from the sample – average of two samples used for 100 MPa.

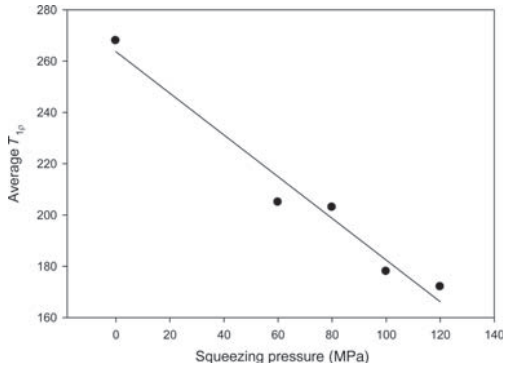

FIG. 7. Average relaxation time as a function of squeezing pressure.

The amount of pore water squeezed out, normalized to 1 g of dry clay mass, is shown in Fig. 6. The squeezed water volume increases linearly with the increasing pressure applied. Approximately 35 wt.% of the collected pore water comes from the IL pores. The proportion of pore water squeezed from the interlamellar spaces and from the remaining pore volume is constant in the pressure range measured.

The analysis of the NMR $T_{1\rho}$ relaxation times shows that the average relaxation time of the samples moves to a faster time for samples squeezed with greater pressure. The larger pores disappear and the average pore size becomes smaller (Fig. 7). A clear linear trend is observed between the average relaxation time and the increasing squeezing pressure.

The estimated IL and non-IL porosity values obtained by SAXS and NMR are listed in Table 6. The values calculated from the NMR results seem to underestimate non-IL porosity because the decay of the time measured signal in the CPMG experiment is proportional to the pore size (smaller decay time, smaller pores). In very high-density samples the difference between the average size of the pores between the clay particles and the interlamellar pores is not large enough to resolve between the two pore types with this method.

Interpretation

Four parallel fully saturated MX-80 bentonite samples were squeezed from an initial dry density of 1.45 g/cm^3 to 1.76, 1.79, 1.82 and 1.88 g/cm^3, by maximum squeezing pressures of 60, 80, 100 and 120 MPa, respectively. The total water content of the samples before squeezing was 33 wt.%, which corresponds to 0.33 mL/g of dry clay at 105°C, where 0.11 mL/g$_{clay}$ was from non-IL space according to the SAXS measurements (Table 6). 32–48 wt.% of pore water was successfully squeezed out, which corresponds to a loss in total water of 0.11 and 0.16 mL/g of bentonite (Table 2).

The microstructural analysis shows a significant difference in the clay structure between the reference

TABLE 6. Comparison of IL and non-IL porosity based on SAXS and NMR measurements.

		SAXS			NMR	
Squeezing pressure (MPa)	Total porosity (vol. %)	Avg IL distance (Å)	IL porosity (vol. %)	Non-IL porosity (vol. %)	IL porosity (vol. %)	Non-IL porosity (vol. %)
0	0.49	18.6	0.33	0.16	0.46	0.03
60	0.37	16.1	0.30	0.07	0.37	0.00
80	0.36	15.9	0.30	0.05	0.36	0.00
100	0.35	16.0	0.31	0.04	0.35	0.00
120	0.32	15.8	0.31	0.02	0.32	0.00

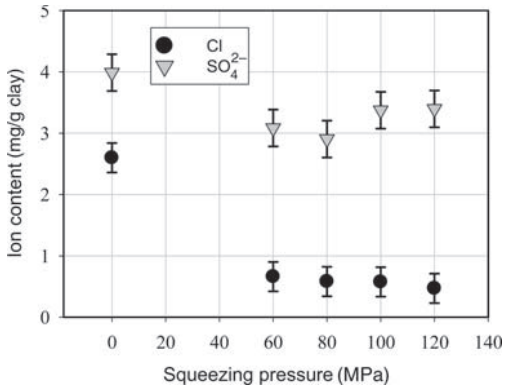

FIG. 8. Chloride and sulfate content as Cl and SO_4^{2-}, respectively, in the clay matrix (mg/g of dry clay). The reference sample (0 MPa) is the average of four parallel samples and the error bar is two times the standard deviation for these samples.

sample and the squeezed samples. A clear reduction in the average basal spacing was observed for an increase in squeezing pressure from 0 to 60 MPa, and a less significant but yet notable decrease was seen as the pressure increased to 80, 100 and then 120 MPa (Fig. 5). At the same time, a decrease was also observed in the volume of the larger pores. The decrease in the calculated values of the porosity shows that the proportion of pore water squeezed from the IL and non-IL pores is constant (Fig. 6).

A clear reduction in the chloride content was observed before and after squeezing (Fig. 8). The calculated chloride-accessible porosities according to equation 4 and based on the analysed values of chloride in the clay matrix and squeezed porewater were 6.6–7.9 vol.% (ρ_{dry} = 1.88–1.76 g/cm^3) for the squeezed samples and 23 vol.% (ρ_{dry} = 1.45 g/cm^3) for the reference sample. These volumes are greater than the measured non-IL porosities using SAXS (2–7 vol.% for the squeezed samples and 16 vol.% for the reference sample). The external water chloride concentration was therefore set at 1 M, when the Cl-accessible porosities decreased to values of 2–3 vol.% for the squeezed samples and to 8.6 vol.% for the reference sample. These values match perfectly with Van Loon *et al.* (2007) with Cl-accessible porosities of 9 ± 2 and 3.5 ± 1 vol.% determined for similar material at 1.6 and 1.9 g/cm^3 dry densities, respectively, in 1 M NaCl solution.

The proportion of the IL, non-IL and chloride-accessible space is presented in Fig. 9. The results match well with previous studies concerning the microstructure of bentonite by Muurinen & Carlsson (2013).

No significant variation in the chemical composition of the squeezed pore water was observed when the

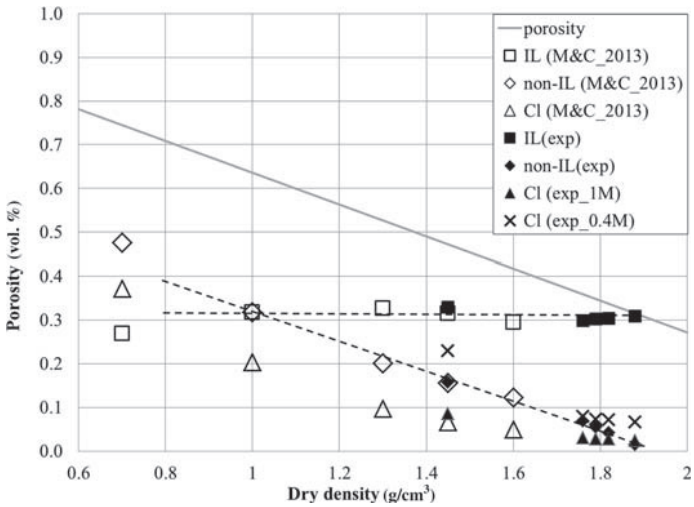

FIG. 9. Porosity *vs.* dry density. Cl is chloride-accessible porosity, IL and non-IL are interlamellar and non-interlamellar porosity, respectively. Exp refers to values measured in the present study. M&C_2013 refers to Muurinen & Carlsson (2013). Dotted lines refer to IL and non-IL porosities *vs.* dry density. 1 M (estimated Cl concentration in Cl-accessible water) and 0.4 M (squeezed pore-water Cl concentration) refers to external water Cl concentrations used to calculate chloride-accessible porosity. Reference sample dry density = 1.45 g/cm^3.

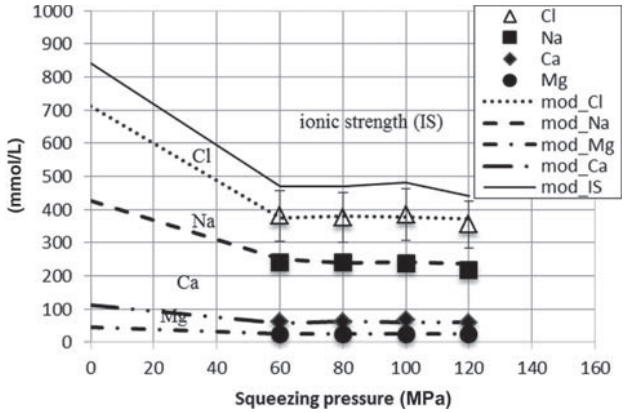

FIG. 10. Exchange isotherm of Na^+ on montmorillonite: squeezed water, as calculated from the squeezed-water composition and exchangeable cations in the present.

pore-water yield increased from 32 to 41 wt.%, *i.e.* from 60 to 100 MPa; a slight dilution of Na and chloride was observed, however, when squeezed pore-water yield increased to 48 wt.% (Table 3).

The modelled results for the initial non-IL and squeezed pore-water compositions are presented together with the squeezed pore-water composition in Figs 10 and 11. The anion-accessible porosities, and diffusion or kinetic limitations were not included in the model.

According to the modelling, the non-IL pore water ionic strength was ~0.840 M which decreased to 0.460 M due to the mixing by IL water during the squeezing process at the pressures studied. The initial non-IL water chloride concentration (0.7 M) according to modelling is smaller than the value (1 M), which corresponds to the chloride-accessible porosities determined by Van Loon *et al.* (2007).

A slight decrease in the total amount of sulfate content was observed to occur during the squeezing according to the clay matrix analyses (Fig. 8). This could be attributed to the dissolution of sulfate due to the mixing of different water types. Only minor concentrations of sulfate (0.7 mM) in the squeezed pore water were analysed. According to geochemical modelling, the dilution of non-IL water dissolves gypsum and calcite at the level of the minerals'

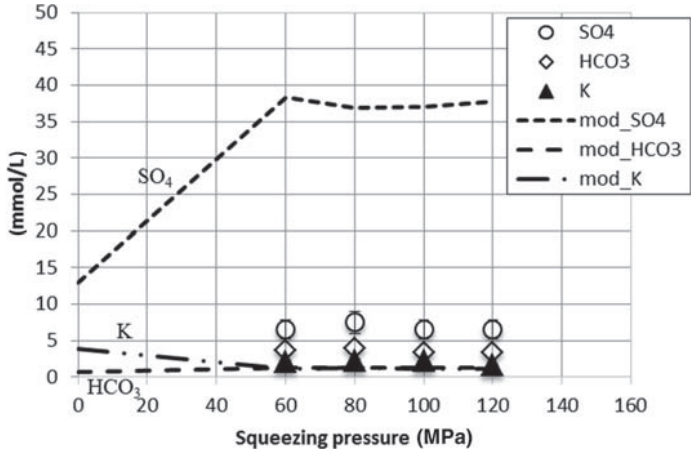

FIG. 11. Initial non-IL water composition according to modelling (0 MPa), and squeezed pore-water (60, 80, 100, 120 MPa) composition according to modelling and experimental results for the main ions. Lines indicate modelling and dots indicate experimental results.

saturation limits, changing the Na/Ca ratio in non-IL water. The exchanger will rebalance the cation ratio and increase dissolution of these accessory minerals. Due to the reaction chain, the sulfate and bicarbonate concentrations should be greater in squeezed pore water than in initial non-IL water (Fig. 11). Such low sulfate concentrations in squeezed pore water may be attributed to the limited space of anions in the real system. This may cause limited migration of large negatively charged ions and greater anion concentrations next to the minerals than predicted by geochemical modelling. Bicarbonate concentration was determined through alkaline titration. Due to the low alkalinity, other compounds such as silicates, organic anions and sulfides may affect the value. This may partly explain high bicarbonate cconcentrations compared with those predicted by geochemical modelling.

Changes before and after squeezing in the exchangeable cation content were not observed (Table 4). The concentration of cations in the squeezed pore water was <6 meq % compared to the CEC of the exchanger, and therefore the possible changes in the cation exchanger cannot be observed in the analyses. The measured Na fraction in the squeezed solution and the exchangeable cations were ~0.77 and 0.33 meq, respectively. In cation-exchange experiments of Na-montmorillonite, the corresponding Na equivalent fraction in solution should be ~0.9 meq or 0.2 meq in the exchanger (Sposito *et al.*, 1983). The different ionic strength established by Sposito *et al*. (1983) and in the present experiment were taken into account by using chemical activities in the calculations (Fig. 12).

The model presented describes the system to some degree but shows that dividing waters into two different water types with simplified compositions cannot explain all the observations. The limited space for anions in non-IL water should be taken into account, as well as varying cation ratios in non-IL water. As anion concentrations are thought to change with the distance from negatively charged surfaces, the change of cation ratios in non-IL pore water could also be considered.

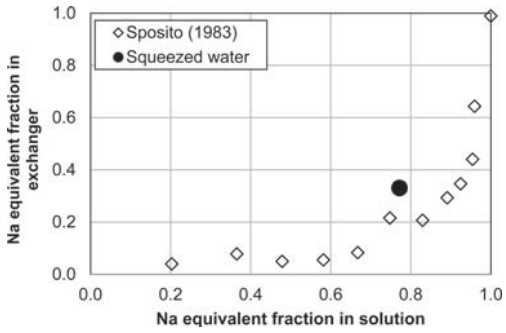

FIG. 12. Initial non-IL water composition according to modelling (0 MPa), and squeezed (60, 80, 100, 120 MPa) pore-water composition according to modelling and experimental results for the minor ions. Lines indicate modelling and dots indicate experimental results.

There is some evidence indicating that the squeezed pore water composition is a mixture of different pore-water types with varying ion concentrations in the squeezing pressure range studied. (1) The decrease in the measured IL, non-IL and Cl-accessible volumes during squeezing indicates mixing of these water types (Fig. 9). (2) The calculated chloride-accessible porosities according to squeezed pore-water chloride concentrations were greater than the measured non-IL porosities (Fig. 9). (3) The imbalance between the squeezed pore water and the cation exchanger indicates that cation composition has changed. A sodium concentration that is too low compared to other cations, indicates that additional calcium was released (Fig. 12).

Rebalancing between squeezed pore water in the syringe and pore water in bentonite was prevented by choosing a relatively short squeezing time (6 days). With a much longer squeezing time, an increase in concentrations of chloride, Na and sulfate and a decrease in concentration of Ca in squeezed pore water in the syringe is expected according to imbalances between bentonite and squeezed pore water observed in these experiments.

CONCLUSIONS

Squeezing experiments, the determination of the chemical composition of aqueous and solid phases and the microstructural analysis of the solid phase, were carried out successfully on ABM samples. The results obtained were used in geochemical modelling with the *PHREEQC* program by mixing IL and non-IL waters in fractions determined by microstructural analysis by means of SAXS measurements.

The pore-water yield increased from 32 to 48 wt.% from the initial amount of pore water in the samples when the squeezing pressure increased from 60 to 120 MPa. About 35 wt.% of collected pore water comes from the IL pores. The ratio between IL and non-IL pore waters, as well as the composition of the squeezed pore water, was constant in this squeezing-pressure range. The results of microstructural measurements by SAXS agree well with previous studies by Muurinen & Carlsson (2013).

Dissolving accessory minerals affects the ratio of cations in the squeezed solution. The limited space for anions in non-IL water affects the chemical activities of the anions and should be taken into account in geochemical modelling. The chloride concentration of the non-IL pore water in compacted bentonite before squeezing was 0.34 M greater than in squeezed pore water, due to the mixing of two main water types.

ACKNOWLEDGEMENTS

The research leading to these results received funding from Posiva Oy (Finland). Andrew Root (MagSol) is acknowledged for carrying out NMR measurements. The authors thank the Alternative Buffer Material (ABM) project and Clay Tech for the opportunity to use the samples for these experiments. Dr A. Muurinen, Dr T. Carlsson and Prof. M. Olin are acknowledged for discussions and ideas on the subject. Dr A.M. Fernández and Dr H. Van Baelen are acknowledged for many constructive comments and suggestions on the manuscript.

REFERENCES

Amman L., Bergaya F. & Lagaly G. (2005) Determination of the cation exchange capacity of clays with copper complexes revisited. *Clay Minerals*, **40**, 441–453.

Blanc P., Lassin A. & Piantone P. (2007) THERMODDEM – A database devoted to waste minerals: (http://thermoddem.brgm.fr).

Bolt G.H. & Warkentin B.P. (1958) The negative adsorption of anions by clay suspensions. *Kolloid-Zeitschrift*, **156**, 41–46.

Bradbury M.H. & Baeyens B. (2002) *Pore water chemistry in compacted re-saturated MX-80 bentonite: Physico-chemical characterisation and geochemical modelling.* Paul Scherrer Institut Berich Nr. 02–10, Villigen, Switzerland, 42 pp.

Fernández A.M., Baeyens B., Bradbury M. & Rivas P. (2004) Analysis of the pore water chemical composition of a Spanish compacted bentonite used in an engineered barrier. *Physics and Chemistry of the Earth*, **29**, 105–118.

Fernández A.M., Sanchez-Ledesma D.M., Tournassat C., Melon A., Gaucher E.C., Astudillo J. & Vinsot A. (2014) Applying the squeezing technique to highly consolidated clayrocks for pore water characterization: Lessons learned from experiments at the Mont Terri Rock Laboratory. *Applied Geochemistry*, **49**, 2–21.

Fernández A.M., Wilhelm S., Wouters L. & Van Baelen H. (2015) Characterizing clay pore water composition of Ypresian clays from Doel and Kallo sites, Belgium. *6th meeting on "Clays in Natural & Engineered Barriers for Radioactive Waste Confinement*". Book of Abstracts, pp. 202–203.

Gran G. (1950) Determination of the equivalence point in potentiometric titration. *Acta Chemica Scandinavica,* **4**, 559–577.

Holmboe M., Wold S. & Jonsson M. (2012) Porosity investigation of compacted bentonite using XRD profile modelling. *Journal of Contaminant Hydrology*, **128**, 19–32.

Itälä A., Järvinen J. & Muurinen A. (2013) CO_2 effect on the pH of compacted bentonite buffer on the laboratory scale. *Clay Minerals*, **48**, 149–152.

Karnland O., Olsson S. & Nilsson U. (2006) *Mineralogy and sealing properties of various bentonites and smectite-rich clay minerals*. Swedish Nuclear Fuel and Waste Management, Stockholm, Sweden, SKB Technical Report TR-06–30.

Kiviranta L. & Kumpulainen S. (2011) *Quality control and characterization of bentonite materials*. Posiva Oy, Olkiluoto, Finland, Working Report 2011–84.

Kumpulainen S. & Kiviranta L. (2010) *Mineralogical and chemical characterization of various bentonite and smectite-rich clay materials*. *Part A. Comparison and development of mineralogical characterization methods Part B: Mineralogical and chemical characterization of clay materials*. Posiva Oy, Olkiluoto, Finland, Working Report 2010–52, 74 p.

Kumpulainen S. & Kiviranta L. (2011) *Mineralogical, Chemical and Physical Study of Potential Buffer and Backfill Materials from ABM Test Package 1*. Posiva Oy, Olkiluoto, Finland, Working Report 2011–41.

Matusewicz M., Liljeström V., Pirkkalainen P., Suurinen J. P., Root A., Muurinen A., Serimaa R. & Olin M. (2013) Microstructural investigation of calcium montmorillonite. *Clay Minerals*, **48**, 267–276.

Meier L.P. & Kahr G. (1999) Determination of the cation exchange capacity (CEC) of clay minerals using the complexes of copper(II) ion with triethylenetetramine and tetraethylenepentamine. *Clays and Clay Minerals*, **47**, 386–388.

Muurinen A. (2001) *Development and testing of analysis methods for bentonite pore water*. Posiva Oy, Olkiluoto, Finland, Working Report 2001–07.

Muurinen A. (2006) *Ion concentration caused by an external solution into the porewater of compacted bentonite*. Posiva Oy, Olkiluoto, Finland, Working Report 2006–96.

Muurinen A. (2009) *Studies on the chemical conditions and microstructure in the reference bentonites of alternative buffer materials project (ABM) in Äspö*. Posiva Oy, Olkiluoto, Finland. Working Report 2009–42.

Muurinen A. (2010) *Studies on the chemical conditions and microstructure in package 1 of alternative buffer materials project (ABM) in Äspö*. Posiva Oy, Olkiluoto, Finland. Working Report 2010–11.

Muurinen A. & Carlsson T. (2013) *Bentonite pore structure based on SAXS, chloride exclusion and NMR studies*. Posiva Oy, Olkiluoto, Finland. Working Report 2013–53.

Muurinen A. & Järvinen J. (2013) *Ion-selective electrodes in pore water chemistry measurement of compacted bentonite*. Posiva Oy, Olkiluoto, Finland. Working Report 2013–24.

Muurinen A. & Lehikoinen J. (1999) *Pore water chemistry in compacted bentonite*. Posiva Oy, Olkiluoto, Finland, Working report 1999–20.

Muurinen A., Karnland O. & Lehikoinen J. (2007) Effect of homogenization on the microstructure and exclusion of chloride in compacted bentonite. *Physics and Chemistry of the Earth, Parts A/B/C*, **32**, 485–490.

Ohkubo T., Kikuchi H. & Yamaguchi M. (2008) An approach of NMR relaxometry for understanding water in saturated compacted bentonite. *Physics and Chemistry of the Earth*, **33**, S169–S176.

Parkhurst D.L. & Appelo C.A.J. (2013) Description of input and examples for PHREEQC version 3 – A computer program for speciation, batch-reaction, one-dimensional transport, and inverse geochemical calculations. U.S. Geological Survey Techniques and Methods, book 6, chapter A43, 497 pp. (http://pubs.usgs.gov/tm/06/a43/)

Posiva (2010) *Nuclear Waste Management at Olkiluoto and Loviisa Power Plants: Review of Current Status and Future Plans for 2010–2012.* TKS-2009, Posiva OY, Eurajoki.

Pusch R., Muurinen A., Lehikoinen J., Bors J. & Eriksen T. (1999) *Microstructural and chemical parameters of bentonite as determinants of waste isolation efficiency.* European Commission. Nuclear Science and Technology. Project Report EUR 18950 EN.

Sacchi E., Michelot J.-L., Pitsch H., Lalieux P. & Aranyossy J. (2001) Extraction of water and solutes from argillaceous rocks for geochemical characterisation: Methods, processes and current understanding. *Hydrogeology Journal*, **9**, 17–33.

SKB (2011) *Long-term safety for the final repository for spent nuclear fuel at Forsmark*. TR-11–01, Svensk Kärnbränslehantering AB, Stockholm.

Sposito G., Holtzclaw K.M., Charlet L., Jouany C. & Page A.L. (1983) Sodium-calcium and sodium-magnesium exchange on Wyoming bentonite in perchlorate and chloride media. *Soil Science Society of America Journal*, **47**, 51–56.

Svensson D., Duek A., Nilsson U., Olsson S., Sandén T., Lydmark S., Jägerwall S., Pedersen K. & Hansen S. (2011) *Alternative buffer material. Status of the ongoing laboratory investigation of reference materials and test package 1*. SKB, TR-11–06.

Van Loon L.R., Glaus M.A. & Muller W. (2007) Anion exclusion effects in compacted bentonites: Towards a better understanding of anion diffusion. *Applied Geochemistry*, **22**, 2536–2552.

Wersin P. (2003) Geochemical modelling of bentonite pore water in high-level water repositories. *Journal of Contaminant Hydrology*, **61**, 405–422.

Series title and number

VTT Science 183

Title	**Chemical behaviour of bentonite in the near field of the KBS-3V concept**
Author(s)	Aku Itälä
Abstract	In Finland the spent nuclear fuel final repository of Posiva Oy is based on the Swedish KBS-3V multi barrier concept. In this concept, the spent fuel rods are placed inside cast iron inserts surrounded by a gastight copper canister. The canister is placed in a vertical borehole and surrounded by bentonite clay rings at a depth of at least 400m in an underground bedrock facility at Olkiluoto. In the KBS-3 concept, the role of bentonite clay is considered to be important. The bentonite acts as a buffer material which gives mechanical and chemical protection, dissipates heat and retards radionuclide diffusion in the event of canister failure. It is crucial to know if the bentonite will retain its performance for at least 100 000 years. This thesis is compiled of 6 publications in which experiments related to bentonite buffer are modelled, or some parameters of bentonite are studied in laboratory/final repository conditions. In the two first publications the aim was to model the chemical evolution of a final repository during the thermal phase, when the bentonite is only partially saturated in the beginning. In these publications, a case called Long term test adverse 2 performed in Äspö Hard Rock Laboratory was adopted as a reference case to make the modelling more concrete and to clarify if the phenomena occurring in the experiment must be taken into account in safety assessment. The main chemical change according to the models and the experiment was anhydrite precipitation near the heater interface. No changes affecting the performance of the bentonite was observed. In addition, during this thesis a few laboratory experiments were conducted and modelled. The effect of temperature on cation exchange behaviour of purified sodium montmorillonite was studied in three different temperatures (25 °C, 50 °C and 75 °C) using calcium/sodium perchlorate mixtures. The observed results showed similar selectivity for all temperatures. In the fourth publication, the carbon dioxide partial pressure effect on the pH of bentonite was modelled using Geochemist's Workbench. The results indicated that only the surface protonation sites buffered the pH changes in the compacted bentonite system since the water amount inside the bentonite was small compared to the amount of surface complexation sites. The buffering capacity was approximated to be 0.3pH units/10g of bentonite. In the fifth publication, a structural model for bentonite was additionally made, which takes into account different kinds of waters inside the bentonite, and the model was compared to state-of-the-art commercial software and was noted to work well. In the last publication a simplified model was made to model the pore water of the squeezing experiments from compacted bentonite in anoxic laboratory conditions. The model worked well on major ions, but some differences were also observed. The conclusion from all these studies is that bentonite is a complex material, and the microstructural behaviour is still under dispute. The most common consensus is that there are three different waters (free pore water, diffuse double layer water and interlamellar water). It is important to understand the microstructure of bentonite so that accurate models can be created which correctly predict the phenomena occurring inside bentonite. Modelling is needed to approximate the final repository behaviour over hundreds of thousands of years, but there are still some uncertainties remaining such as chemical and mechanical parameters, parameters related to saturation and high temperature behaviour, lack of kinetic data for some minerals as well as reactive surface areas and grain radii.
ISBN, ISSN, URN	ISBN 978-951-38-8670-7 (Soft back ed.) ISBN 978-951-38-8669-1 (URL: http://www.vttresearch.com/impact/publications) ISSN-L 2242-119X ISSN 2242-119X (Print) ISSN 2242-1203 (Online) http://urn.fi/URN:ISBN:978-951-38-8669-1
Date	November 2018
Language	English, Finnish abstract
Pages	60 p. + app. 67 p.
Name of the project	
Commissioned by	
Keywords	bentonite, modelling, nuclear waste, final repository, transport, diffusion, KBS-3V
Publisher	VTT Technical Research Centre of Finland Ltd P.O. Box 1000, FI-02044 VTT, Finland, Tel. 020 722 111

Julkaisun sarja ja numero

VTT Science 183

Nimeke	**Bentoniitin kemiallinen käyttäytyminen KBS-3V konseptin lähialueella**
Tekijä(t)	Aku Itälä
Tiivistelmä	Käytetyn ydinpolttoaineen loppusijoitus Suomessa Posiva Oy:n loppusijoituspaikalla perustuu ruotsalaiseen KBS-3V moniestekonseptiin. Tässä konseptissa käytetyt polttoainesauvat asetetaan valurautaholkkiin, joka ympäröidään ilmatiiviillä kuparikapselilla. Kapseli asetetaan pystysuoraan kairareikään ja ympäröidään bentoniittirenkailla vähintään 400 m syvyyteen Olkiluodon maanalaiseen laitokseen. KBS-3 konseptissa bentoniittisavella on tärkeä rooli. Bentoniitti toimii puskurimateriaalina, joka antaa mekaanista ja kemiallista suojaa, johtaa lämpöä ja hidastaa radionuklidien diffuusiota kanisterivian sattuessa. On tärkeää tietää, säilyttääkö bentoniitti suorituskykynsä vähintään 100 000 vuotta. Tämä väitöskirja on koottu kuudesta julkaisusta, joissa bentoniittiin liittyviä kokeita on mallinnettu tai joitakin bentoniitin parametreja tutkittu laboratorio/loppusijoitus olosuhteissa. Kahdessa ensimmäisessä julkaisussa tarkoituksena oli mallintaa loppusijoitustilan evoluutiota termisen vaiheen aikana, kun bentoniitti on alussa osittain saturoitunut. Näissä julkaisuissa koe nimeltä Long term test adverse-2, joka tehtiin Äspöön Hard Rock laboratoriossa, otettiin referenssitapaukseksi. Tällä saatiin mallinnusta konkreettisemmaksi, ja pystyttiin selventämään, tarvitseeko kokeissa tapahtuvia ilmiöitä huomioida turvallisuusanalyysissä. TOUGHREACT mallinnusohjelmaa käytettiin tekemään kytketty termo-hydro-kemiallinen malli. Olennaisin kemiallinen muutos mallien ja kokeiden perusteella oli anhydriitin saostuminen lämmittimen lähellä. Bentoniitin suorituskykyyn vaikuttavia muutoksia ei havaittu. Väitöskirjassa tutkittiin myös joitain mallinnettuja laboratoriokokeita. Työssä tutkittiin lämpötilan vaikutusta kationinvaihtoon puhdistetussa natrium montmorilloniitissa kolmessa eri lämpötilassa (25 °C, 50 °C and 75 °C) käyttämällä kalsium/natrium perkloraatti seoksia. Havaitut tulokset näyttivät samansuuntaisia selektiivisyyksiä kaikissa lämpötiloissa. Neljännessä julkaisussa mallinnettiin Geochemist's Workbenchillä hiilidioksidin osapaineen vaikutusta bentoniitin pH:n. Tuloksista havaittiin, että vain pintakompleksaatiopaikat puskuroivat pH:n muutoksia kompaktoidussa bentoniitti systeemissä, sillä vesimäärä bentoniitin sisällä on pieni verrattuna pintakompleksaatiopaikkojen määrään. Puskurikapasiteetin arvioitiin olevan 0.3 pH yksikköä/10 grammaa bentoniittia. Viidennessä julkaisussa tehtiin bentoniitille rakenteellinen malli, joka ottaa huomioon erilaiset vedet bentoniittissa ja mallia verrattiin johtavaan alan kaupalliseen malliin, ja sen todettiin toimivan hyvin. Viimeisessä julkaisussa tehtiin yksinkertaistettu malli puristuskokeille mallintamaan huokosvettä hapettomissa laboratorio olosuhteissa. Malli toimi hyvin merkittävimmille ioneille, mutta joitakin eroja havaittiin myös. Johtopäätöksenä väitöskirjassa tehdyistä tutkimuksista voidaan sanoa, että bentoniitti on monimutkainen materiaali, ja mikrorakenteellinen käyttäytyminen on kiistanalaista. Yleisin mielipide on, että bentoniitti sisältää kolmenlaista vettä (vapaata huokosvettä, diffuusikerrosvettä ja lamellien välistä vettä). Bentoniitin mikrorakenne on tärkeä ymmärtää, jotta voidaan luoda tarkkoja malleja, jotka kuvaavat oikein bentoniissa tapahtuvia ilmiöitä. Mallinnusta tarvitaan arvioimaan loppusijoitustilan käyttäytymistä satojen tuhansien vuosien aikana, mutta joitakin epävarmuuksia liittyen bentoniittiin on yhä olemassa, kuten kemialliset ja mekaaniset parametrit, parametrit liittyen bentoniitin saturaatioon ja korkean lämpötilan käyttäytymiseen, joidenkin mineraalien kineettisen datan puute sekä reaktiiviset pinta-alat ja raekoko.
ISBN, ISSN, URN	ISBN 978-951-38-8670-7 (nid.) ISBN 978-951-38-8669-1 (URL: http://www.vtt.fi/julkaisut) ISSN-L 2242-119X ISSN 2242-119X (Painettu) ISSN 2242-1203 (Verkkojulkaisu) http://urn.fi/URN:ISBN:978-951-38-8669-1
Julkaisuaika	Marraskuu 2018
Kieli	Englanti, suomenkielinen tiivistelmä
Sivumäärä	60 s. + liitt. 67 s.
Projektin nimi	
Rahoittajat	
Avainsanat	bentoniitti, mallinnus, ydinjäte, loppusijoitus, kulkeutuminen, diffuusio, KBS-3V
Julkaisija	Teknologian tutkimuskeskus VTT Oy PL 1000, 02044 VTT, puh. 020 722 111

Chemical behaviour of bentonite in the near field of the KBS-3V concept

In Finland the spent nuclear fuel final repository of Posiva Oy is based on the Swedish KBS-3V multi-barrier concept. In this concept, the spent fuel rods are placed inside cast iron inserts surrounded by a gastight copper canister. The canister is placed in a vertical borehole and surrounded by bentonite clay rings at a depth of at least 400m in an underground bedrock facility at Olkiluoto.

In the KBS-3 concept, the role of bentonite clay is considered to be important. The bentonite acts as a buffer material which gives mechanical and chemical protection, dissipates heat and retards radionuclide diffusion in the event of canister failure. It is crucial to know if the bentonite will retain its performance for at least 100 000 years.

This thesis is compiled of 6 publications in which experiments related to bentonite buffer are modelled, or some parameters of bentonite are studied in laboratory/final repository conditions. In the thesis there are four main parts. In the first part, the Finnish spent nuclear fuel disposal concept is discussed with its main features. In the second part, the structural and chemical behaviour of bentonite and its main mineral, montmorillonite, are introduced. The third part consists of experimental studies on bentonite, and the fourth part is about thermo-hydro-chemical modelling of bentonite buffer.

ISBN 978-951-38-8670-7 (Soft back ed.)
ISBN 978-951-38-8669-1 (URL: http://www.vttresearch.com/impact/publications)
ISSN-L 2242-119X
ISSN 2242-119X (Print)
ISSN 2242-1203 (Online)
http://urn.fi/URN:ISBN:978-951-38-8669-1